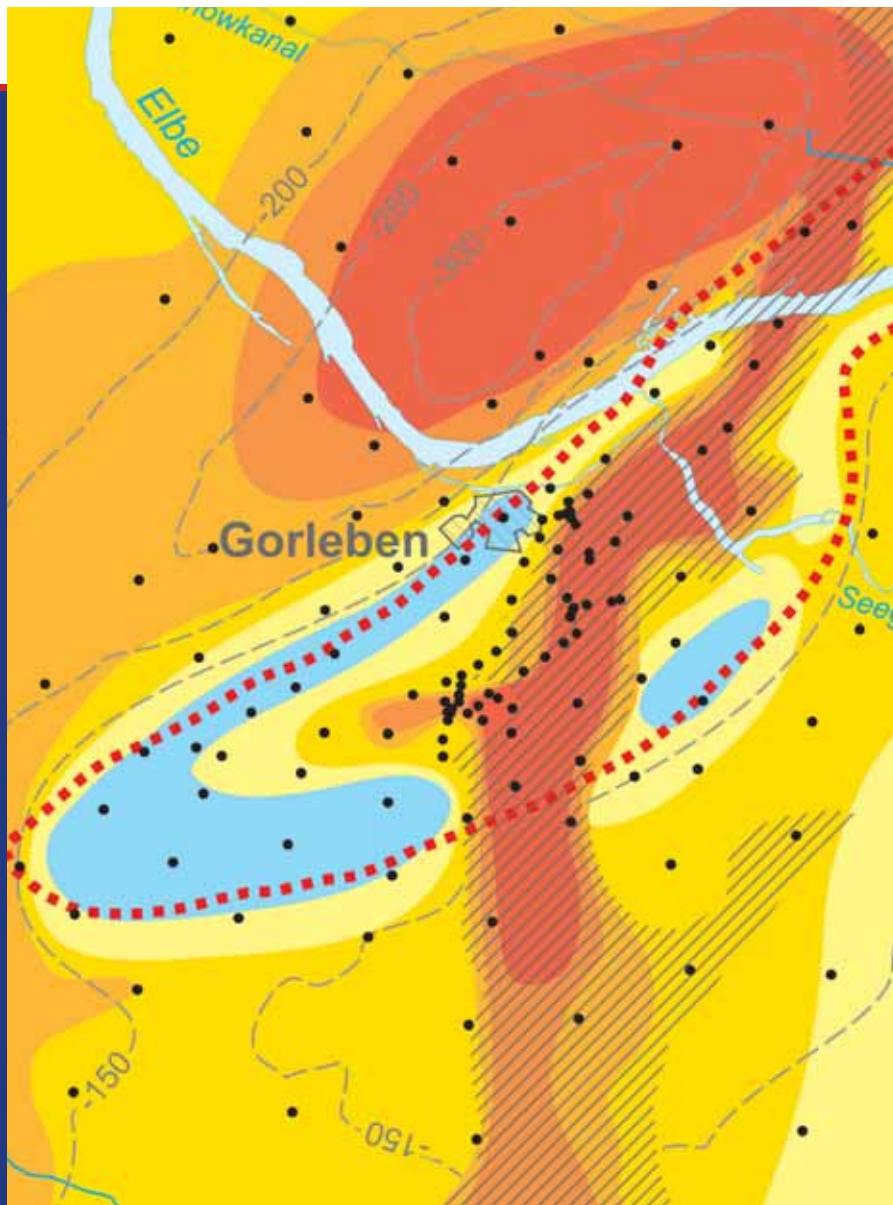


Description of the Gorleben site
Part 1:

Hydrogeology of the overburden of the Gorleben salt dome



Description of the Gorleben Site
Part 1:
Hydrogeology of the overburden
of the Gorleben salt dome

Description of the Gorleben site
Part 1:

Hydrogeology of the overburden of the Gorleben salt dome

A topographic map of the Gorleben area in Germany. The map shows contour lines with elevations of 150, 200, and 250 meters. The Elbe river is visible on the left side, and the Seesee is on the right. The Gorleben site is marked with a square and labeled 'Gorleben'. The map is overlaid with a grid of dots and lines, representing the hydrogeological data discussed in the report.

HANS KLINGE
JENS BOEHME
CHRISTOPH GRISSEMANN
GEORG HOUBEN
ROLF-RÜDIGER LUDWIG
ANDRÉ RÜBEL
KLAUS SCHELKES
FRIEDRICH SCHILDKNECHT
AXEL SUCKOW

Hannover, 2007

German edition:

Standortbeschreibung Gorleben Teil 1
Die Hydrogeologie des Deckgebirges des Salzstocks Gorleben

ISBN 978-3-510-95962-4, Price: 34.00 €

More information/Purchase: <http://www.schweizerbart.de/9783510959624>

© Bundesanstalt für Geowissenschaften und Rohstoffe (BGR)
Geozentrum Hannover
Stilleweg 2
30655 Hannover
Germany

www.bgr.bund.de

ISBN 978-3-9813373-4-1

Foreword

Research has been carried out since 1979 on the Gorleben salt dome, located in the rural district of Lüchow-Dannenberg in Lower Saxony, to investigate its suitability as a geologic repository for radioactive waste. The investigation programme consists of surface and underground geological and mine engineering exploration, as well as analysing and evaluating all of the issues necessary to competently assess its suitability and long-term safety. The Gorleben site was investigated in detail for a period of more than twenty years to understand the internal structure of the salt dome, the overburden and the adjoining rock. The preliminary results of these investigations were published in interim reports in 1983, 1990 and 1995. The findings published in these reports substantiated the potential suitability of the salt dome as a geologic repository for radioactive waste.

The investigation work at the Gorleben site was suspended as a consequence of the agreement reached on 14 June 2000 between the German government and the power supply industry. This moratorium applied for a period of at least three years, but a maximum of ten years. Notwithstanding the moratorium, the German government issued a statement on Gorleben which confirmed that the previous findings from its investigation did not contradict the site's potential suitability.

It is now possible after the termination of the surface investigation programme, and for the purpose of documenting the results of the extensive underground exploration, to present the findings of the geoscientific investigation of the Gorleben site in an overall report. The first part presents the hydrogeology of the overburden. The second part presents the results of the geological and structural geological exploration of the overburden and the adjoining rock, and the third part covers the results of the exploration of the salt itself. These findings are supplemented in the fourth part by a description of the geotechnical investigations.

This compilation of the data, and the presentation of the technical evaluation of the geoscientific investigation results, as well as the documentation, should also help to bring more objectivity into the controversially discussed public and political debate concerning the Gorleben site.



(Volkmar Bräuer)

- Repository Project Manager -

Abstract

The Gorleben salt dome has been investigated since 1979 to ascertain its suitability as a repository for radioactive waste. A wide-ranging drilling and exploration programme was carried out from 1979 to 1998 to investigate the hydrogeological conditions and the geology of the overburden above the salt dome. This report brings together all of the most important results of this hydrogeological investigation.

The Tertiary and Quaternary strata covering the salt dome form a system of aquifers and aquitards with a maximum thickness of 430 m. These can be hydrogeologically divided up into Tertiary and Elsterian sands and gravels forming a lower aquifer, overlain by Saalian and Weichselian deposits forming an upper aquifer. The most dominant structural element in the overburden of the Gorleben salt dome is the Elsterian Gorleben channel (Gorlebener Rinne). The central part of the channel above the salt dome is filled with channel sands of good permeability lying directly on the cap rock, and locally also on Zechstein salts.

The Elsterian channel sands are separated from the shallow aquifer by the low permeability Lauenburger-Ton-Komplex. However, to the north and south of the salt dome, they are in hydraulic contact with the trans-regionally widespread important aquifer formed by Tertiary Braunkohlensande.

The Gorleben channel is of considerable importance when assessing the long-term safety of a repository within the salt dome. Because of the direct contact between the Zechstein evaporites and the lower aquifer in the centre of the channel, there is a considerable increase in the salinity of the groundwater. An assessment of any potential migration paths out of the salt dome is closely connected with the issue of the transport of saline water within the overburden. Two migration paths for this brine can be defined on the basis of the current freshwater/salt water distribution: a) lateral migration of highly concentrated brines in the northwestern rim syncline where the water collects at the base of the aquifer because of its higher density; b) vertical rise of the brine in the upper aquifer as a result of locally increased permeability within the overlying aquitard. This brine reaches the groundwater surface in the Elbe lowland.

Numerical modelling of the flow of water using three-dimensional flow models indicates that it would take several thousand to a few ten thousand years for freshwater to flow from the contact zone in the Gorleben channel to the groundwater surface. In contrast, 2D modelling of groundwater flow in the Gorleben channel, considering the brine-concentration-dependent water density, indicates that other flow patterns develop when brine is present, and that these have lower flow velocities on average and thus longer travel times within the salt water zone.

This is also indicated by the isotopic composition of the brine, which in some cases still bears a Pleistocene signature or in other cases represents mixtures of Pleistocene and Holocene waters. It can be concluded from this that the flow of groundwater in the post-glacial period in the Gorleben channel also includes brine. On the other hand, the presence of Pleistocene water reveals that there is only a minor amount of salt water flow overall in the channel.

Table of contents		Page
1	Introduction	9
2	The hydrogeological investigation programme at Gorleben	10
3	Morphology and hydrology of the study area	13
3.1	Location, morphology, hydrography, land use	13
3.2	Climate and precipitation	16
3.3	Groundwater recharge	17
4	Overburden hydrogeology	20
4.1	Introduction	20
4.2	Hydrostratigraphic classification of the sedimentary sequence	20
4.2.1	Tertiary	22
4.2.2	Quaternary	24
4.3	Hydrogeological structure	25
5	Hydraulic properties	31
5.1	Long-term pumping tests	32
5.1.1	Objectives	32
5.1.2	Evaluation method	34
5.1.3	Results	35
5.1.3.1	Hydraulic parameters	35
5.1.3.2	Spatial drawdown behaviour over time	36
5.2	Hydraulic conductivity	40
6	Geothermal investigations	43
6.1	Objective	43
6.2	Datebase	43
6.3	Expected geothermal field	44
6.4	Groundwater temperatures in the overburden	44
6.5	Distribution of heat flow density	45
6.6	Thermal indications of groundwater flows	50
7	Hydrochemistry	55
7.1	Spatial distribution of total dissolved solids	55
7.1.1	Data evaluation procedure	55
7.1.2	Description of freshwater/salt water distribution	57
7.2	Chemical composition of the groundwater	66
7.2.1	Groundwater classification	66
7.2.2	Geochemical interactions between groundwater and sediments	69

7.3	Isotope-hydrological investigations	74
7.3.1	Tritium	74
7.3.2	Stable oxygen and hydrogen isotopes	76
7.3.3	¹⁴ C age dating	82
7.3.4	Analysis of core samples from the Hamburg-Ton and Lauenburger-Ton-Komplex	86
8	Groundwater dynamics	91
8.1	Groundwater levels	91
8.2	Groundwater dynamics in the freshwater body	95
8.2.1	Shallow groundwater	95
8.2.2	The freshwater body of the lower aquifer in the Elbe-Löcknitz lowland	99
8.3	Groundwater dynamics in the salt water body	100
9	Numerical groundwater modelling	103
9.1	Three-dimensional groundwater model with constant density	103
9.2	Modelling of groundwater flow with variable densities	106
9.3	Paleohydrogeological investigations	110
9.4	Conclusions from groundwater flow modelling	114
10	Final discussion on freshwater/salt water dynamics within the overburden of the Gorleben salt dome	115
	References	132
	Abbreviations	139
	List of tables	141
	List of figures	142
	List of appendices	145

1 Introduction

The Federal Institute for Geosciences and Natural Resources (BGR), as the German government's central authority on geoscientific issues, works on the geoscientific aspects of the investigation of the Gorleben site as part of the geologic repository measures of the Federal Ministry for the Environment, Nature Conservation and Nuclear Safety (BMU) and the Federal Office for Radiation Protection (BfS). All of the investigation findings resulting from the surface and underground geological exploration activities are interpreted and presented by the BGR. The results of the exploration and the safety analysis form the basis for the assessment of the site and the subsequent approval procedures conducted pursuant to the Atomic Energy Act.

In accordance with the coalition agreement of the German Federal Government, and as a consequence of the decision to abandon nuclear power, the Nuclear Consensus Agreement of June 2000 between the German Federal Government and the energy utilities created the statutory basis for a moratorium on the investigation of the Gorleben salt dome. On the basis of this agreement, work at the site was stopped and the underground investigations were preliminarily suspended in October 2000. The hydrogeological investigations of the overburden and adjoining rock had already been completed by this time. The results of these investigations could therefore be presented in full despite the moratorium (KLINGE et al. 2004).

The results of the hydrogeological investigation of the overburden and adjoining rock of the salt dome have been published continuously in numerous internal BGR publications throughout the long period of investigation. These publications were forwarded to the Federal Office for Radiation Protection as the agency with overall responsibility. In addition, the current status of the investigations at the time was published with a broad technical audience in mind in PTB (1983), and in BfS (1990) and ALBRECHT et al. (1991). Later publications mainly dealt with sub-aspects of the investigation programme in the form of conference papers or articles in technical journals. There has so far been no publication giving an overall presentation of the hydrogeological conditions in the overburden above the Gorleben salt dome.

Now that the surface exploration programme has been completed, it is possible to present the hydrogeological facts and results of this exploration in a publication. Three additional volumes of the *Geologisches Jahrbuch* published in parallel bring together all of the geological results of the surface exploration (KÖTHE et al. 2007), the results to date of the underground exploration (BORNEMANN et al. 2008) and of the geotechnical underground investigations (BRÄUER et al. in prep.).

The focus of this publication is a presentation of the hydrogeology of the overburden and its interpretation with respect to potential migration paths for contaminants from the surface of the salt dome and into the biosphere via the groundwater. It does not draw any conclusions about the suitability of the Gorleben salt dome as a repository for radioactive waste. An assessment of the suitability in this context requires an overall evaluation of the properties of the salt dome and the overburden at Gorleben. However, a final assessment of the barrier properties of the Gorleben salt dome will only be possible after completing and evaluating the whole of the investigation programme.

2 The hydrogeological investigation programme at Gorleben

The Gorleben salt dome was proposed by the government of Lower Saxony in 1977 as a possible location for a mine repository for radioactive waste. The German Federal Government adopted this proposal at the time and initiated investigations to ascertain the suitability of the site for the disposal of waste of this type. The aim of these investigations was to confirm the safety of the construction and operation of a repository in the salt dome, as well as confirm its long-term safety. For this purpose, the geology and hydrogeology of the site were investigated at the surface and underground. The surface investigations were carried out to determine the geology and hydrogeology at the site, and primarily to provide the basis for estimating and calculating the potential transport of nuclides within the overburden as part of the assessment of scenarios on the long-term safety of the repository.

The investigations were carried out in two phases. From 1979 to 1984, an area of approx. 390 km² was first investigated, whose boundaries were defined by hydrological and hydrogeological aspects. This area was bounded in the north by the river Elbe, which formed the political boundary at the time between West and East Germany.

The general lack of natural outcrops of the overburden meant that exploration was primarily based on a comprehensive drilling programme. 158 exploration boreholes were drilled to a depth of 200 to 450 m in most cases, and 322 groundwater observation wells were drilled additionally (Fig. 1). The observation wells were used for the extraction of water samples and for the measurement of water levels. Furthermore, special logging methods were also carried out in the observation wells, with the main aim of estimating the flow of highly saline groundwater.

The hydrogeological investigations were supplemented by:

- four long-term pumping tests lasting three weeks each
- pedological mapping to determine the rate of water percolation and groundwater-recharge

- permeability tests at drilling cores
- sorption test at sediments
- a geo-electrical ground survey to identify the freshwater/salt water interface
- short-term pumping tests in observation wells
- an investigation programme to reveal the presence of shallow salty groundwater
- helicopter-borne electromagnetic surveying to investigate occurrences of salty groundwater

A large number of cuttings and core samples were collected in the exploration and water observation wells. The samples underwent sedimentary, micropaleontological and palynological analysis. The results were used to determine the stratigraphy of the Cretaceous to Quaternary sediments.

Other investigation programmes largely concerned with geological questions were:

- surface geological mapping of the Quaternary sediments
- a drilling programme with a total of 44 boreholes drilled to the salt table to investigate the cap rock, plus four deep drillings, and two additional boreholes investigating the site for the planned mine shaft
- a core drilling in the Southern rim syncline to investigate the Tertiary sediments
- a reflection seismic survey to investigate the salt dome structure
- a shallow seismic survey to explore the surface of the salt dome and the Quaternary channel structures

The hydrogeological results of these investigation programmes were documented in numerous internal BGR reports, which are not generally accessible. In this specific report, references are only made to those BGR reports which summarise the investigation results. With respect to the study area to the south of the Elbe, this is BOEHME et al. (1995).

As mentioned in the introduction, the boundaries of the study area were determined by hydrological and hydrogeological considerations. The area was bounded to the north by the Elbe river. Extending the investigations to the north would have been desirable because the Elbe and the Lößnitz, running a few kilometres to the north of the Elbe, lie at a similar height, and because the Elbe-Lößnitz lowland is a discharge area for the groundwater flowing in from the south and the north (and it is not possible to clearly delineate the southern and northern flows from one another). However, inclusion of this

area at the start was not possible because the Elbe formed the political boundary at the time between East and West Germany, and investigations within the German Democratic Republic were not permitted.

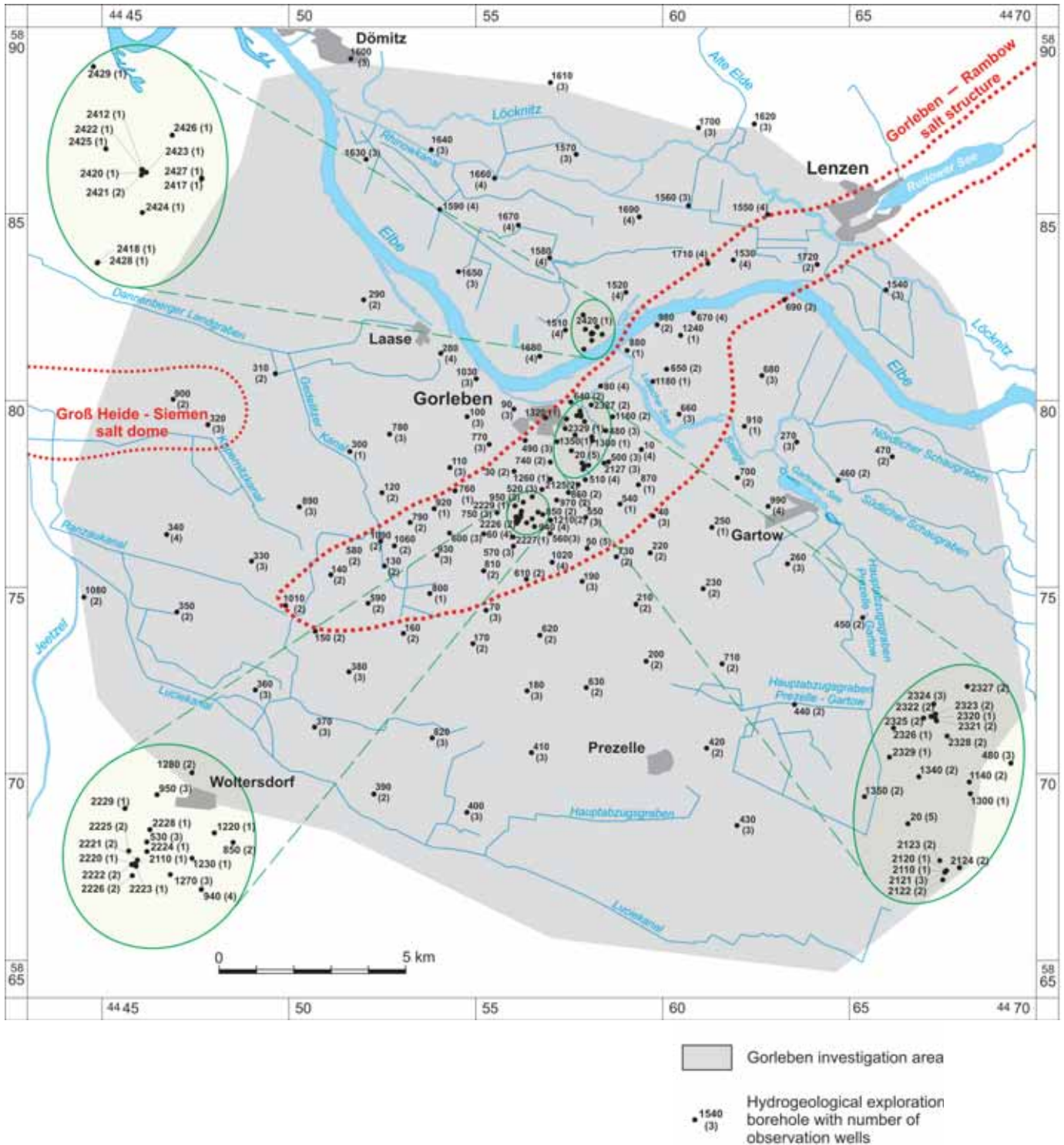


Figure 1: Location map of the exploration boreholes and observation wells for the hydrogeological investigation programme

Reunification of the two German states in 1990 first made it possible to investigate the lowland between the Elbe and the Lößnitz. This was carried out between 1996 and 1998 and also largely involved a drilling and testing programme. 27 exploration boreholes were drilled overall, in addition to 76 groundwater observation wells. This drilling programme was supplemented by pedological mapping to determine the water percolation rate. Other exploration programmes included a geological mapping and shallow drilling programme looking at the Quaternary sediments, as well as a shallow seismic survey exploring the subsurface Quaternary structures. The hydrogeological results of the investigation of the Elbe-Lößnitz lowland were presented in KLINGE et al. (2001). The results of both investigation programmes were again brought together in KLINGE et al. (2004).

According to the Atomic Energy Act, the German Federal Government is responsible for the construction of radioactive waste repositories. When the project began, this responsibility lay with the National Metrology Institute (PTB). It was transferred to the Federal Office for Radiation Protection (BfS) when this was founded in 1989.

The Federal Institute for Geosciences and Natural Resources (BGR) has been responsible for providing PTB/BfS with technical advice, geoscientific monitoring and quality assurance during the investigation of the site, and the overall geoscientific evaluation of the results – in addition to extensive investigations on behalf of PTB and BfS.

3 Morphology and hydrology of the study area

3.1 *Location, morphology, hydrography, land use*

Figure 2 shows the location and morphology of the 475 km² study area. The area to the south of the Elbe is all in Lower Saxony. The area to the north of the Elbe is largely in Brandenburg but also includes a small portion in Mecklenburg-Western Pomerania to the north of the Lößnitz around Dömitz.

The study area lies in the glacial valley of the Elbe, which is particularly wide at this point. It can be divided into three typical land forms:

1. The late glacial to Holocene lowlands and floodplains of the Elbe and its tributaries
2. The Weichselian glacial valley of the Elbe
3. The Weichselian to Saalian geest ridges

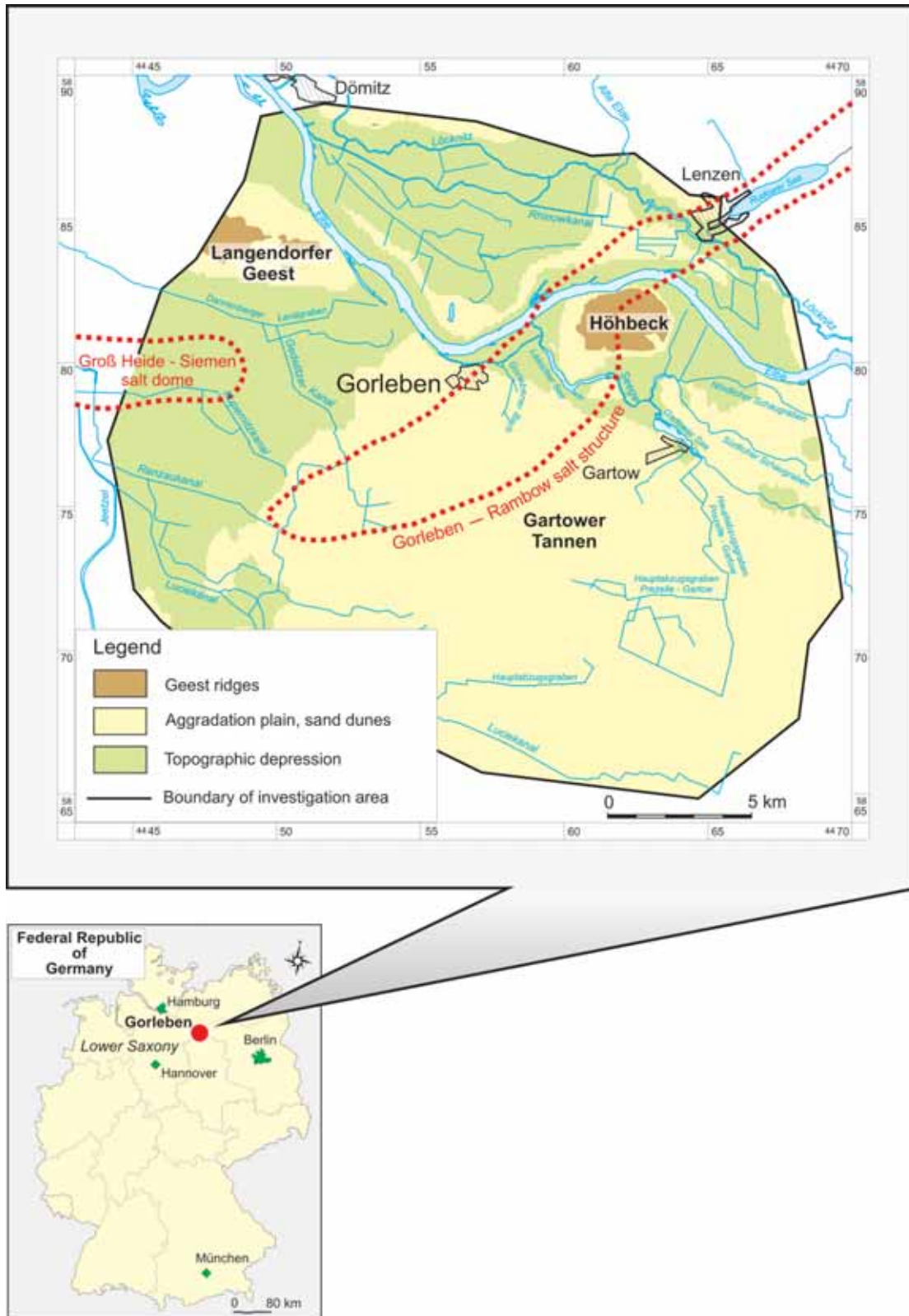


Figure 2: Location and morphology of the Gorleben study area

1. Lowlands and alluvial valleys of the Elbe and its tributaries

This is an extremely flat area that extends parallel to the current river bed and is up to several kilometres wide. In addition to the lowland between the Elbe and the Lößnitz in the north of the study area, these lowlands also exist at the western edge of the area occupied by the tributaries and drainage system of the Jeetzel river, as well as along the Seege in the south and the Hühbeck in the west. All of these areas are covered by water every year during annual flooding if they are not protected by dikes. Because of the regular flooding, this area is covered by alluvial and flood clays. These are the youngest sediments in the area. Typical features of the lowlands are the numerous small water-filled abandoned river courses.

The land mainly lies at a height between 13 m and 17 m above sea level. The deepest point is 12 m above sea level in the northwest near Dömitz, where the Rhinow canal enters the Elbe.

2. Aggradation plain of the last glaciation (Weichselian glacial valley)

This land form covers most of the study area. Most of the area is in the glacial valley of the Elbe. The aggradation of this Pleistocene water course by the Elbe during the last ice age left behind an extensive plain, which gradually rises to its edges in the northeast and southwest. The ancient plain is cut by the flood plain of the current Elbe and its tributaries, and the higher land formed by the geest ridges. Aeolian sand was deposited outside of the lowlands at the end of the last glaciation and continuing into the Holocene. This aeolian sand covers the aggradation plain with a sheet a few decimetres to a few metres thick, or in the form of dunes and dune fields a few metres high. Aeolian sand determines the present day relief which is particularly irregular with small scale structures in the areas covered by the dune fields. Extensive dune fields of this kind are found in the Gartower Tannen area in particular.

The relief of this land form in the study area is primarily between 20 m above sea level and 30 m above sea level.

3. Geest ridges

The so-called geest "islands" form isolated ridges in the glacial valley of the Elbe. Those which extend into the study area are the eastern extensions of the Langendorfer geest and primarily the Hühbeck. The oldest sediments are found on the surface of the geest "islands". These are primarily Saalian sediments.

The relief of this land form in the study area primarily lies between 30 m above sea level and 50 m above sea level. The H6hbeck forms the highest point in the area with a relief of 76 m above sea level.

Figure 2 shows the position of the most important water courses. The main water course is the Elbe into which the Seege flows directly in the centre of the area. The study area is also drained by a network of ditches and canals. This drainage water flows into the Jeetzel to the west. At the northern edge of the study area, the L6ocknitz, which runs approximately parallel to the Elbe, is the main water course into which the tributaries flow from the northeast. South of D6omitz, the L6ocknitz is redirected to the north into a canal and flows into the Elbe around 7 km west-northwest of D6omitz.

The lowland between the Elbe and the L6ocknitz is protected from flooding by dikes. This area needs to be continuously drained because some of it lies below the mean water level of the Elbe. Drainage involves a system of canals which flow into the centrally located Rhinow canal. The water level of this canal is artificially controlled by the Gaarz water scoop lying to the south of D6omitz.

The elevated terrain at the Gartower Tannen, H6hbeck and Langendorfer geest has remarkably few water courses. This is due to the high infiltration capacity of the aeolian and meltwater sands which are present in these locations. Precipitation infiltrates very quickly here. The few ditches and channels in the area only rarely carry any water and are regularly dry, particularly in the summer months.

Around 40 % of the study area is forested, primarily by pine forests. Most of these forests lie in the southeast of the study area in the zones characterised by sheets of aeolian sand and dunes. Around 30 % of the area is used for arable farming – primarily in the southwestern part of the study area. Most of the approx. 25 % grass land and wet lands lie in the Elbe-L6ocknitz lowland.

3.2 *Climate and precipitation*

Compared to western North Germany, the Gorleben area is characterised by relatively minor precipitation and a more continental-type climate. An average precipitation of 556 mm/year was determined at the L6uchow station for the 25-year period from 1955 to 1980. In the 1984 to 1997 hydrologic years, a much higher average of 636 mm/year was measured for the study area (PORTMANN & MENDEL 1999). These relatively large differences in average values are attributable to the above-average amount of precipitation in 1984 and in the periods 1986 to 1988 and 1993 to 1994, of over 700 mm/year to a maximum of 841 mm/year (cf. Fig. 3).

The average annual temperature for 1983 to 1997 was 8.9 °C, with a minimum and maximum of 7.3 °C (1996) and 10.0 °C (1990) respectively. The sun shone on average 1655 hours/year, with minimum and maximum figures of 1458 hours/year in 1987 and 1859 hours/year in 1989 respectively.

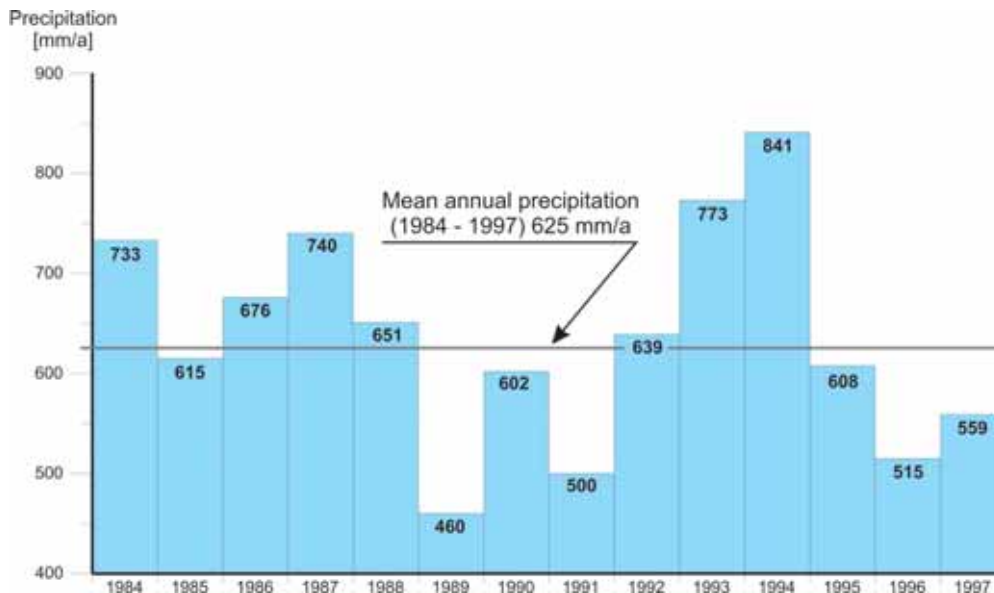


Figure 3: Annual precipitation for 1984 – 1997 hydrologic years (according to PORTMANN & MENDEL 1999)

3.3 Groundwater recharge

The percolation water rate was used to calculate groundwater recharge in the Gorleben study area. The method used by SPONAGEL & STREBEL (1981) in the area to the south of the Elbe is based on empirically determined dependencies between the percolation water rate and amount of precipitation, physical soil parameters, and depth of the water table. The method enables differentiated determination of groundwater recharge at a fine scale, making allowance for soil-related and land use-related aspects.

The method calculates the amount of water seeping into and remaining in the groundwater every year, i.e. the difference between annual percolation and annual capillary rise from the groundwater.

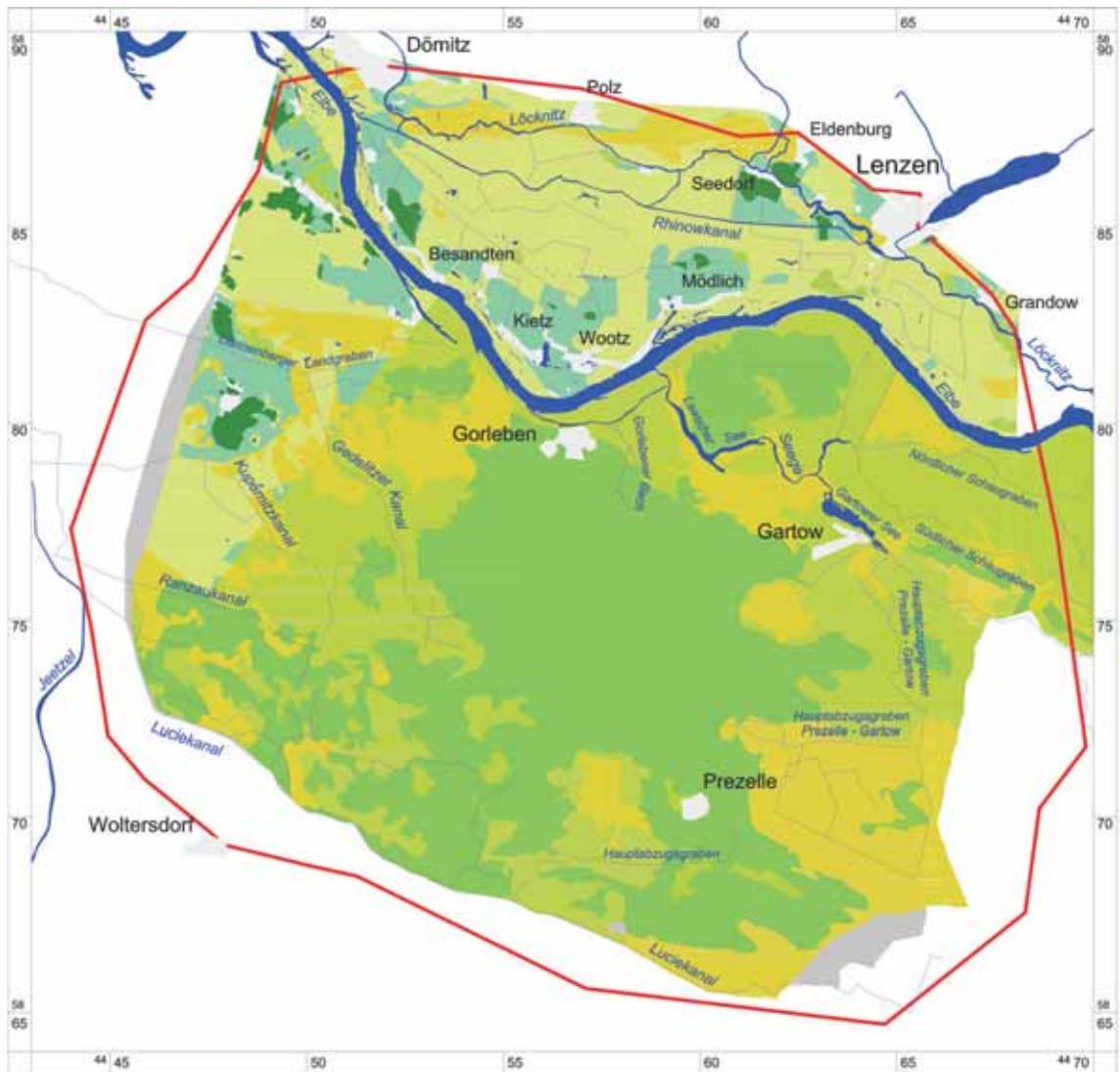
The 25-year averages of the Lüchow weather station form the basis for the climatic data input. The soil parameters for the amount of soil water available to vegetation were determined from pedological mapping (SPONAGEL & STREBEL 1981; HENNINGS & DUIJNISVELD 1997).

A method further developed by Renger & Wessolek (1990) was used in the Dömitz-Lenzen study area. The main difference to the method applied by Spönagel & Strebels (1981) in the area to the south of the Elbe is the incorporation of seasonal precipitation differences. Both methods produce comparable results overall (Hennings & Duijnsveld 1997).

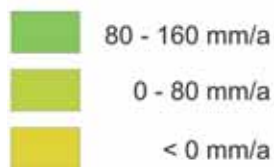
Figure 4 summarises the calculation results for both sub-areas. In the area to the south of the Elbe, Spönagel & Strebels (1981) differentiate between five different recharge types with recharge rates of between -80 mm/year and +200 mm/year. The figure shows a large contiguous area of groundwater recharge with rates over 80 mm/year to 160 mm/year in the central area, characterised by aeolian sand deposits and the sand dune deposits of the Gartower Tannen.

The central zone with high rates of groundwater recharge is bounded by areas with minor to absent recharge in lowlands where water courses drain into the Elbe. Because of the shallow water table and the cohesive soils, evaporation in these areas exceeds precipitation by up to 80 mm/year. 84 % of the area to the south of the Elbe has average groundwater recharge rates of 64 mm/year. The remaining 16 % of the area has negative recharge rates.

The percolation water rates calculated by Renger & Wessolek (1990) in the Dömitz-Lenzen study area vary from area to area between -61 mm/year and +161 mm/year. Because of the low water tables and the widespread outcropping of alluvial flood clays, large areas have very low, and even in some cases negative recharge rates, particularly in the Lößnitz floodplains and in the area to the north of Lößnitz. Areas with significant groundwater recharge rates of > 100 mm/year are mainly limited to the agriculturally used areas near the Elbe with average water table depths of usually more than 1.5 m. In the area to the north of the Elbe, the average overall groundwater recharge rate is only 28 mm/year.



Groundwater recharge (southern investigation area)
(SPONAGEL & STREBEL 1981)



Groundwater recharge (northeastern investigation area)
(HENNING & DUJNISVELD 1997)

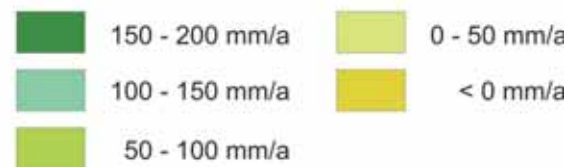


Figure 4: Groundwater recharge calculated from the soil water balance (percolation water rate in mm/year)

4 Overburden hydrogeology

4.1 Introduction

The geology of the overburden and adjoining rock of the Gorleben salt dome is described in detail in KÖTHE et al. (2007) and will therefore only be described here to the degree required to understand the hydrogeological structures.

Figure 5 is a schematic geological section through the study area. The main structural element is the Gorleben salt dome. It has rim synclines on both sides, which developed from the migration of salt into the salt structure.

Whilst the rim synclines are characterised by approx. 1 000 m to 2 500 m thick Mesozoic sequences, these are almost completely absent on top of the Gorleben salt dome, with the exception of a few thin Cretaceous erosional remnants.

The distribution and thickness of the Tertiary sequences are similar to the Mesozoic section. Diapirism of the salt means that only a few stratigraphic elements – mainly Eocene clays – are present and usually only in very thin layers. The Tertiary rocks have been dragged up on the flanks of the salt dome to form a circular area of uplift known as a “ring wall”. The Tertiary sediments exceed the normal thicknesses in the rim synclines. The stratigraphic sequence ranges from Early Tertiary (Paleocene) to Late Tertiary (Miocene).

This is followed by a stratigraphic gap which extends far into the Quaternary. Unlike the older sediments referred to above, the Quaternary sequence is fully developed over the salt dome.

4.2 Hydrostratigraphic classification of the sedimentary sequence

The Tertiary and Quaternary overburdens form a system of aquifers and aquitards with a maximum thickness of 430 m. This chapter first deals with a hydrostratigraphic classification of the sediments on the basis of their hydraulic properties, as well as discussing their lithology and their stratigraphic classification.

A tripartite division into aquifers ($k_f > 10^{-5}$ m/s), aquitards (10^{-5} m/s $\leq k_f < 10^{-7}$ m/s) and aquitards ($k_f \leq 10^{-7}$ m/s) is carried out on the basis of the main petrographic components and reflecting the hydrogeological mapping recommendation (Ad-Hoc Arbeitsgruppe Hydrogeologie 1997) (Fig. 6). Chapter 4.3 then goes into the hydrogeological structure of the area.

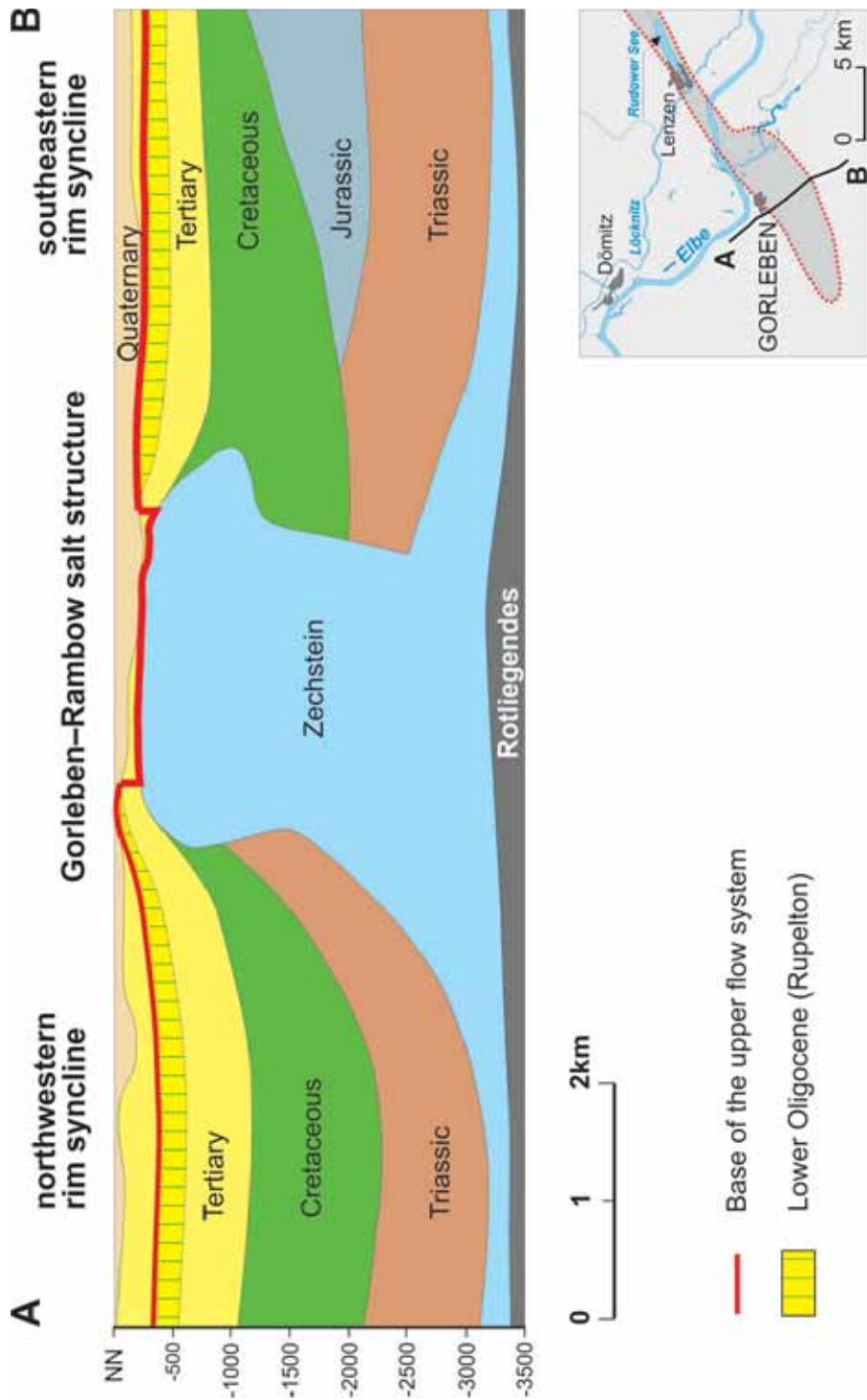



Figure 5: Simplified geological cross section through the Gorleben salt dome (according to ZIRNGAST in ALBRECHT et al. 1991)

		Stratigraphy		Petrography	Hydrogeology
Quaternary	Pleistocene	qN	Lower terrace Weichselian glaciation	Sand, gravely	
		qs	Saalian glaciation	Sand Silt Boulder clay	
		qhol	Holsteinian interglaciation	Silt, clayey, sandy	
		qL	Lauenburger-Ton-Komplex Elsterian glaciation	Clay, silty, sandy	
		qe	Elsterian glaciation	Sand Boulder clay	
		qpe	Bavel-Cromer- Komplex Menapian glaciation	Silt, peat clay, fine sand Sand, gravely	
Tertiary	Middle Miocene Pliocene		Hyatus		
	Lower Miocene	tmiBS2	Obere Braunkohlensande	Fine sand	
		tmiHT	Hamburg-Ton	Fine sand, silt, clayey Fine sand Clay, silt	
		tmiBS1	Untere Braunkohlensande	Fine sand	
	Oligocene	toloN	Upper Oligocene Neochattian	Fine sand, silt	
		toloE	Upper Oligocene Eochattian	Silt, sandy	
		tolu	Lower Oligocene Rupelton	Clay, silty	
Eocene - Paleocene	teo + tpa	Eocene - Paleocene	Clay, silt, sandy		

 Aquifer
 $k_f > 10^{-5}$ m/s

 Aquitard
 $k_f = 10^{-7} - 10^{-5}$ m/s

 Aquitard
 $k_f < 10^{-7}$ m/s

Figure 6: Summary of the hydrostratigraphic structural units of the overburden in the Gorleben study area.

4.2.1 Tertiary

The **Paleocene** and **Eocene** sediments consist mainly of silty-clayey aquitards. The clays more or less cover the whole study area.

The **Rupelton** (Rupelian Clay), a sequence of mainly clayey layers of Lower Oligocene age, are of major significance for groundwater flow in the Gorleben study area. Its top forms the base of the regional groundwater flow system investigated in the area. The

areally widespread aquitard is several tens of metres thick and separates the post-Lower Oligocene aquifer system from the generally highly saline deeper aquifers in the rim synclines.

In the rim synclines where the Tertiary sequence is generally fully developed, with the exception of the Pliocene and the Middle and Upper Miocene, the Rupelton is overlain by approx. 55 – 110 m thick low permeable silts and clayey silts of the **Eochattian**. These aquitards are only of minor significance for groundwater flow because of their low permeability.

The overlying approx. 25 m thick moderately permeable fine sands and silts of the **Neochattian** form a trans-regionally widespread major groundwater aquifer together with the overlying Lower Miocene **Untere Braunkohlensande** (Lower Brown Coal Sands).

The thickness of the Untere Braunkohlensande varies in the rim synclines between around 60 m to 130 m. Generally, permeability decreases with depth within the aquifer. The layers with the coarsest grain sizes – the so-called Graupelsande – occur as lenses in the upper part of the Untere Braunkohlensande. Localised lignite seams up to a few metres thick have also been penetrated in the Untere Braunkohlensande. The lignite seams have no economic or hydrogeological significance.

The Untere Braunkohlensande are overlain by the regionally widespread Lower Miocene **Hamburg-Ton** (Hamburg Clay) aquitard. The Hamburg-Ton can be divided up into three parts on the basis of its hydraulic permeability: a lower mainly clayey sequence, a middle fine-sandy sequence with varying proportions of silt and medium-grained sand, and an upper sequence consisting of clay and silt with varying proportions of sand. The thickness of the whole sequence varies from 60 m to > 100 m (KÖTHE et al. 2004). The Untere Braunkohlensande and the Hamburg-Ton primarily occur in the northwest rim syncline and the southwest end of the Gorleben salt dome. Occurrences southwest of the salt dome are very patchy because of the Quaternary erosion.

The **Obere Braunkohlensande** (Upper Brown Coal Sands) which normally overly the Hamburg-Ton are only present in the form of relicts in the study area. They were almost completely eroded during the Quaternary. The main area of distribution is in the centre of the northwest rim syncline. Compared to the Untere Braunkohlensande, these sediments have much lower permeability because of the higher fraction of fine-grained sediments.

4.2.2 Quaternary

The Quaternary sediments overlie the Tertiary sequence with a hiatus of approx. 14 million years. The distribution and depositional conditions of the sediments are no longer dominated by underlying halokinetic movements, but by erosive, accumulative and ice-tectonic processes associated with the Nordic continental glaciation. In general, the Quaternary sedimentary sequence consists of interbedded meltwater sands, glacial tills and basin sediments (clays, silts and fine sands).

In the Gorleben study area, the Quaternary sequence begins with sediments which are unusual in North Germany: a small, approx. 3 km² deposit of Pre-Elsterian sands is preserved above the western part of the Gorleben–Rambow salt structure in a fossil subsidence trough. The sands were possibly deposited in a river system which flowed into the North Sea from the area lying to the east of the Gorleben study area. Sedimentation in the subsidence trough ended with a generally low permeable interbedded sequence of interglacial limnic silts, muds and fine sands.

The main period of sedimentation in the Quaternary began with the **Elsterian Glaciation**, and is closely associated with glacial and meltwater channel erosion forms, and the Gorleben channel in particular. The channels are typically filled with highly permeable channel sands with usual thicknesses of approx. 10 m to 50 m.

Elsterian glacial tills, which were originally widespread but today mainly occur only in the form of erosional remnants within Quaternary channels, can be present at the base of the channels.

The upper sequence filling the channels consists primarily of low permeable silts and clays of the **Lauenburger-Ton-Komplex** (Lauenburg Clay Complex). This sequence occurs in places in compact homogeneous form consisting of thick clay/silt packages, whilst in other places, it is characterised by rapid lateral and vertical changes of silty, clayey and sandy facies. Its thickness varies between approx. 5 – 25 m at the margins of the channel and 50 – 90 m in the centre.

The topographic depressions of the incompletely filled channels then became depositional areas for the silts and muds laid down in the following **Holsteinian Interglacial**. These sediments often have a notable olive-green colour and were deposited in limnic to limnic-fluviatile environments. The dominant low permeable silts and clay silts are mainly of importance for geological reasons. Because of their characteristic, easily datable pollen spectrum, these sediments form a marker horizon, which simplifies classification of the glacial sediments in the overlying and underlying sequences whose stratigraphic

identification is either difficult or impossible because of their in part large proportion of redeposited sediments. These sediments are not particularly significant hydrogeologically but are mainly assigned to the Weichselian and Saalian aquifers because of their minor thickness and patchy distribution.

Unlike the Elsterian and Holsteinian sequences, which are restricted to the channels, the Saalian deposits are spread throughout the study area. The ice sheet crossed the area of investigation three times during the **Saalian Glaciation**. This was associated with the deposition and glacial deformation of highly permeable meltwater sands, glacial tills and glacio-limnic silts/clays, which interfinger over short distances. The glacial till, silt and clay aquitards only form approx. one third of the total volume of Saalian sediments.

The advances of the ice sheet caused widespread glacio-tectonic deformation of the underlying beds, and particularly the upper part of the Lauenburger-Ton-Komplex and the Holsteinian sediments as well as the Hamburg-Ton in areas with shallow Tertiary sequences. The compressional tectonics extended approx. 40 m to 60 m beneath the base of the Saalian, up to a maximum of 140 m below ground level. The glacio-tectonic deformation is particularly visible and deep in the compressional area of the H \ddot{o} hbeck and its poorly definable southern extension (K \ddot{O} THE et al. 2004).

The main elements of today's morphology, i.e. the geest "islands" and the glacial valley of the Elbe, were already recognisable at the end of the Saalian Glaciation. Eemian sediments have only been penetrated in one borehole. These sediments consisted of fine-grained silts, which have not been dealt with separately because of their localised nature.

The top of the Pleistocene sequence consists of fluvial, highly permeable sands and gravels of the **Weichselian Lower Terrace**, which is present throughout the study area and masks an only slightly differentiated Saalian relief. Thin and low permeable flood plain and fluvial sediments were deposited in the lowlands from the end of the Weichselian Glaciation into the Holocene. The youngest deposits outside of the depressions are the highly permeable and very homogeneously structured aeolian sand sheets and dune fields. This is where most present-day groundwater recharge takes place (cf. Chapter 4.3).

4.3 Hydrogeological structure

The hydrogeological structure of the study area is described in the following, on the basis of Figures 7 to 9 and four vertical cross sections (Appendix 1).

The sediments in the Gorleben area can be roughly divided into an **upper** and a **lower aquifer**. Figure 7 shows the spatial distribution of these two aquifers along a vertical section (B – B', Appendix 1), which crosses the Gorleben salt dome NW-SE. The Weichselian and Saalian deposits throughout the study area consist of a sequence of highly permeable sands as well as low permeable basin silts and glacial tills. Sediment types change rapidly over short distances, which makes the establishment of clear boundaries impossible, despite the large number of exploratory drillings. Because sandy deposits are dominant, the Weichselian and Saalian sediments can be bundled together and considered as a uniform, laterally and vertically strongly interbedded inhomogeneous upper aquifer.

In the rim synclines, the Untere Braunkohlensande and the Eochattian form a much more homogeneous lower aquifer compared to the upper aquifer. This is bounded at the top by the Hamburg-Ton (Hamburg Clay) aquitard. In the channel structures, and the Gorleben channel in particular, in the areas where the Untere Braunkohlensande and Hamburg-Ton have been eroded, the positions of the lower aquifer and the overlying aquitard are occupied by the Elsterian channel sands and the Lauenburger-Ton-Komplex.

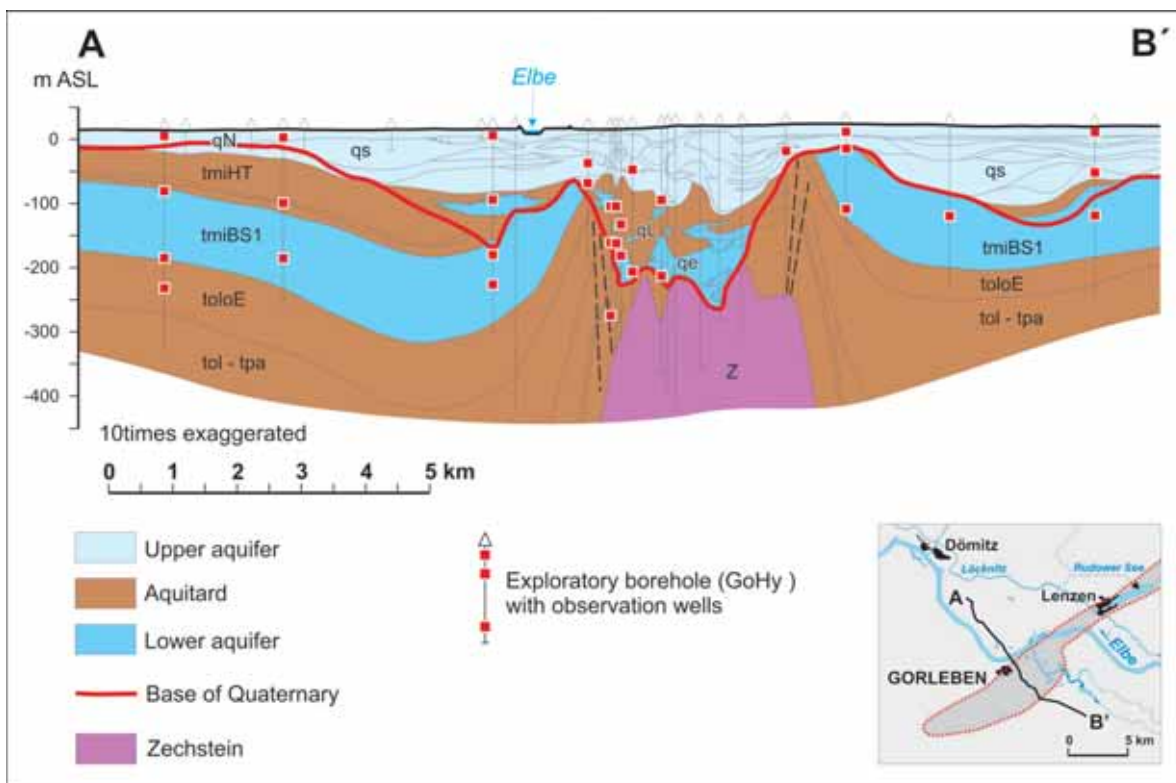


Figure 7: Aquifer subdivision in the overburden of the Gorleben salt dome

In detail, the study area can be divided up into the following four hydrogeological and geological units:

1. The rim synclines to the northwest and southeast of the salt structure
2. The Elsterian Gorleben channel
3. The subsion trough over the western part of the Gorleben salt dome
4. The transition zone between the Gorleben and Rambow salt domes

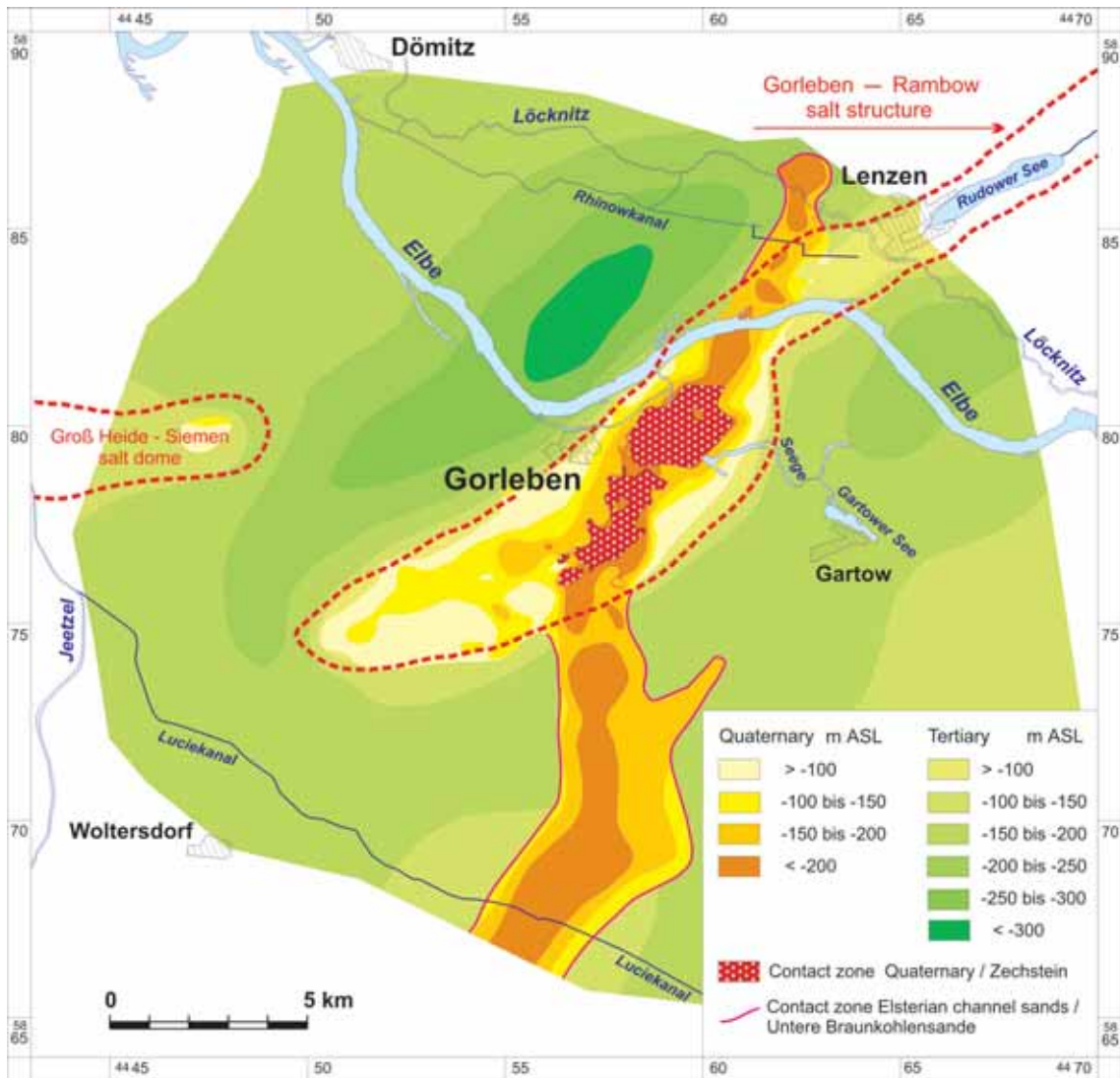


Figure 8: Base of the lower aquifer (according to KÖTHE et al. 2004)

1. The **rim synclines** in the northwest and southeast of the Gorleben–Rambow salt structure developed as a consequence of salt movement towards the salt structure. This led to the formation of a long, closed trough in the northwest, whose axis runs NE-SW parallel to the salt structure.

The base of this lower aquifer is in the centre of this trough, at a depth of approx. -330 m above sea level. At the northwestern edge of the study area, near Dömitz, the base of the lower aquifer is at > -150 m above sea level (Fig. 8). On the flanks of the salt dome, where a circular uplift or ring wall of Tertiary sediments has formed, the base of the aquifer throughout lies at > -100 m above sea level (vertical section B – B', Appendix 1).

The southeastern rim syncline is smaller than the northwestern rim syncline. The base of the aquifer in the centre of the trough in the southwest of the Rambow salt dome is much shallower, at around -220 m above sea level.

The lower aquifer in the northwestern rim syncline occupies the full thickness of the Untere Braunkohlensande, with a thickness of approx. 100 to 120 m. It is covered throughout the area by the Hamburg-Ton, whose thickness varies considerably. The Hamburg-Ton and Untere Braunkohlensande were eroded to a varying degree by the formation of the Elsterian channel structures. In these areas, the Lauenburger-Ton-Komplex replaces the Hamburg-Ton as the aquitard separating the aquifers, so both aquitards are present throughout virtually all of the northwestern rim syncline. The only small gaps are in the area to the west of Gorleben, on top of the Groß Heide–Siemen salt structure, and at the northwestern edge of the study area around Dömitz (Fig. 9).

The Hamburg-Ton and parts of the Untere Braunkohlensande are eroded over large parts of the southeastern rim syncline. They are replaced here by Elsterian channel sands, which are partially overlain by the Lauenburger-Ton-Komplex. Unlike in the northwestern rim syncline, there are major gaps in the two aquitards, so the upper and lower aquifers come into direct contact.

2. A system of elongated meltwater channels developed during the Elsterian Glaciation. The largest contiguous structure is the Gorleben channel, which cuts NNE-SSW through the whole study area. Other channel structures are located in the southeastern rim syncline around Gartow and west of Gorleben, in the northwestern rim syncline. The areal extent of the Lauenburger-Ton-Komplex in Figure 9 highlights the location of these channel structures.

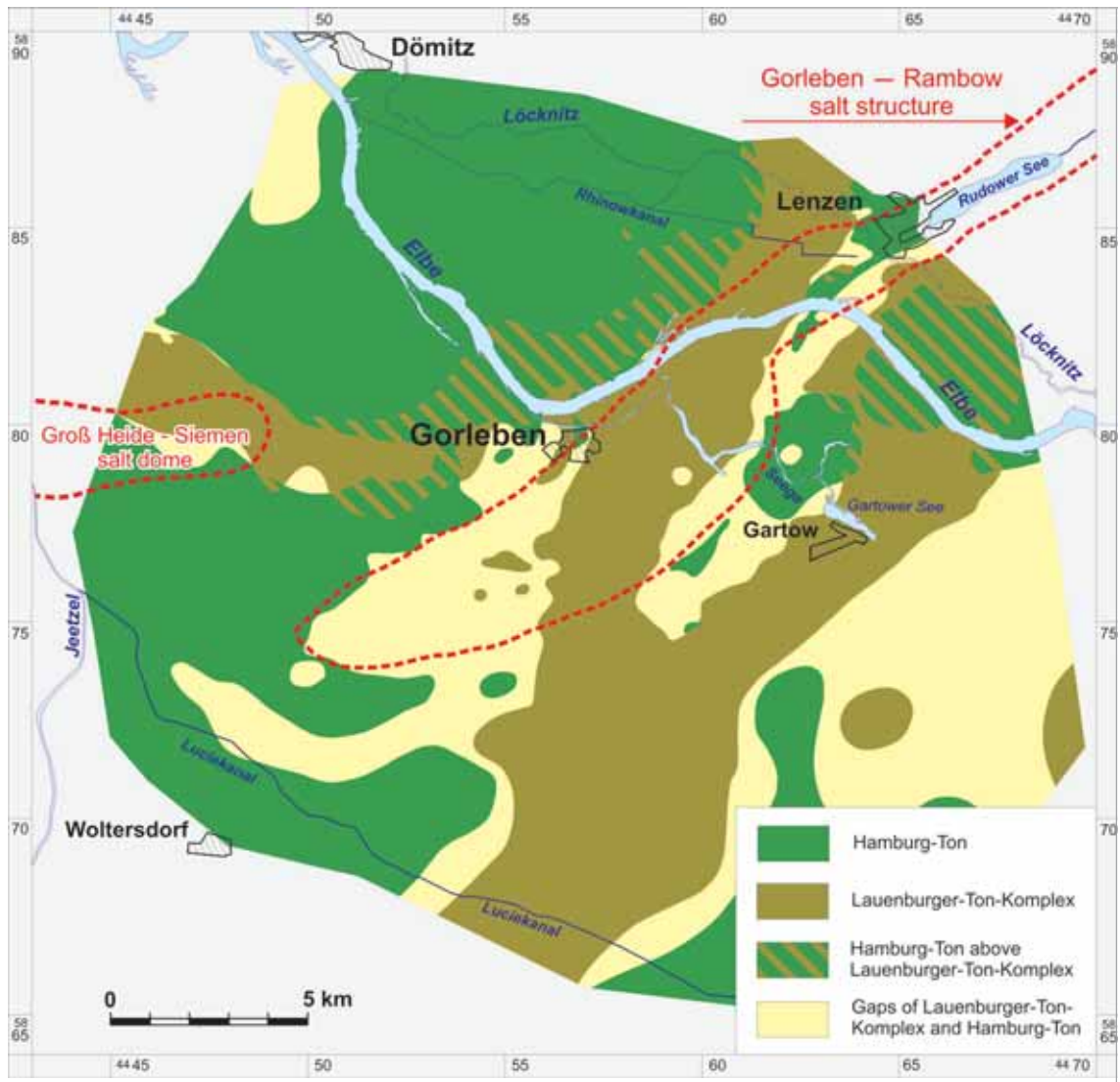


Figure 9: Distribution of the Hamburg-Ton and Lauenburger-Ton-Komplex aquitards (according to KÖTHE et al. 2004).

The Gorleben channel cuts across the Gorleben salt dome over a length of around 7 km (vertical cross section D – D', Appendix 1). In the lowest parts of the channel at depths below -200 m above sea level, the low permeable Tertiary clays, which probably completely covered the salt dome at the beginning of the Pleistocene, have been fully eroded in an area that is approx 5 km long and approx. 1 km - 1.5 km wide (Fig. 8). Elsterian meltwater sands directly overlie the cap rock and in parts even the evaporite rocks in this area. The lowest sediments in the deepest parts of the channel consist of gravelly medium-coarse sands grading upwards into finer grained sands. These channel sands are overlain by the primarily low permeable silts and clays of the Lauenburger-Ton-Komplex (KLINGE et al. 2002). The drilling results indicate the

continuous presence of this aquitard in the channel structure above the salt dome, which means that there is no direct contact between the upper and lower aquifers in this area. However, the upper parts of the Lauenburger-Ton-Komplex have been strongly disturbed by ice tectonics in some areas. In addition, long-term pumping tests as well as local salt water highs above the salt dome (cf. Chapter 7.1.2) indicate areas of localised higher vertical and lateral permeability. The significance of this is discussed in detail in Chapter 10.

The Gorleben channel continues in the rim synclines to the north and south of the salt dome. The Untere Braunkohlensande were almost completely eroded here and are replaced by Elsterian channel sands, which are laterally hydraulically connected at the flanks of the channel by the trans-regionally widespread Untere Braunkohlensande (Fig. 8).

3. The overburden above the **western part of the Gorleben salt dome** has a special hydrogeological structure. The Zechstein evaporite sequence including the cap rock is extensively overlain here by low permeable pre-Miocene clays, although with varying thicknesses and deformed bedding in parts as a result of subsidence. The Tertiary clays here are overlain by Menapian Glacial sands, which are themselves overlain by silts and peat muds of the Bavelian and Cromerian Complex. The latter were deposited in a **subsidence trough** as limnic sediments in a shallow lake. Overall, these sediments are equivalent to the lower aquifer in the Elsterian sediments of the Gorleben channel, with which they are hydraulically connected in the east of the trough. In other areas, the lower aquifer in the subsidence trough is laterally bounded by the ring wall of clays and silts of the Lower Oligocene, which are relatively shallow at this point. This is why there is no hydraulic connection to the lower aquifer of the rim synclines (vertical section D – D', Appendix 1). Unlike the situation in the Gorleben channel, the lower aquifer is only weakly separated from the upper aquifer above the western salt dome, where the aquitard usually consists of glacial till and silts.
4. In the **transition zone between the Gorleben and Rambow salt domes** between the Rudower See lake and the Elbe, the diapiric rise of the salt led to the formation of a crestal trench accompanied by numerous en echelon faults and strong block faulting of the overburden (ALBRECHT & ZWIRNER 1999; vertical cross section C – C', Appendix 1). The Zechstein evaporite sequence is covered throughout by thick, low permeable Oligocene and Eocene Tertiary clays. However, these clays are cut by numerous faults which reach down into the evaporite sequence and which are potential water migration paths. Nevertheless, compared to the Gorleben salt dome south of the Elbe, the cap rock is unusually thin, at only 1.5 to 4 m thick. This means that,

because of the depth and the continuous relatively thick clay cover, there has been no major salt subsidence for a long period of time. It also indicates that the numerous faults in the clays have had hardly any hydraulic effect.

The upward movement of the salt means that the thickness of the Untere Braunkohlensande is much thinner over the salt structure compared to the rim synclines. The overlying Hamburg-Ton was largely eroded during the Quaternary because of the elevation of the salt dome so the lower and upper aquifers are now locally in direct hydraulic contact. With respect to the regional groundwater flow within the Elbe glacial valley, which runs approximately parallel to the present day Elbe, there is a much lower cross sectional area of flow compared to the rim synclines. The salt structure, which runs orthogonal to the Elbe, is therefore in figurative terms a partial barrier bar to regional groundwater flow.

5 Hydraulic properties

Comprehensive investigations were conducted as part of the hydrogeological investigation programme to determine the hydraulic properties of the sediments. These investigations primarily involved:

- grain size analysis of samples from cores and both shafts of the exploration mine
- permeability tests at drilling cores
- evaluation of geophysical well logs
- short-term pumping tests in groundwater observation wells
- a total of five long-term pumping tests involving a great deal of technical input

Long-term pumping tests enable the hydraulic parameters to be determined and also support hydrogeological and structural interpretations.

This chapter presents the results of the hydraulic permeability investigations. Because of the overall importance of the long-term pumping tests, the objectives and results of these pumping tests will be presented first in a separate section. The following subchapters then discuss the other evaluation results.

5.1 *Long-term pumping tests*

5.1.1 Objectives

Five long-term pumping tests were carried out to clarify the hydrogeological interrelations between the lower and upper aquifers and to quantify their hydraulic properties. The pumping tests had three main objectives:

1. To determine the relevant hydraulic material properties (transmissivity, hydraulic conductivity and storage coefficient)
2. To investigate the hydraulic effect of the aquitards (Hamburg-Ton-Komplex and Lauenburger-Ton-Komplex) separating the two aquifers
3. To identify geohydraulically effective connections between the lower aquifer and other aquifer systems, particularly the connection between the Elsterian channel sediments and the Untere Braunkohlensande to the north of the Elbe.

Each pumping test above the Gorleben salt dome was named after the location of the production well: “Weißes Moor 1”, “Weißes Moor 2”, “Gorlebener Tannen”, and “Meetschow” (Fig. 10). The pumping test to the north of the Elbe was named after the study area “Dömitz-Lenzen”.

Table 1 summarises the most important technical data from the long-term pumping tests. The production wells were generally fully screened. The pumping phase of the pumping tests lasted approx. 3 weeks in each case at constant production rates. The recovery of the water table after shutting off the pumps was observed for a similar length of time. The pumping tests were each preceded by a 24-hour preliminary test to check the technical systems under operating conditions.

During the long-term pumping tests, the water levels in the tested aquifers as well as in the overlying and underlying aquifers were observed.

This was carried out by installing nine observation wells in the lower aquifer in each case, and up to nine more observation wells in the upper aquifer. The observation wells were located concentrically around the well, at distances of around 10 m, 200 m and 500 m. The observation wells were spaced at angles of approx. 120 ° and each group was offset from the next. In addition, several dozen observation wells of the existing monitoring network were observed in different layers during all of the pumping tests.

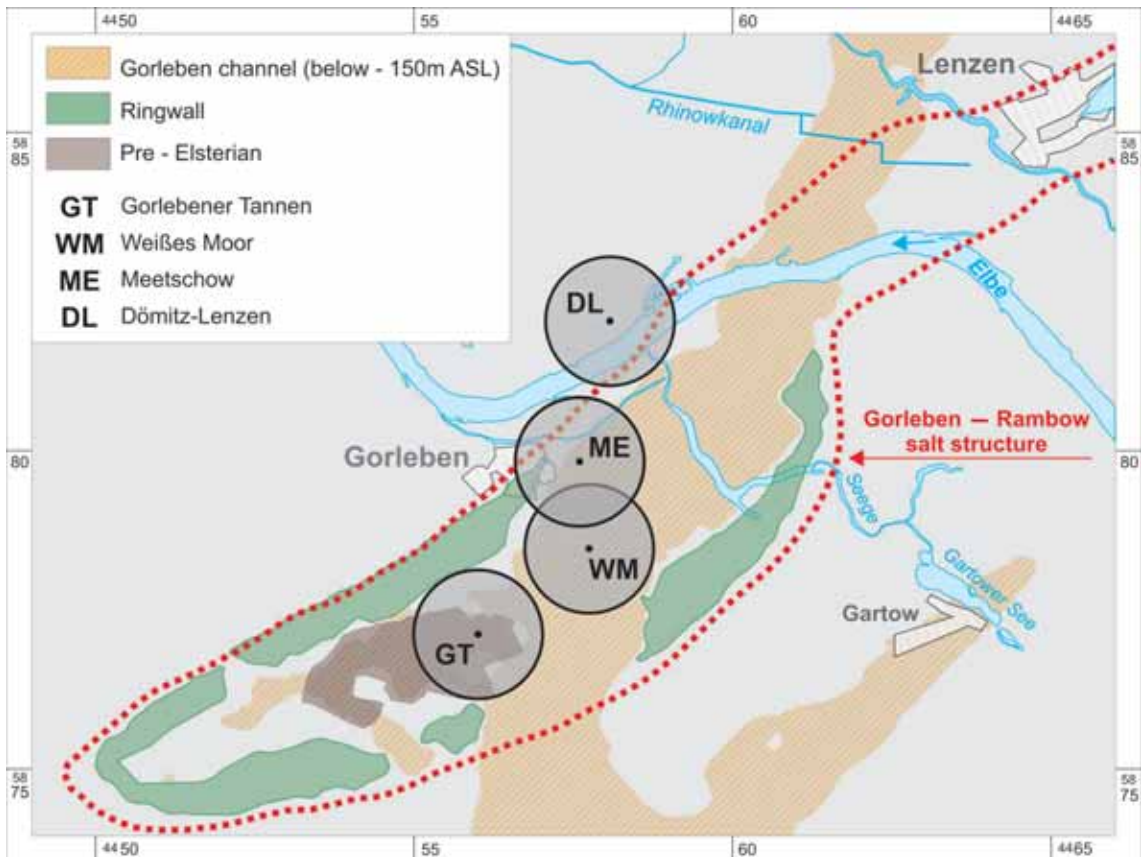


Figure 10: Location of the long-term pumping test sites

Table 1: Technical data on the long-term pumping tests

Name	Abbreviation	Aquifer (stratigraphy)	Production well depth [m BGL]	Screen length [m]	Production rate [m ³ /h]
Weißes Moor 1	WM 1	Upper (qs)	136.5	43.5	98.1
Weißes Moor 2	WM 2	Lower (qe)	250.2	26.4	29.9
Meetschow	MS	Lower (qe)	236.0	28.0	90.0
Gorlebener Tannen	GT	Lower (qpe)	245.0	70.0	99.5
Dömitz-Lenzen	DL	Lower (qe)	225.0	82.0	100

Whilst the observation wells in the lower aquifer were specially installed during the pumping test to observe the drop in pressure in the proximity of the production well, the observation wells in the upper aquifer were installed to provide information on the extent to which the, in some cases, high drawdown within the lower aquifer close to the production well, affected the water levels in the upper unconfined aquifer, and to provide information on any vertical permeability within the aquitards separating the aquifers.

The data from the observation wells in the area south of the Elbe were recorded with data loggers and by manual logging. The data from the Dömitz-Lenzen pumping tests were recorded on electronic systems. Climatic data were continually recorded to correct the measured data for fluctuations in air pressure. The water levels in the Elbe as the main regional water course have a major effect on the groundwater levels in the surrounding aquifers – particularly the shallow aquifers. The water levels of the Elbe at Lenzen, Gorleben and Dömitz were therefore also taken into consideration.

The salinity of the water produced during the pumping tests was measured by continuous conductivity measurements and occasional water sampling. No unusual changes were observed, in general. The salt concentration ranged from approx. 0.16 g/l TDS (Total Dissolved Solids) in the upper aquifer to 180 g/l TDS in the lower aquifer within the Gorleben channel.

The water was pumped into the Elbe with the authorisation of the responsible authorities.

5.1.2 Evaluation method

The hydraulic parameters transmissivity and storage coefficient were determined mainly using the type curve method according to THEIS (1935). This involves considering the drawdown during the production phase and the recovery after the pumping phase. Evaluation was carried out manually for the pumping tests located to the south of the Elbe. The **AquiferWin32** (Environmental Simulations Ltd.) and **Interpret/2** (Scientific Software Intercomp) analysis software applications were used to analyse the Dömitz-Lenzen pumping test.

The THEIS method is based on several assumptions, including a constant density and salinity distribution within the groundwater. However, the salt concentrations within the groundwater vary over three orders of magnitude from around 0.2 g/l TDS to saturated brine with approx. 320 g/l TDS at the base of the Gorleben channel. Modelling the Weißes Moor 2 and Dömitz-Lenzen pumping tests using the ROCKFLOW (KRÖHN 1991) and SUTRA (VOSS 1984) software revealed that the salt concentration of the groundwater only has a minor effect on the draw down behaviour (WOLLRATH & ARENS 1992). This means that the assumption of a constant density distribution is a viable simplification for the purpose of the evaluation.

The influence of the strong fluctuations in the water levels of the Elbe was clearly noticeable in the upper aquifer in the groundwater levels measured in observation wells located close to the Elbe. This also applies to a lesser extent to the lower aquifer. This superimposed effect on the draw down and recovery curves decreases as the distance from the Elbe increases. Corrections were not required for the pumping test areas to the south of the Elbe because of the minor fluctuations in Elbe water levels as well as the larger distance away from the river. However, because the Elbe was in flood some of the time during the Dömitz-Lenzen pumping tests, a correction factor for distance to the Elbe was determined and used to correct the groundwater levels (KLINGE et al. 2004).

5.1.3 Results

5.1.3.1 Hydraulic parameters

The hydrogeological parameters transmissivity (T), hydraulic conductivity (k_f) and storage coefficient (S), determined by the analytical THEIS method (THEIS 1935) for the drawdown and recovery are listed in Table 2.

Table 2: Pumping test results: hydraulic parameters

	Aquifer (stratigraphy)	Transmissivity [m ² /s]		Hydraulic conductivity k_f [m/s]		Storage coefficient	
		min	max	min	max	min	max
WM 1	Upper (qs)	2 x 10 ⁻²		3 x 10 ⁻⁴	4 x 10 ⁻⁴	5 x 10 ⁻⁴	8 x 10 ⁻⁴
WM 2	Lower (qe)	1 x 10 ⁻³	2 x 10 ⁻³	2 x 10 ⁻⁵	5 x 10 ⁻⁵	3 x 10 ⁻⁴	9 x 10 ⁻⁴
MS	Lower (qe)	7 x 10 ⁻⁴	2 x 10 ⁻³	2 x 10 ⁻⁵	7 x 10 ⁻⁵	1 x 10 ⁻⁴	8 x 10 ⁻⁴
GT	Lower (qpe)	3 x 10 ⁻³	1.2 x 10 ⁻²	4 x 10 ⁻⁵	1.7 x 10 ⁻⁴	2 x 10 ⁻⁴	8 x 10 ⁻⁴
DL*	Lower (qe)	2 x 10 ⁻²	3.4 x 10 ⁻²	2.1 x 10 ⁻⁴	3.6 x 10 ⁻⁴	1.4 x 10 ⁻³	2.6 x 10 ⁻³
	Lower (tmiBS1)	9.5 x 10 ⁻³	1.1 x 10 ⁻²	1 x 10 ⁻⁴	1.2 x 10 ⁻⁴	8.4 x 10 ⁻⁴	1.2 x 10 ⁻³

*geometrical mean for minimum and maximum influence of the Elbe

These values lie in the expected range for aquifers with sandy lithologies. The hydraulic conductivity values for the Saalian glacial/fluviol sands in the upper aquifer at Weißes Moor are higher by a factor 6 - 20 than the Elsterian meltwater sands. The hydraulic conductivity k_f for the Elsterian channel sands in Dömitz-Lenzen are around one order of magnitude higher than those south of the Elbe.

The vertical hydraulic conductivity of the aquitard (Lauenburger-Ton-Komplex) between the two main aquifers in the Gorleben channel south of the Elbe is $< 5 - 10 \times 10^{-9}$ m/s from a numerical simulation of the pumping test (HOFFMANN & RADELFAHR 1986). A corresponding evaluation of the Dömitz-Lenzen pumping test was not possible because of the flooded state of the Elbe.

5.1.3.2 Spatial drawdown behaviour over time

The **Weißes Moor 1** pumping test was mainly carried out to acquire hydraulic data. The cone of depression at the end of the extraction phase in the unconfined upper aquifer was remarkably small, with a radius of approx. 1 000 m. It was almost radially symmetrical and had no hydraulically restricted boundaries (Fig. 11).

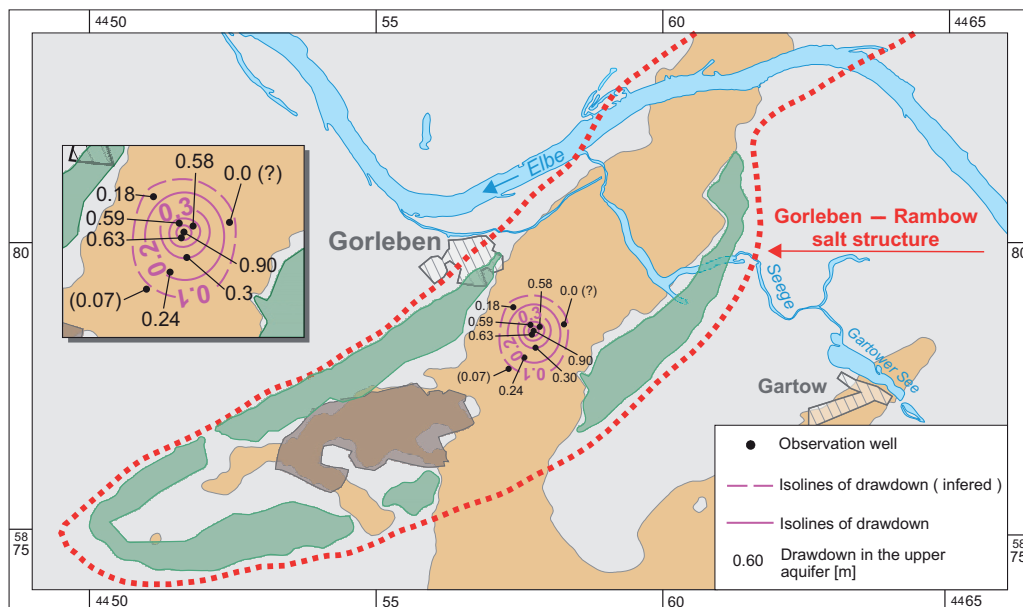


Figure 11: Drawdown at the end of the pumping test phase – Weißes Moor 1 pumping test

The main objective of the **Meetschow** and **Weißes Moor 2** pumping tests was to investigate any possible hydraulic connection between the upper and lower aquifers in the Gorleben channel, i.e. the vertical permeability of the Lauenburger-Ton-Komplex or any hydraulic short circuits that may be present. Both tests revealed that even after drawdowns of several metres and pumping for approx. three weeks, there was no clearly measurable drawdown in the upper aquifer. This means that highly effective hydraulic short circuits between the aquifers are unlikely, at least in the vicinity of the wells. However, these findings contradict other investigation results as discussed in detail in Chapter 10.

The cone of depression in both pumping tests was almost symmetrical in a SW-NE direction, i.e. the shape corresponded to the structure of the Gorleben channel (Figs. 12 and 13). This means that the margins of the channel have low permeability. The maximum extent of the drawdown in the channel axis was more than 6 km in each direction during the Meetschow pumping test. Drawdown probably extended northwards into the area to the north of the Elbe. However, because the Elbe formed the boundary to the former German Democratic Republic when the pumping tests were carried out, it was not possible to carry out any measurements to the north of the river. In addition, the Meetschow pumping test also had a minor measurable effect in the pre-Elsterian subsrosion trough. The extent of the drawdown during the Weißes Moor 2 pumping test was much smaller because of the lower production rate. No effect on the subsrosion trough was observed.

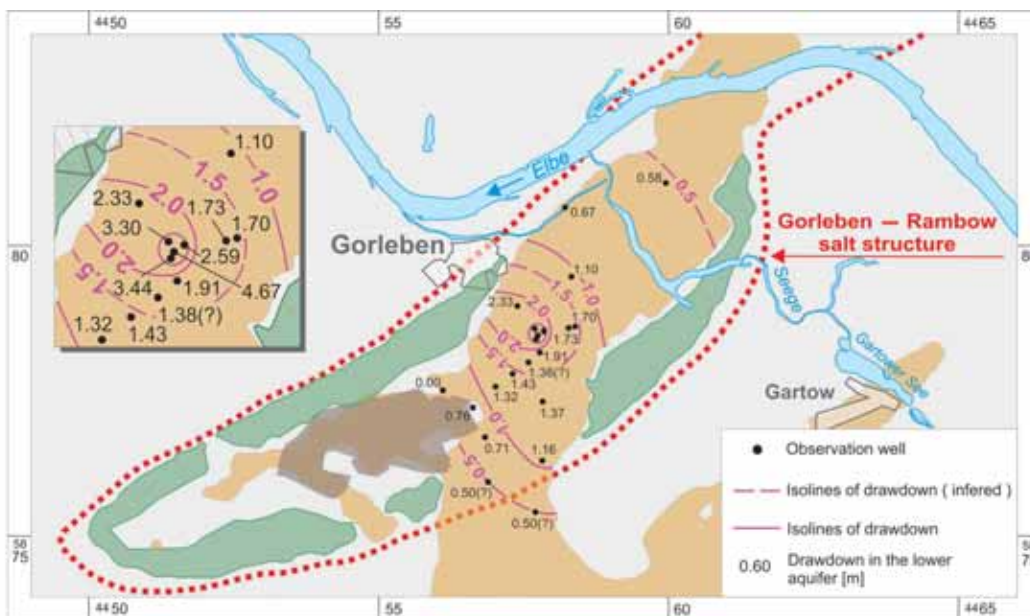


Figure 12: Drawdown at the end of the pumping test phase – Weißes Moor 2 pumping test

The main objective of the **Gorlebener Tannen** pumping test was to investigate the lateral hydraulic connection between the Gorleben channel and the pre-Elsterian subsrosion trough, which extends above the southwestern part of the salt dome. The well was screened in the pre-Elsterian sands but lies at the transition zone between the subsrosion trough and the channel. The main drawdown occurred within the trough, where the cone of depression reflected the shape of the structure (Fig. 14). The maximum drawdown extent was approx. 4 km and occurred in the southwest of the trough. The drawdown extended approx. 3 km northeast in the Gorleben channel, approximately as far as the village of Gorleben. This confirms hydraulic contact between the subsrosion trough and the channel as already indicated by the Meetschow pumping test. However, transmissivity must be lower in the transition zone between the two structures because the drawdown only continued to a lesser extent and there is a narrow space between the lines representing the same level of drawdown.

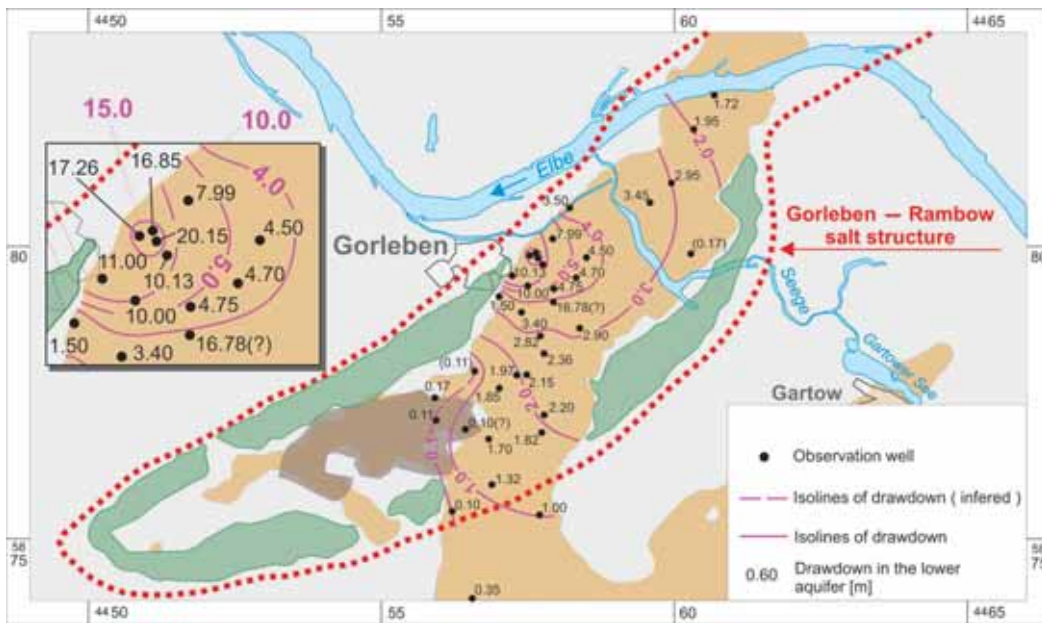


Figure 13: Drawdown at the end of the pumping test phase – Meetschow pumping test

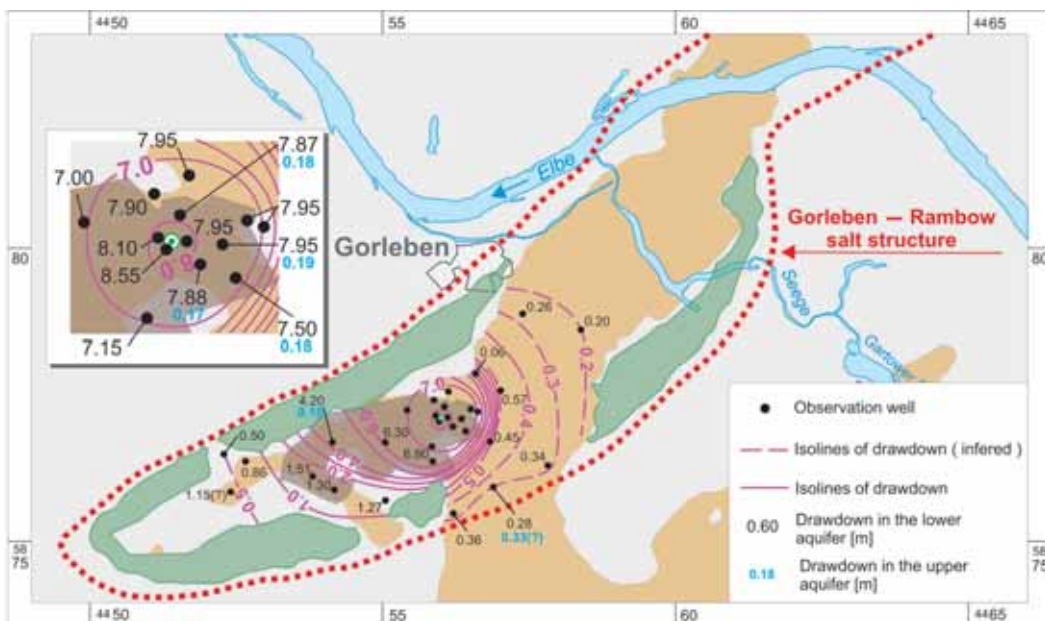


Figure 14: Drawdown at the end of the pumping test phase – Gorlebener Tannen pumping test

Another objective of the Gorlebener Tannen pumping test was to clarify the vertical connection between the aquifers separated by glacial till within the subsidence trough. The results of the pumping test revealed that a vertical connection is present. Observation wells in the upper aquifer close to the production well in particular reacted to the extraction of

water in the lower aquifer. Drawdown ranged from 0.16 – 0.19 m. The glacial till is therefore a less effective barrier between the two aquifers than the Lauenburger-Ton-Komplex. Confirmation of the hydraulic contact between the aquifers here is consistent with the finding that freshwater lies at a greater depth in the subsidence trough than in the Gorleben channel (cf. Chapter 7.1.2). It appears that the freshwater percolates into the trough from above, particularly because this area is a recharge zone with downward groundwater flow.

The observation wells in the cap rock reacted during this pumping test with a clear drawdown, just as they did during the Meetschow pumping test. This shows that the cap rock is in direct hydraulic contact with the lower aquifer.

The objective of the **Dömitz-Lenzen** pumping test was to investigate the hydraulic connection of the northwestern rim syncline to the Gorleben channel. The main aim was to determine the presence of any hydraulic contact between the Untere Braunkohlensande and the Elsterian channel sands in the vicinity of the northwestern ring wall above the salt dome. The reaction of the observation wells in the Gorleben channel to the south of the Elbe was particularly important to clarify this point. Another aim was to provide additional evidence of the direct hydraulic connection between the Gorleben channel and the Untere Braunkohlensande in the northwestern rim syncline as already indicated by the drilling results (cf. Chapter 4.3).

Because of a strong rise in the water level of the Elbe, it was not possible to quantify the possible impact of the extraction of water from the lower aquifer on the water levels in the upper aquifer. The maximum reach of the drawdown within the lower aquifer after approx. three weeks of production was 7 km (Fig. 15) as recorded within the rim syncline, i.e. to the northwest and northeast. The extent of the drawdown towards the southeast, i.e. in the direction of the ring wall, was much lower at approx. 2.5 – 3 km, with the drawdown also extending into the Gorleben channel to the south of the Elbe.

The drawdown in the Gorleben channel against time and distance indicates that a local hydraulic connection exists above the northwestern ring wall, between the lower Elsterian channel aquifer and the lower aquifer in the northwestern rim syncline. As a result of this connection, the drawdown can already be observed at an early stage south of the Elbe during the pumping test in the Gorleben channel. The pressure drawdown in the northern rim syncline within the Gorleben channel extended along the channel axis from northeast to southwest as the pumping test progressed. This confirms that the Gorleben channel and the Untere Braunkohlensande within the northwestern rim syncline form a uniform aquifer. It also indicates that the permeability of the ring wall zone is much lower than at the northern end of the Gorleben channel (KLINGE et al. 2001).

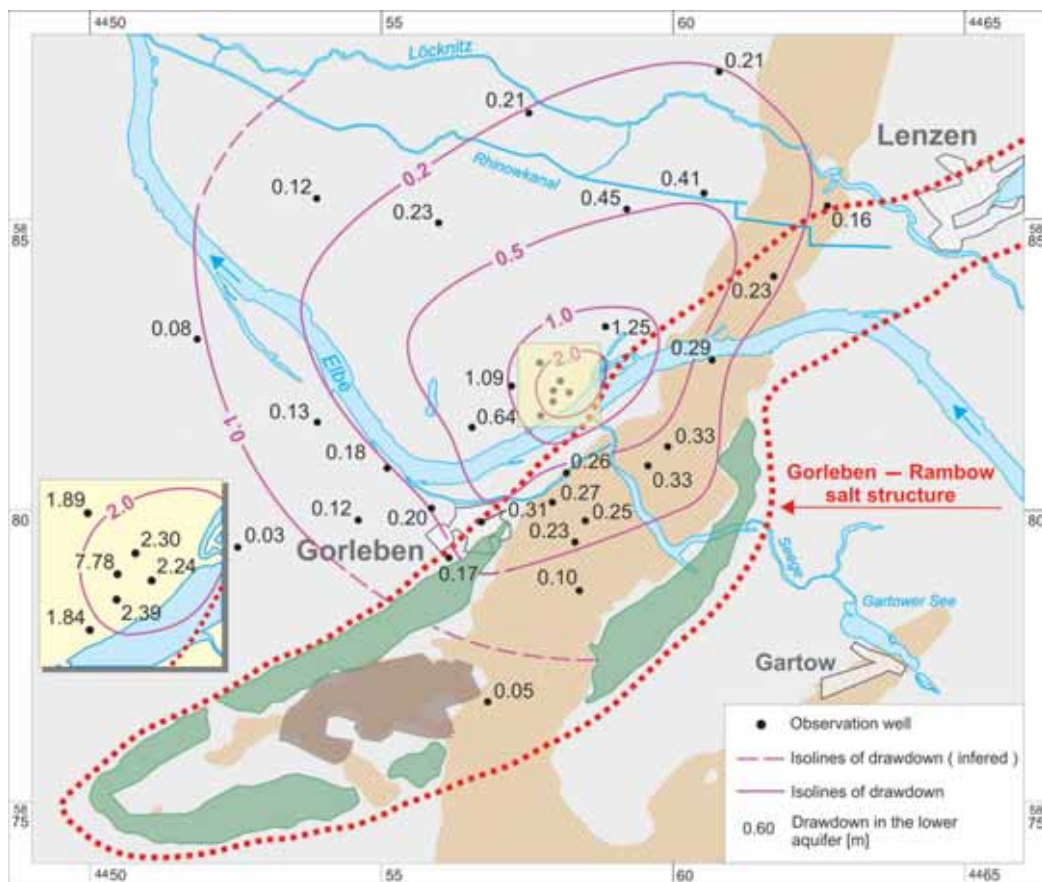


Figure 15: Drawdown at the end of the pumping test phase – Dömitz-Lenzen pumping test

Numerical modelling applying PM Win 5.1.7 (Processing Modflow; CHIANG & KINZELBACH 1991) confirms this assumption. The modelling shows that the actual drawdown within the Gorleben channel can only be successfully matched by assuming partial permeability of the ring wall (GEO-DATA 2001). Transmissivity above the ring wall needs to be lower than at the northern channel exit in the model.

5.2 Hydraulic conductivity

In addition to the aforementioned results of the long-term pumping tests, the hydraulic conductivities are also determined on the basis of grain size analysis of core samples, direct laboratory permeability measurements on cohesive sediments, as well as short-term pumping tests in groundwater observation wells.

Approx. 950 sieve analyses of sediment samples are available. They were used to calculate the hydraulic conductivities using the BEYER (1964), HAZEN (1893) and ZIESCHANG (1961) calculation methods. These mutually comparable empirical methods were derived from the comparison of pumping test results with grain size measurements. Empirical values of this kind are naturally only approximations.

In addition to the k_f calculations from grain size analysis, 50 samples of cohesive sediments from 18 cores were subjected to water permeability measurements in triaxial cells in accordance with DIN 18130 (WD tests).

Short pumping tests lasting approx. four hours were carried out in connection with the well development of the observation wells and the initial water sampling in 75 groundwater observation wells. With the use of only a minor amount of additional equipment, these short pumping tests could be used to acquire more information on the hydraulic properties of the aquifer in the screened zone. These pumping tests were evaluated using a method according to STRELTSOVA (1988), which makes allowance for errors associated with the skin effects in the observation wells and the potential influence of short screens.

The methods used differ in principle with respect to the representativity of the recorded values. **Sieve analysis** was carried out on core samples. Care was taken to select representative samples, and a relatively large number of samples were analysed to avoid randomness. Nevertheless, the parameters determined in this way are only viable for the immediate proximity of the sample location, particularly in heterogeneous sediments such as the Quaternary deposits.

This is also true to a limited extent for the **short-term tests** in the groundwater observation wells. The effective radius of these pumping tests is limited to the aquifers within only a few metres or decametres of the screen (screen length: 2 m) at the observation well.

In the **long-term pumping tests**, the whole thickness of the lower aquifer was tested, in each case within a radius of several kilometres around the production well. The k_f value derived from the transmissivity value is therefore a large-scale integral value for the permeability of the section between the production well and the observation well over the whole thickness of the aquifer.

Figure 16 is a synopsis of the k_f values determined using different evaluation methods. The figure shows in each case the range of the hydraulic conductivities at a logarithmic scale, and their geometrical means. This figure shows that the hydraulic conductivity coefficients determined for the main aquifer from the short-term pumping tests and sieve analyses in the Saalian, Elsterian and pre-Elsterian sands (q_s , q_e and q_{pe}) as well as in the Untere Braunkohlensande (tmiBS1) produce comparable results. The means predominantly lie between 1×10^{-4} to 4×10^{-4} m/s. The values show major fluctuations of several orders of magnitude because of the methods used. This is particularly apparent in the short-term pumping tests in the Untere Braunkohlensande. The large variation is attributable to the lithological differences. Within the aquifers, the grain size continually decreases with depth, alongside a continuous increase in clay content. The associated reduction in permeability

is clearly demonstrated by the short-term pumping tests, because of the short test intervals and the uniform distribution of the observation well screens throughout the formation.

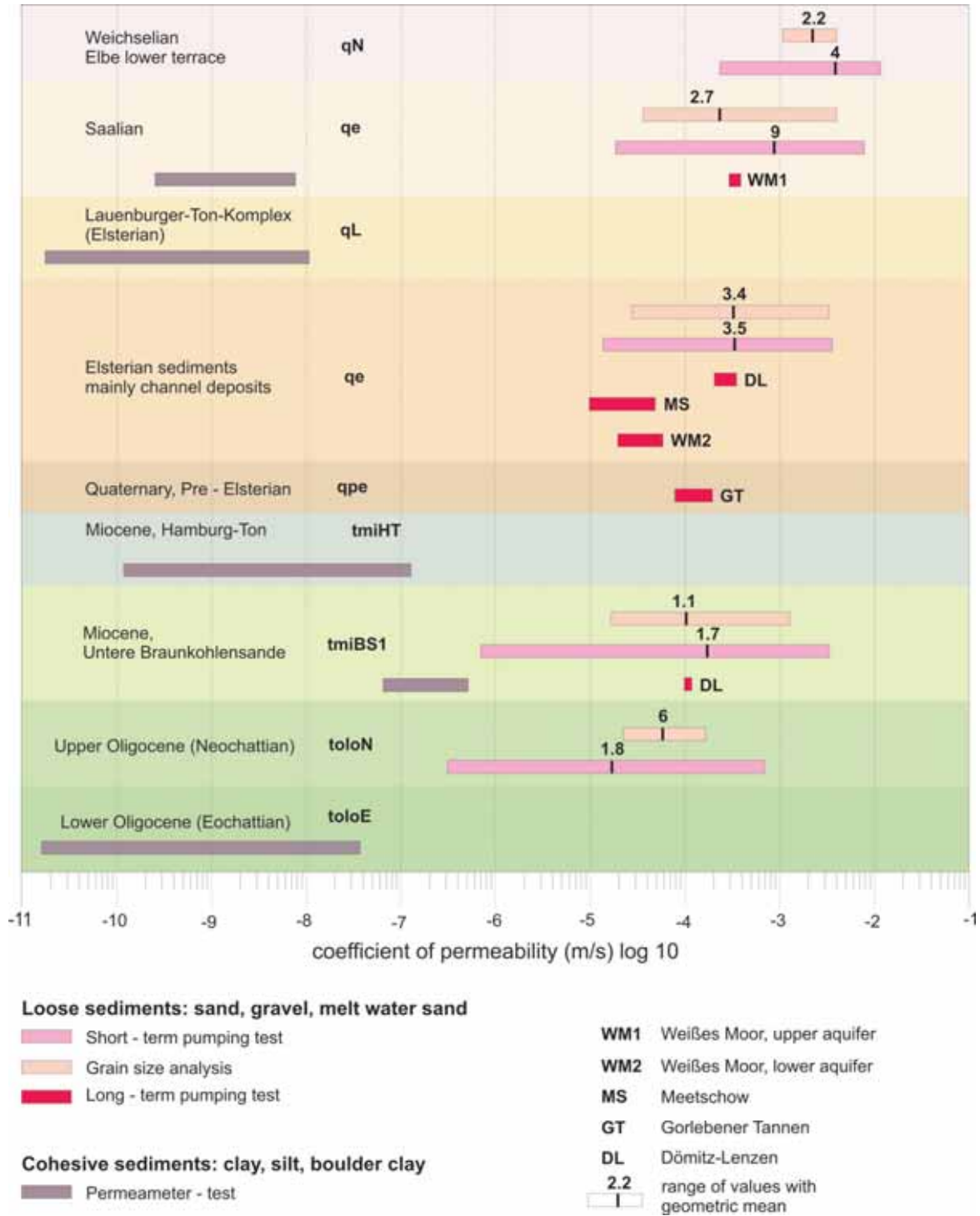


Figure 16: Hydraulic conductivity coefficients from pumping tests and laboratory tests

A comparison of the hydraulic conductivities determined from the long-term pumping tests and the results of the short-term pumping tests and the sieve analysis shows that these are comparable to the values determined from the pumping tests at Dömitz-Lenzen and Weißes Moor 1. In contrast, the hydraulic conductivities determined to the south of the Elbe in the lower aquifer within the Gorleben channel are much lower by around one order of magnitude. This is probably attributable to the location of the Weißes Moor (lower aquifer) and Meetschow pumping test areas at the northwestern edge of the Gorleben channel. The lower channel aquifer at this location has numerous glacial till interbeds and therefore has lower transmissivity than the sediments in the central part of the channel.

The k_f values determined for the Weichselian Glacial sediments are around one order of magnitude higher than the Saalian and Elsterian aquifers. The tested sediments were in the Elbe Lower Terrace and were all very coarse grained.

The values determined for cohesive sediments in laboratory WD tests have a spread of around four orders of magnitude between 10^{-11} and 10^{-7} m/s, and therefore fall within the typical range for aquitards.

6 Geothermal investigations

6.1 Objective

The objective of the thermal investigations, in addition to the general geothermal characterisation of the Gorleben site, was to acquire additional thermal indications of groundwater flows at depth to supplement the hydrogeological and hydraulic findings. Geothermal indications of groundwater flow come from the observation of anomalies within the natural temperature field. These anomalies arise from the superimposition of the additional advective heat flow associated with the transport of groundwater from other temperature zones on top of the normal conductive geothermal heat flow rising up from deeper zones.

6.2 Database

The data were acquired from high-resolution temperature logs taken from 167 exploration boreholes and groundwater observation wells, including salt table and salt dome exploration boreholes. Detailed synthetic profiles of sedimentary composition are also available in digital form for 116 of these boreholes (sand content, clay content and water content). These were calculated from the geophysical well logs. Together with laboratory data on the thermal conductivity of the clay, quartz sand and water matrix components, these data were used to generate detailed sedimentary thermal conductivity profiles.

6.3 *Expected geothermal field*

The natural geothermal field within the geological sequence is generally determined by the terrestrial heat flow rising up from below, as well as the thermal conductivity and structural relationships of the rocks. Because of the much higher thermal conductivity of evaporites compared to the surrounding sedimentary rocks, the area surrounding a salt dome has a typical anomalous heat flow distribution and an associated abnormal temperature field. Because the rising heat reaching the surface is concentrated by the evaporitic rock, the inside of the evaporite as well as the directly overlying overburden have much higher heat flow densities than the surrounding areas. The excess heat flow in the immediate vicinity of the salt dome is compensated by an associated widespread reduction in heat flow density in the area surrounding the salt dome.

The temperature field around the Gorleben salt dome was calculated by DELISLE (1980) on the basis of a schematic cross section. This model calculates a concentration of the natural heat flow in the central part of the salt dome with a value of approx. 120 mW/m². This is twice the regional average value of approx. 50 – 60 mW/m² (HÄNEL 1998). This conductive temperature field derived from pure thermal conductivity can be locally superimposed by advective heat transported by groundwater flow within the overburden.

6.4 *Groundwater temperatures in the overburden*

Because of the higher thermal conductivity of the evaporitic rock, the Gorleben–Rambow and Groß Heide–Siemen salt structures are associated with zones of raised temperatures in the overburden.

The temperature map at a depth of -150 m above sea level shown in Figure 17 clearly shows the superimposition of the temperature anomaly on the outline of the Gorleben salt dome. Measured temperatures locally exceed 19 °C and differ by over 9 °C from the lowest temperatures recorded in the rim synclines. The raised temperature zone within the margins of the salt dome is not uniformly distributed throughout this area, but associated with strong local anomalies. The Groß Heide–Siemen salt dome that lies to the west of the study area is also shown, although its outline is not precisely reflected in the isotherms because less is known about the shape of the salt dome, which has only been penetrated by two boreholes.

In addition to the temperature maxima above the salt domes, the thermal distribution map shows marked temperature minima in the rim synclines of the Gorleben–Rambow salt structures: there are localised patches where the temperature is only 10 °C, whilst the “normal” temperature at this depth would be approx. 13.3 °C. The zone of lower temperatures is more extensive in the southeast of the structure than in the northwest.

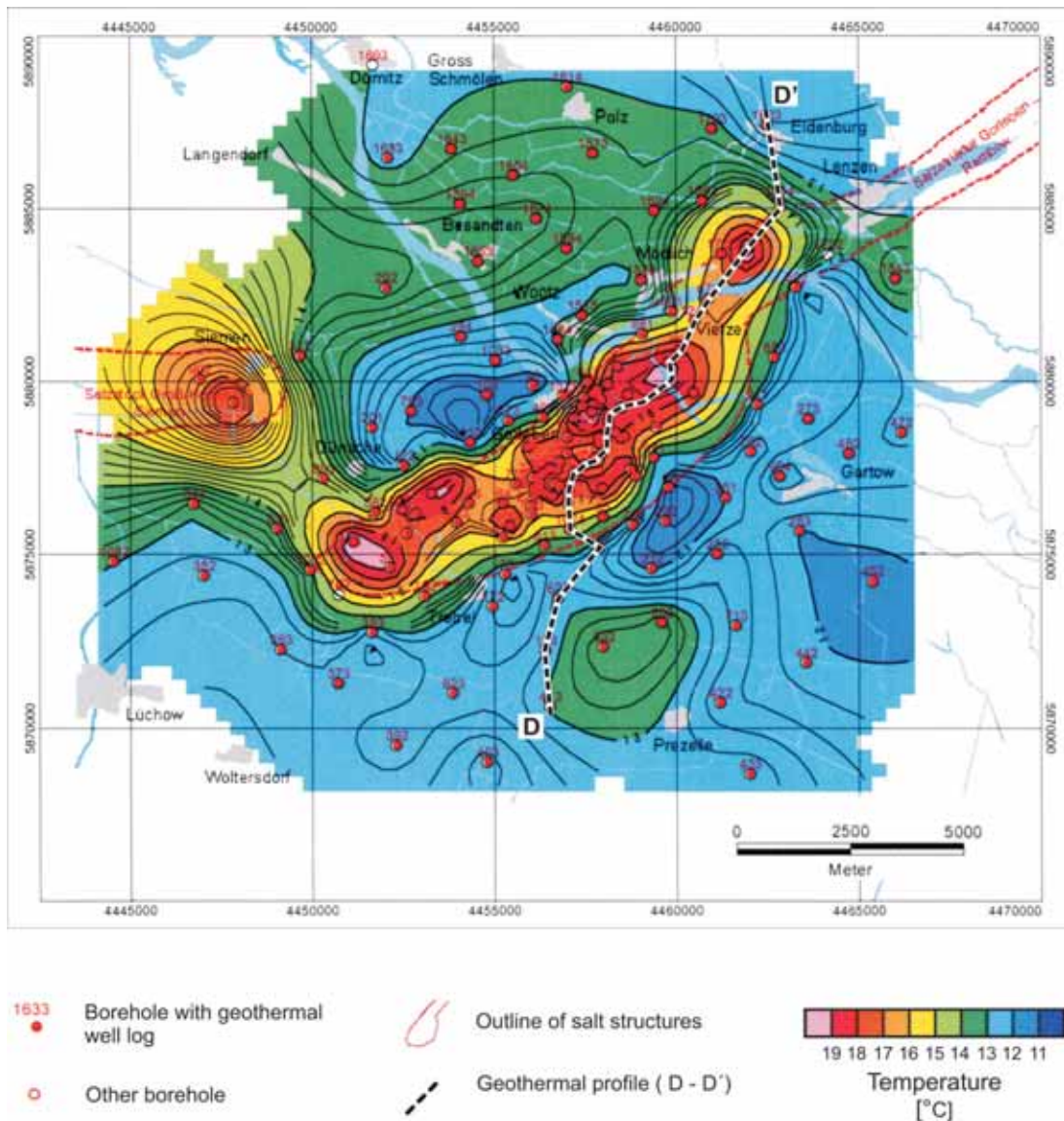


Figure 17: Groundwater temperature distribution at -150 m above sea level

6.5 Distribution of heat flow density

The vertical heat flow density was determined in all suitable boreholes to determine whether the observed temperature distribution can be adequately explained by the distribution of the geological layers within the overburden and at deeper levels, and whether groundwater flow also has an influence. This is achieved by modelling as accurately as possible in synthetic profiles the measured temperature logs and/or the temperature gradients derived from these logs.

The synthetic profiles are calculated for the local stratigraphic sequence assuming a constant vertical heat flow throughout the section penetrated by the borehole and also assuming pure thermal conductivity:

$$T_i = T_0 + q * \sum_{j=1}^i dj / kj \quad (6-1)$$

$$\text{grad } T_i = q / k_i \quad (6-2)$$

where

T_0	Annual average temperature at the surface
q	Heat flow density in [W/m ²]
i	Number of layers, starting from the surface
T_i	Temperature at the base of layer i in [°C]
$\text{grad } T_i$	Temperature gradient in layer i in [K/m]
k_i	Thermal conductivity in layer i in [W/m*K]

This method is refined by dividing up the unconsolidated sediments into 1 m thick layers (all $d_i = 1$ m; $i = \text{depth}$), whose thermal conductivities are synthesised from the relative volume proportions and thermal conductivities of the components sand, clay and water:

$$k_i = k_{\text{syn}} = \{V_{\text{wa}} * k_{\text{wa}} + V_{\text{to}} * k_{\text{to}} + V_{\text{sa}} * k_{\text{sa}} * (1 + kf * i)\} \quad (6-3)$$

where

$V_{\text{wa}}, V_{\text{to}}, V_{\text{sa}}$	relative volume proportions of water, clay and sand respectively
$k_{\text{wa}}, k_{\text{to}}, k_{\text{sa}}$	thermal conductivities of water, clay and sand (quartz) resp.
kf	compression factor

The relative volume proportions were determined from the gamma ray, density and electrical resistivity recorded by the geophysical well logs.

The following values measured in the BGR laboratory or derived from the literature (LANDOLT-BÖRNSTEIN 1967) were used for the thermal conductivities:

Table 3: Thermal conductivities for the sedimentary components clay, quartz sand and water used in the calculations

Sedimentary components	Thermal conductivity K [W/m ² x K] at 15 °C
Clay	$k_{\text{to}} = 1.3$
Quartz sand	$k_{\text{sa}} = 3.3$
Water	$k_{\text{wa}} = 0.6$

Using the compression factor kf incorporated in (6-3), enables the approximate increase in effective thermal conductivity with increasing depth to be approximately taken into

consideration. This is due in part to the larger area of contact between individual sand grains attributable to the increase in pressure. The temperature profile modelling was improved by using an assumed figure of $k_f = 0.01$.

Depth zones where this adjustment fails, i.e. where significant differences remain between the calculated and the measured temperatures, indicate the presence of flow processes (advective temperature differences). In addition, significant deviations in the heat flow density from the expected value of 60 mW/m^2 outside of the salt dome or 120 mW/m^2 within the salt dome – where they cannot be explained by anomalous geological situations – indicate additional positive or negative advective heat flow components associated with flowing groundwater.

Figure 18 shows examples of measured temperature curves, synthetic thermal conductivity curves and calculated temperature curves for the GoHy 1092 and GoHy 1534 groundwater observation wells.

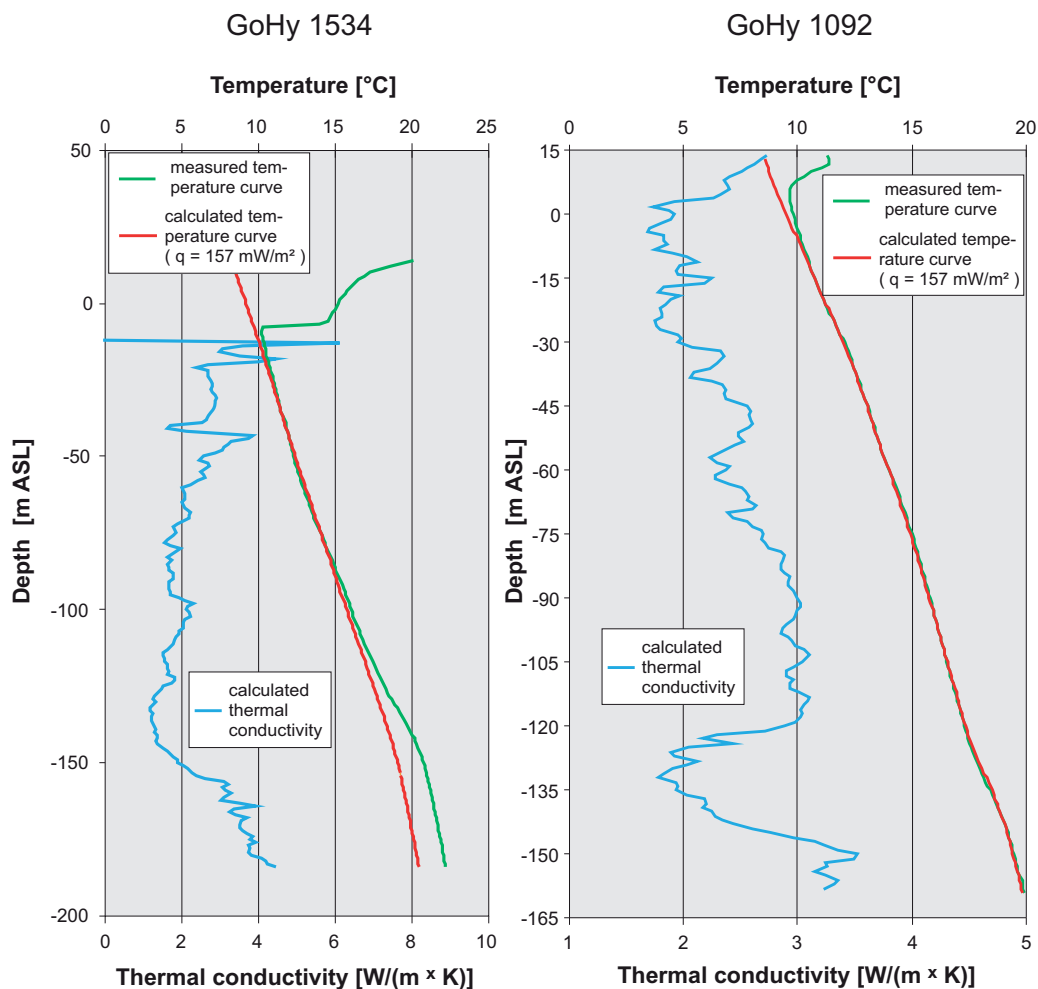


Figure 18: Measured and calculated temperature and thermal conductivity logs in the GoHy 1092 and GoHy 1534 groundwater observation wells

The GoHy 1092 observation well is screened in the Eocene sands at a depth of -160 m above sea level, and is located in the ring wall in the southwestern part of the salt dome. In the figure, this mainly argillaceous sequence between approx. -125 to -145 m above sea level with its low thermal conductivity values clearly stands out from the overlying sandy sections with their higher thermal conductivity values.

The synthetic and measured temperature logs are largely comparable. This shows that the temperature profile in the borehole is completely determined by vertical conductive heat flow and that the logged section of the borehole has no water flow.

The GoHy 1534 observation well is in the north of the Gorleben salt dome in the Gorleben channel. It is screened at a depth of -185 m above sea level within the Elsterian channel sands, which are overlain here by an around 100 m thick Lauenburger-Ton-Komplex sequence. Unlike GoHy 1092, this observation well has a marked positive temperature anomaly within the Elsterian channel sands, which indicates the lateral inflow of warmer groundwater.

The heat flow density distribution shown in Figure 19 reveals, as expected, the outline of the salt dome in a similar way to the temperature distribution map. Local differences in anomaly structures provide additional information on potential groundwater flow, as discussed in the following section.

The lowest heat flows of below 40 mW/m² are observed in the southeastern rim syncline, whilst the highest heat flow densities of over 160 mW/m² in parts occur at several points above the Gorleben salt dome. These top values considerably exceed the expected value of 120 mW/m² derived from the simplified model calculation. The highest heat flow density zones lie almost completely within the outline of the salt dome, or within the ring wall, which suggests a reason for the difference between the model calculation and the highest measured values: the low thermal conductivity of the pre-Miocene Tertiary clays, which surround the evaporite and overlie it in part, causes the zone in which the heat flow (which has already been concentrated by the evaporite body) preferentially enters the Quaternary overburdens to be further narrowed and thus causes additional concentration of the heat flow.

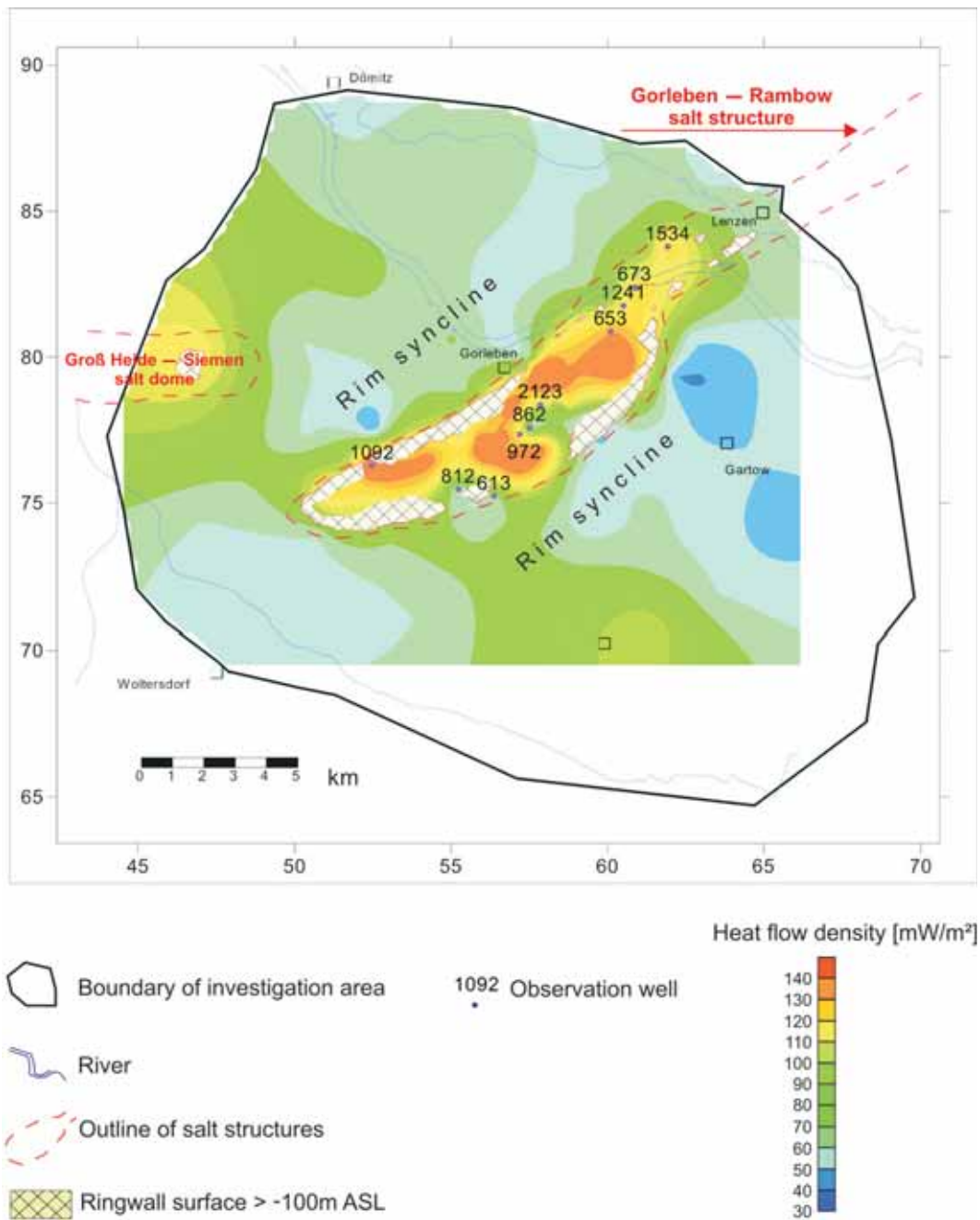


Figure 19: Heat flow density map

6.6 *Thermal indications of groundwater flows*

As discussed above, unusually low heat flow densities are encountered in the **southeastern rim syncline**. The Holocene dune sands and aeolian sand sheets occurring in this area form a favourable groundwater recharge area, beneath which there is a marked rise in the water table (cf. Chapter 8.2.1.). The downward flow of cold shallow groundwater reduces the formation temperature, i.e., the rising geothermal heat flow is cooled down by the downward moving advective components.

A comparison of the heat flow density in Figure 19 with the water table contour map in Figure 43 shows that the heat flow density minima and the high in the shallow groundwater are not superimposed. Quite the reverse: the heat flow densities beneath the high water table in the southeast of the study area are relatively high. The heat flow density minima are located further to the northeast. This could be attributable to the extensive distribution of the Lauenburger-Ton-Komplex to the southeast, which is patchily distributed further northeast (cf. Fig. 9). Whilst the downflowing groundwater flow beneath the high water table in the southeast is limited to the shallow aquifer by the low permeable Lauenburger-Ton-Komplex, it appears to extend down as far as the lower aquifer further to the northeast, which is in direct hydraulic contact with the upper aquifer.

Because of the geometry of the salt dome, a higher but more uniformly distributed heat flow density would be expected above the **Gorleben salt dome**. However, the heat flow map shows a remarkably differentiated picture with local reductions in heat flow well below the expected values. Two main zones are involved here:

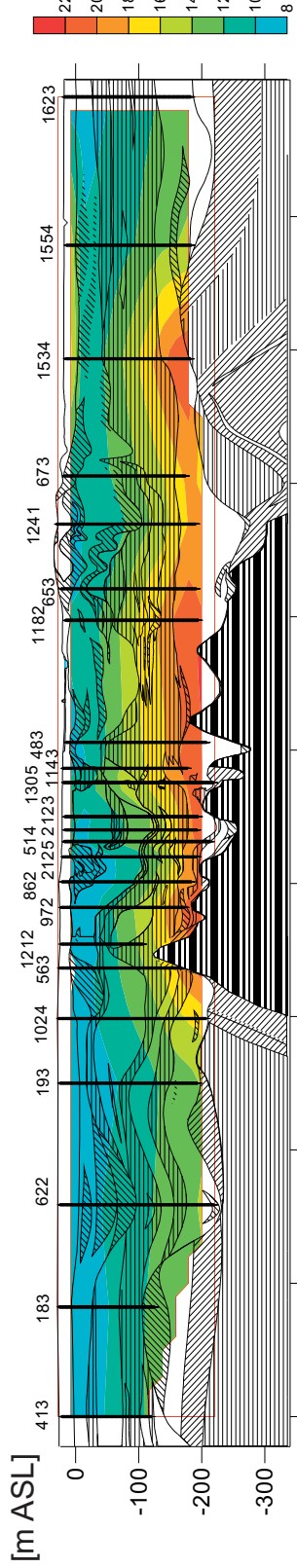
- Above the ring wall in the southwest of the salt dome (around the GoHy 812 and 613 observation wells)
- Above the salt dome to the south of Gorleben between the GoHy 862 boreholes and the Weißes Moor pumping test area (GoHy 2123)

In both cases, zones of low heat flow extend from the southeast into the area of the salt dome overburden.

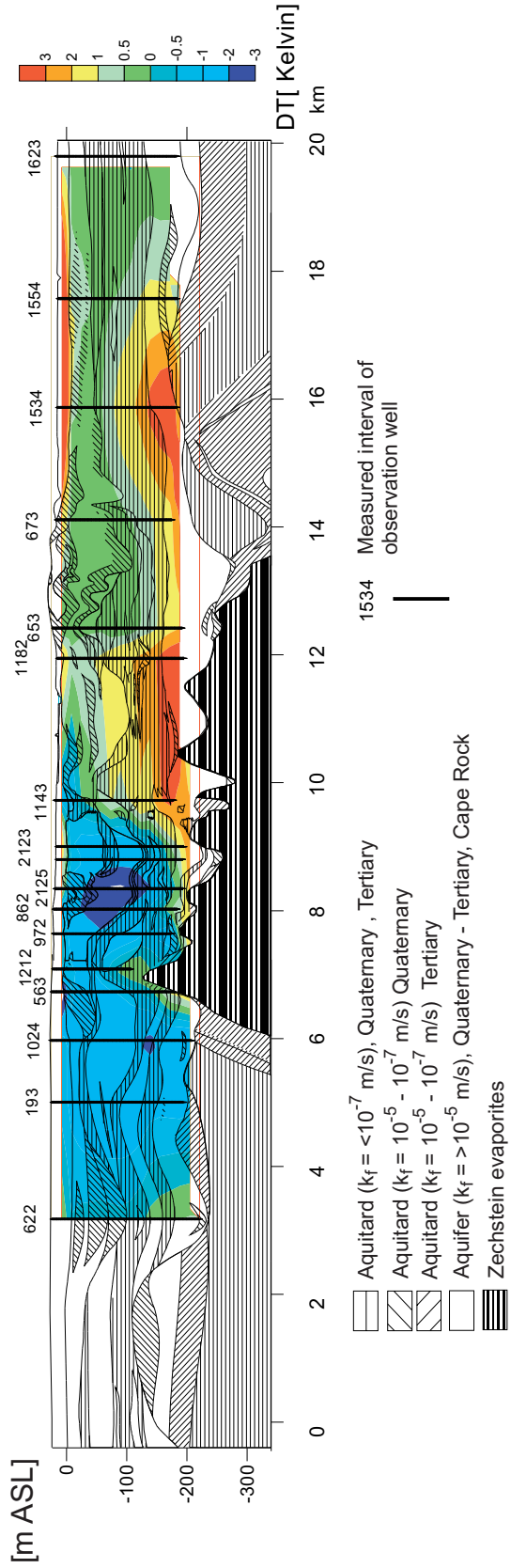
Both the GoHy 812 and GoHy 613 observation wells are located above the salt dome ring wall. The surface of the ring wall is deeper here than in the neighbouring areas to the southwest and northeast, due to Quaternary erosion. This erosion gives rise to a local hydraulic connection between the fossil subsidence trough above the western salt dome and the southwestern rim syncline, through which cold groundwater can flow in from the area of the Gartower Tannen into the fossil subsidence trough. The inflow of cold groundwater reduces the heat flow in the inflowing area.

D'

a) Grundwater temperatures



b) Advective temperature differences



- Aquitard ($k_f = <10^{-7}$ m/s), Quaternary, Tertiary
 - Aquitard ($k_f = 10^{-5} - 10^{-7}$ m/s) Quaternary
 - Aquitard ($k_f = 10^{-5} - 10^{-7}$ m/s) Tertiary
 - Aquifer ($k_f > 10^{-5}$ m/s), Quaternary - Tertiary, Cape Rock
 - Zechstein evaporites
- 15.34 Measured interval of observation well

Figure 20: Groundwater temperatures and advective differential temperatures along the Gorleben channel (cf. Fig. 17 for cross section location).

The second zone, which lies further to the northeast, shows a similar picture. The thermal/hydrogeological cross section A – A' (Fig. 20) through the Gorleben channel shows that the temperatures (Fig. 20a) corresponding to the salt dome geometry are generally raised above the whole salt dome. The isotherms in the upper part of the overburden between the GoHy 972 and GoHy 2123 observation wells are much lower. The temperature differences shown in Figure 20b (difference between measured and synthetic temperatures) indicate that the zone of anomalous low temperatures is limited to the upper aquifer, whose lower boundary corresponds here to the unusually deep lying top of the Lauenburger-Ton-Komplex. The influence of the cold water flowing in from the groundwater high beneath the Gartower Tannen therefore appears to reach right down to the upper aquifer.

A second, although much weaker temperature low is under the H hbeck around the GoHy 653, 1241 and 673 groundwater observation wells. This is also attributable to the downward flow of cold groundwater beneath the topographic high of the H hbeck.

Figure 20 b shows that there are also positive temperature differences within the lower aquifer in the **Gorleben channel** which cannot be completely explained by conductive influences, even with high heat flow values.

Interpreting the temperature distribution across the central part of the channel is made more complex by the fact that most of the observation wells in the Gorleben channel are screened in the uppermost part of the aquifer. This means that there are no continuous temperature profiles available down to the base of the channel – which would considerably simplify interpretation. There are generally two models to explain the positive temperature differences:

1. It can be concluded from the observed vertical distribution of salt concentration within the channel aquifer, and on the basis of the 2D freshwater/salt water model calculations, that there is a northeastward flow of water in the uppermost part of the channel aquifer within the Gorleben channel. In the lower parts, however, it is also possible for salt dissolution at the base of the channel to give rise to convection cells, with reverse flow in parts (cf. Chapters. 8.3 and 10, Fig. 55). The positive temperature differences in the upper part of the channel aquifer could also be interpreted as a possible thermal indicator for the existence of such convection cells which transport conductive heat from the base of the channel into the upper part of the channel aquifer.

2. The upper boundary of the channel aquifer formed by the base of the Lauenburger-Ton-Komplex rises over the Gorleben salt dome from south to north by around 30 m. An alternative explanation could therefore be that the warmed-up groundwater flowing from the south leads to the positive temperature differences in the central and northern parts of the channel above the salt dome.

A remarkable positive thermal anomaly of over 3 degrees (cf. Fig. 18) occurs within the Elsterian channel sands in the GoHy 1534 observation well which, although still in the Gorleben channel, actually lies to the north outside the outline of the salt dome. The map of temperature differences at -180 above sea level level in Figure 21 shows that this temperature anomaly extends to the west into the centre of the **northwestern rim syncline**, although with a strong decline in amplitude.

The distribution and extent of this temperature anomaly in the Gorleben channel and the northern rim syncline correlate strongly with the distribution of salt concentration within the lower aquifer (Chapter 7.1.2). The relatively highest temperatures occur in each case above the centre of the zone, with salt concentrations exceeding 200 g/l – the isotherms indicate a further rise in temperatures towards the centre of the salt water body.

The spatial distribution of the temperature anomaly within the lower aquifer, with its decreasing amplitudes to north and west, as well as its correlation with the salt concentrations, supports the interpretation that the temperature anomaly reflects permanent salt water transport out of the Gorleben channel into the northwestern rim syncline. The warmed-up salt water flow continually gives off conductive heat to the surrounding area as it flows. This leads to the observed excess temperatures within the overlying freshwater-bearing part of the lower aquifer. This heat loss reduces the temperature of the salt water flow along the direction of flow with increasing distance from the point it flows out of the salt dome overburden.

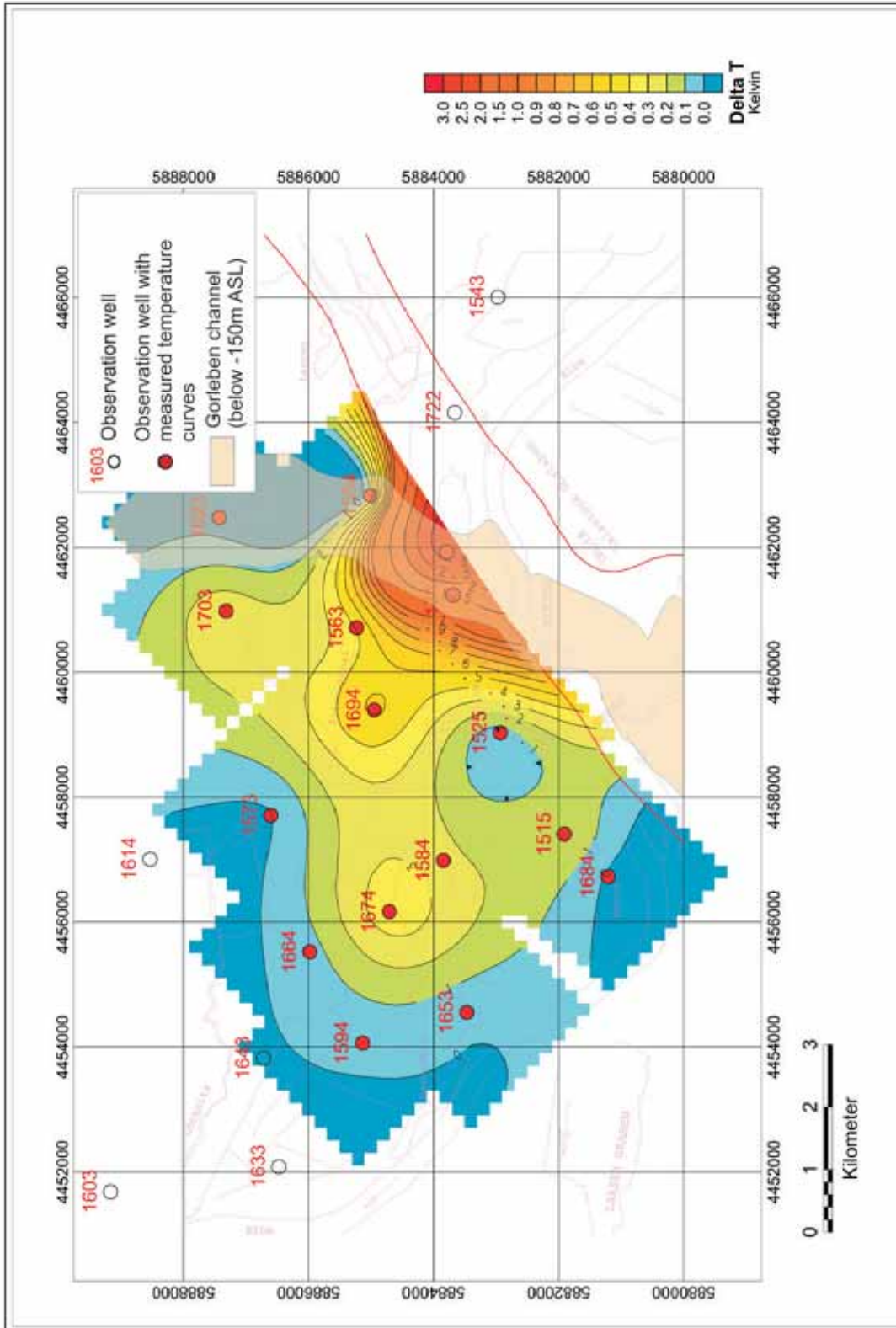


Figure 21: Distribution of advective temperature differences in the northwestern rim syncline at -180 m above sea level

7 Hydrochemistry

7.1 *Spatial distribution of total dissolved solids*

The study area has the typical subdivision within the North German Plain of an upper body of freshwater of varying thickness and low total dissolved solids (TDS) throughout, underlain by a body of salt water with saline groundwater. Freshwater in this context is defined as all water with less than 1 g/l TDS.

It already became clear during the early phase of the investigation that groundwater is in direct contact with the Zechstein evaporite sequence in some areas above the salt dome. The direct contact between Zechstein salt and Quaternary sediments in the centre of the Gorleben channel gives rise to a strong increase in the salt content of the groundwater. The search for potential migration paths out of the salt dome is therefore closely linked with the question of salt water flow within the overburden. Investigating the freshwater and salt water systems is therefore a key part of the investigation programme. Part of this programme involved the systematic installation of groundwater observation wells within salt water-bearing sediments, and geophysical borehole logging to evaluate the vertical distribution of salinity.

Chapter 7.1 starts with a general description of the freshwater/salt water distribution within the Cenozoic aquifer system. An interpretation of this distribution within the context of salt water flow, and of the origin and genesis of this water, requires the consideration of additional criteria such as the isotopic geochemical composition of the water. This will therefore be undertaken in Chapter 10.

7.1.1 **Data evaluation procedure**

The main data used to assess the spatial distribution of the total dissolved solids in the groundwater originate from a chemical analysis of groundwater samples from 404 observation wells as well as from the evaluation of geophysical logs carried out in 106 main boreholes. The results of this analysis and logging from the wells in the Gorleben channel in the area south of the Elbe and from all boreholes north of the Elbe are continuous vertical profiles of pore water electrical conductivities and densities. The salinity and density profiles were calculated from a combined evaluation of borehole logs, specifically the formation density, specific electrical resistance and natural gamma ray intensity (FIELITZ & GIESEL 1991, cf. Chapter 8.3).

In the vertical sections of freshwater/salt water distribution discussed in the following chapters, the waters are divided into the following six salinity classes:

0 – 1 g/l TDS

1 – 10 g/l TDS

10 – 50 g/l TDS

50 – 100 g/l TDS

100 – 200 g/l TDS

> 200 g/l TDS TDS (Total Dissolved Solids) = Total salt concentration

Evaluation of the geophysical borehole logs is best suited to salt water-bearing sediments where there is a high conductivity contrast between the pore water and the formation matrix. Because of the low conductivity contrast between the matrix and the pore water in zones with freshwater or groundwater with low salinity, using this method gives rise to large errors. For this reason, the depth of the freshwater/salt water interface of 1 g/l, as well as the salt concentration boundary of 10 g/l was derived directly from the resistivity log on the basis of an empirically determined correlation between formation resistivity in the filter zones of the observation wells and the total dissolved solids within the groundwater (Fig. 22).

Unlike the evaluation of the geophysical borehole logs, this empirical method is in principle only applicable to sandy sediments because of the high electrical conductivity of clays – and therefore does not in principle allow any conclusions to be drawn about the vertical distribution of salinity within homogeneous clay sediments. However, because there are numerous thin sandy interbeds in the study area, particularly in the Hamburg-Ton-Komplex as well as in the Lauenburger-Ton-Komplex, it is actually possible to draw conclusions based on the distribution of salt concentration within the water in these interbeds and thus interpret the vertical distribution of salinity within the overall formation. This assumes that the salinity of the pore water in the sandy layers does not generally differ from that in the surrounding clay. Special investigations carried out on the pore water in the sediments by RÜBEL (2000) confirm the validity of this assumption.

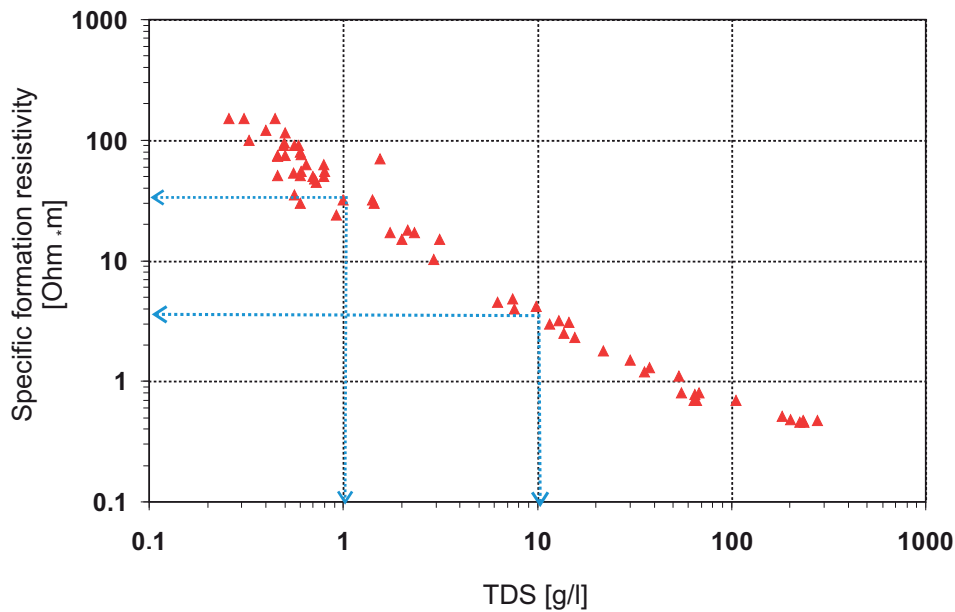


Figure 22: Correlation between total dissolved solids in the water sample from observation wells and the formation resistivities derived from induction logs

7.1.2 Description of freshwater/salt water distribution

The following description of the freshwater/salt water distribution is based on four hydrochemical cross sections (Appendix 1), as well as thematic maps and profiles in Figures 23 to 28. The locations of the hydrochemical cross sections are identical to the hydrostratigraphic sections. In addition to freshwater/salt water distribution, the sections also show the spatial distribution of the aquifers and aquitards. In addition, the total dissolved solids (in g/l) of the groundwater and its hydrochemical classification are given for the filter zones in each observation well.

The vertical cross sections A – A' and B – B' (Appendix 1) which cross the Gorleben salt dome and its rim synclines in a NW-SE direction, show the vertical subdivision typical for this area into an upper **freshwater body** with total dissolved solids well below 1 g/l, and a lower **salt water body** with total dissolved solids exceeding 10 g/l. A typical feature of the **rim synclines** in the area south of the Elbe are the widespread large thicknesses of freshwater exceeding 100 m, as well as the very low total dissolved solids throughout, which either remain constant with depth or only increase very slightly. The freshwater is separated from the underlying salt water by a transition zone a few tens of metres thick, within which the salt concentration rises downwards almost exponentially to above 10 g/l TDS (KLINGE 1994). The freshwater/salt water interface within the rim synclines mainly lies within the Untere Braunkohlensande.

Because of the marked hydrogeological subdivision of the aquifer system within the Elbe-Löcknitz lowland around the northwestern rim syncline, there is a much stronger vertical differentiation into freshwater and salt water bodies (vertical cross section C – C'). The base of the freshwater body here lies within the upper aquifer throughout. The freshwater body is underlain by relatively low salinity salt water with total dissolved solids of well below 10 g/l. In the centre of the lowland, the Hamburg-Ton and Lauenburger-Ton-Komplex aquitards also contain salty pore water with associated relatively low total dissolved solids. The two aquitards are directly underlain by another thin freshwater body with very low salt concentrations of 0.4 to 0.7 g/l TDS. This lower freshwater body reaches its greatest thickness of around 40 to 50 m at the northern edge of the study area. This thickness decreases continuously towards the southwest to zero at the transition zone to the salt water. Figure 23 shows the distribution and total dissolved solids of this freshwater body. It extends southwards to the Elbe in the west. In the east, it is bounded by the Gorleben–Rambow salt structure. In the centre of the lowland, it only extends to a position directly south of the Rinow canal.

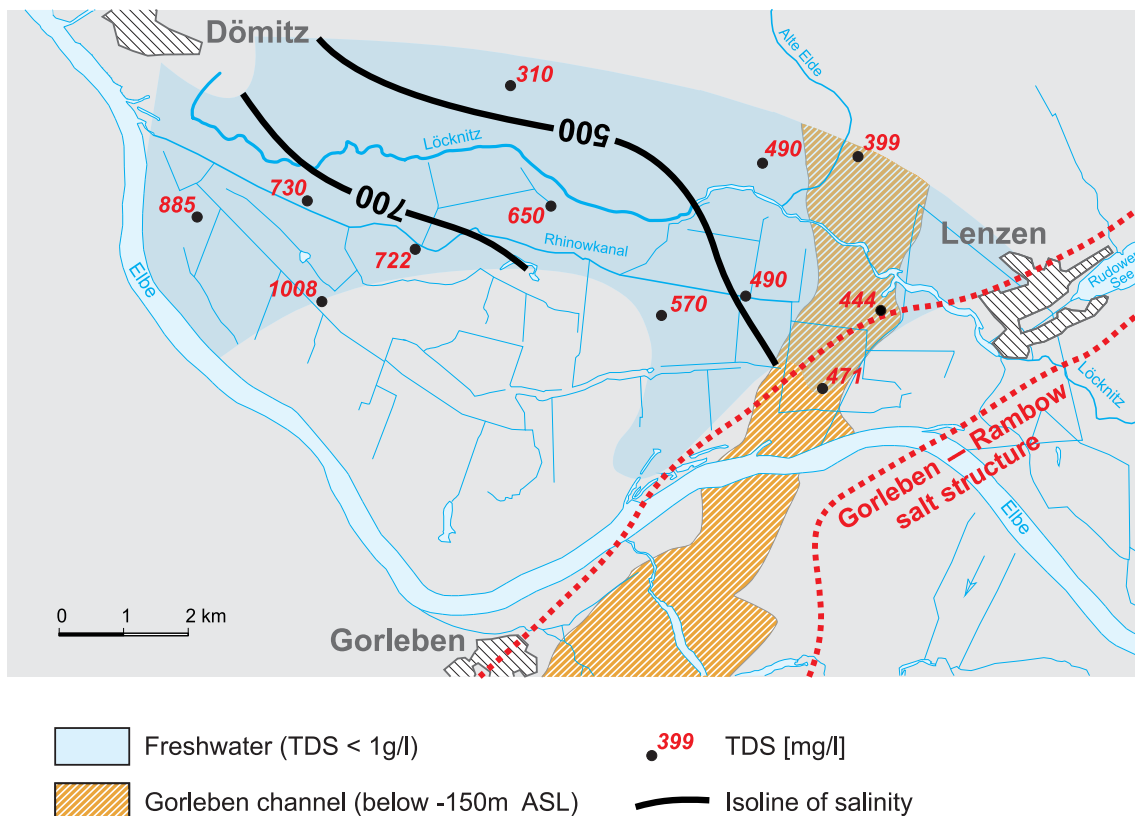


Figure 23: Distribution and total dissolved solids of the lower freshwater body in the Elbe-Löcknitz lowland

The TDS distribution in this lower freshwater body shows a general increase in mineralisation to the southwest. The zone of very low salt concentrations of less than 0.5 g/l TDS extends all the way to the immediate southern distribution boundary of the Gorleben channel, whilst the salt concentration in the west rises continually towards the Elbe to almost 0.9 g/l TDS. The shape and extent of this freshwater body, as well as the zonation of the salt concentrations, point to the inflow of freshwater from the areas bordering it to the northeast (KLINGE et al. 2001).

Highly saline water with total dissolved solids of more than 200 g/l to around 280 g/l lies under the freshwater body beneath a thin transition zone, and extends down to the base of the lower aquifer. The distribution of this salt water body with over 200 g/l TDS is limited to the central part of the northwestern rim syncline. Its upper surface is roughly horizontal, while its lower surface tracks the base of the lower aquifer and follows the trough-like structure of the rim syncline.

The pore water within the Chattian silts in the underlying sequence has much lower salt concentrations compared to the overlying brine. This vertical distribution of pore water salinities in the transition zone between the lower aquifer and the underlying aquitard is shown as an example in Figure 24. The pore water in the uppermost part of the Untere Braunkohlensande is only slightly salty with total dissolved solids of 1.1 g/l. The conductivity of the groundwater increases continuously from around 2 mS/cm to a maximum of around 90 mS/cm at the base of the Untere Braunkohlensande. A declining conductivity trend occurs in the underlying Neochattian. The conductivity of the pore water then increases again beneath a depth of 250 m. A TDS of 66 g/l was measured in an observation well located in the conductivity maximum. The TDS at an observation well within the Eochattian at a depth of 246 m BGL is only 15 g/l.

A corresponding vertical distribution of pore water salinities is shown in all boreholes in the centre of the rim syncline: a rise in salt concentration with depth within the Untere Braunkohlensande, a maximum at around the base of the aquifer, and a reverse trend in the underlying Chattian silts.

Above the **Gorleben salt dome**, there is a basic difference in the spatial distribution of TDS and the position of the freshwater/salt water interface between the southwestern part and the northeastern part: in the area of the pre-Elsterian subsrosion trough in the southwest of the salt dome, the Zechstein evaporite is covered throughout by low permeable early Tertiary clays. The freshwater/salt water interface at around -100 m above sea level is at a comparable depth to the interface in the rim synclines. The mineralisation of the salt water at the base of the lower aquifer is also comparably low, at around 20 g/l TDS. The aquifer is filled with freshwater right down to the base in the higher lying areas at the edges of the structure (vertical cross section A – A').

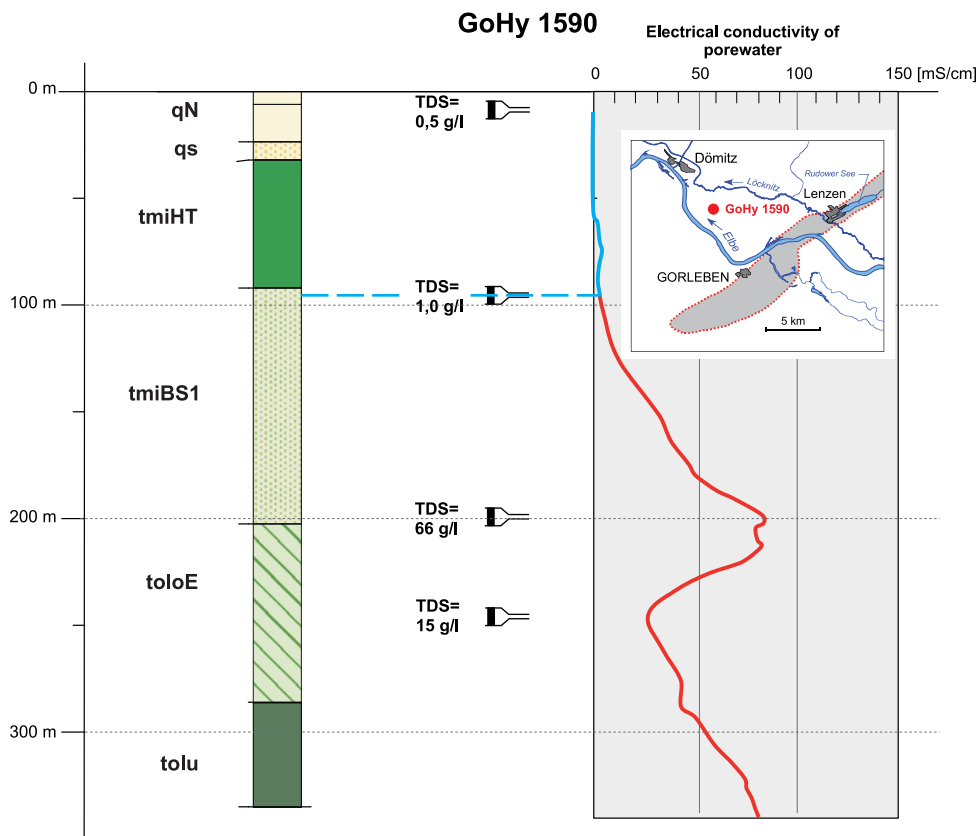


Figure 24: Vertical change in pore water conductivity in GoHy 1590 exploration well

By contrast, the spatial distribution of salt concentrations above the central and northeastern part of the salt dome is strongly affected by the Gorleben channel. Because of the direct contact between groundwater and the Zechstein evaporites in the central part of the channel, the base is marked by a strong increase in the salinity of the water, ranging as high as NaCl saturation. This addition of salt strongly influences the pore water within the lower channel aquifer as well as in the overlying sediments. The freshwater/salt water interface above the Gorleben channel lies at very irregular depths within the upper aquifer. The Lauenburger-Ton-Komplex is salt water-bearing throughout, with the TDS of the pore water compared with the Elbe-Lößnitz-lowland being much higher, at 10 – 30 g/l. The salt concentration generally increases with depth.

The vertical distribution of groundwater salinity within the lower aquifer in the Gorleben channel is as follows: in the upper part of the Elsterian sands, the TDS within the groundwater rises with increasing depth within a 20 to 30 m transition zone from around 20 to 40 g/l to over 200 g/l. The top of this transition zone parallels the base of the Lauenburger-Ton-Komplex. In those observation wells screened at the base of the channel, the measured salt concentrations range from around 250 g/l up to the salt saturation level of around 320 g/l TDS.

Figure 25 highlights the salinity distribution, reflecting the vertical density and salinity distribution at a groundwater observation well on the basis of an induction log interpretation. Because of the close, approximately linear correlation between the measured groundwater densities and the water TDS, the density/depth distribution in the boreholes can be used to directly interpret the TDS distribution within the groundwater.

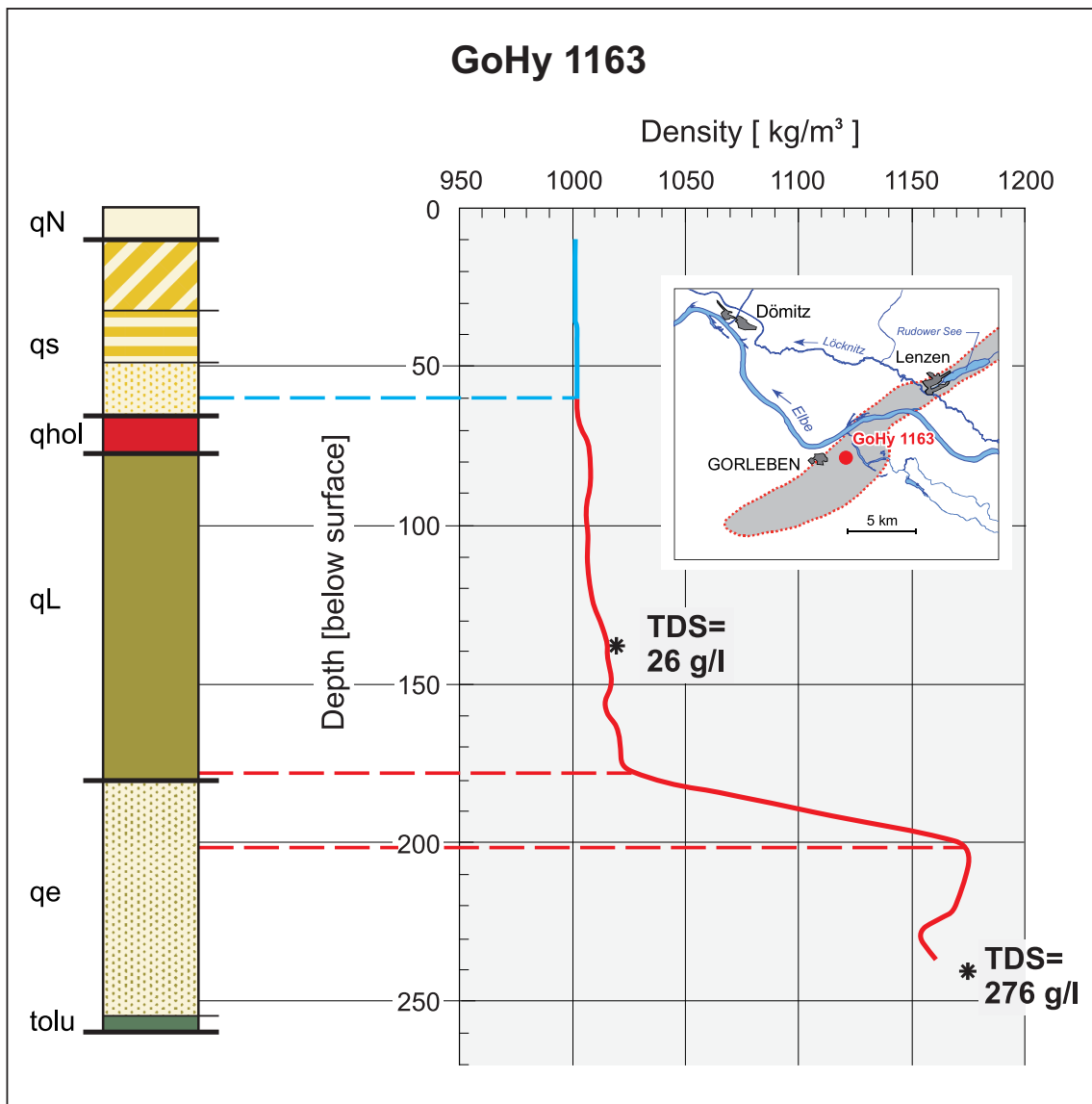


Figure 25: Vertical density distribution of groundwater at the GoHy 1163 observation well on the basis of induction log interpretations.

The spatial distribution of salt concentration in the groundwater at the base of the lower aquifer shown in Figure 26 highlights the clear correlation between TDS zonation and the structure of the lower aquifer. The distribution of the highly saline water with more than 200 g/l TDS is limited to the contact between the evaporite body and the Quaternary

sediments within the Gorleben channel, including the immediately neighbouring areas to the north and south, as well as the central part of the closed trough structure of the northwestern rim syncline. The saline waters of the Gorleben channel and the rim syncline are in direct connection. Salt concentrations decrease continually within the northwestern rim syncline towards the structural highs and drop down to values of well below 50 g/l TDS. However, even outside the brine distribution area, the salinity of the salt water in the northwestern rim syncline is higher than in the southwestern rim syncline, where the salinity of the water at the base of the aquifer largely lies below 10 g/l. The salt concentrations over the southwestern part of the salt dome are also generally of the same order of magnitude – higher salt concentrations only occur in the immediate vicinity of the Gorleben channel. The lower aquifer above the ring wall is filled with freshwater, all the way down to the base of the aquifer in places.

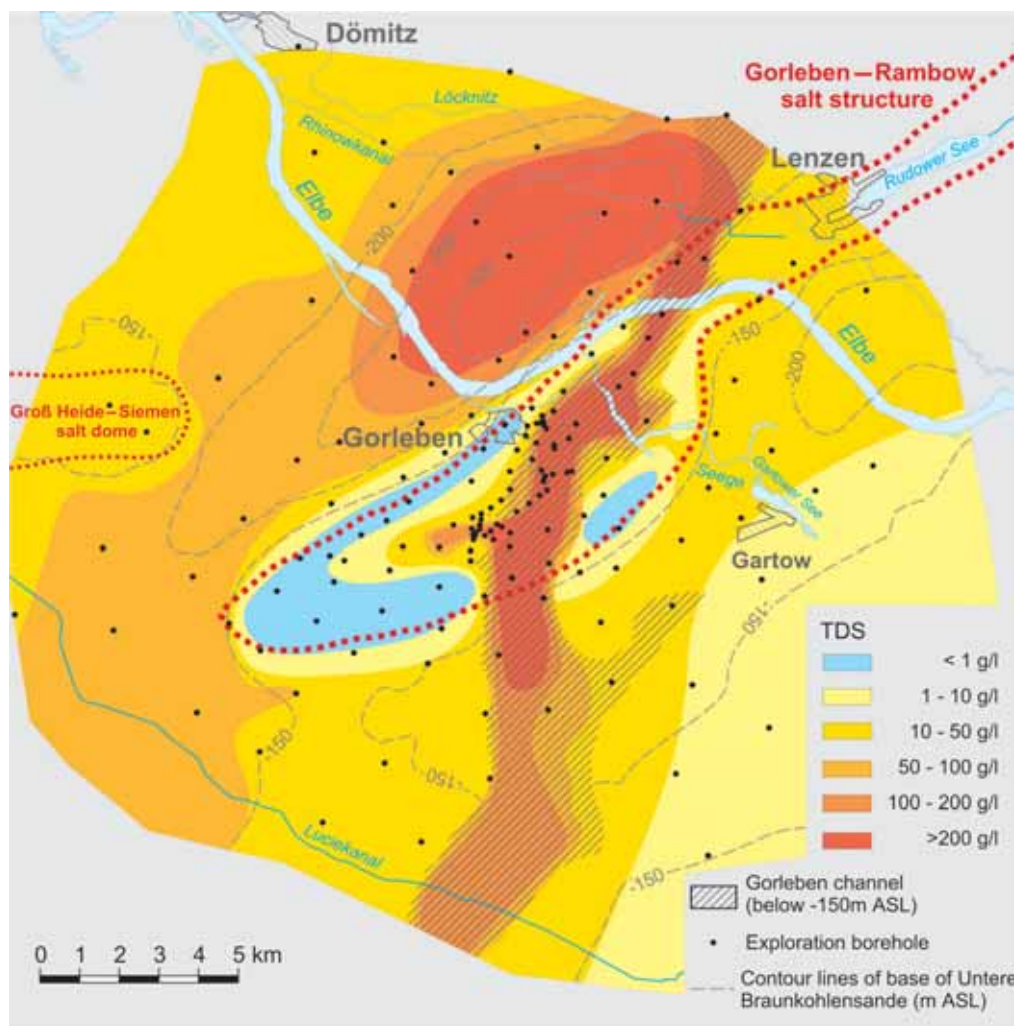


Figure 26: Groundwater TDS at the base of the lower aquifer

Figure 26 shows the depth of the base of the freshwater body. The considerable relief of this horizon reflects the regional hydrogeological structure – and the distribution of the aquitards in particular – as well as the regional groundwater flow. Because of the local lateral interdigitation and overlapping of freshwater and salt water bodies, the depth of this horizon can vary over a short distance by up to 100 m. The largest thickness of the freshwater body of more than 100 m to a maximum of 170 m is located in the rim synclines to the northwest and southeast of the salt dome in areas with downward groundwater flow, and areas where there is also direct hydraulic contact between the upper and the lower aquifers. Comparable thicknesses also occur in parts of the pre-Elsterian subsion trough above the western part of the salt dome.

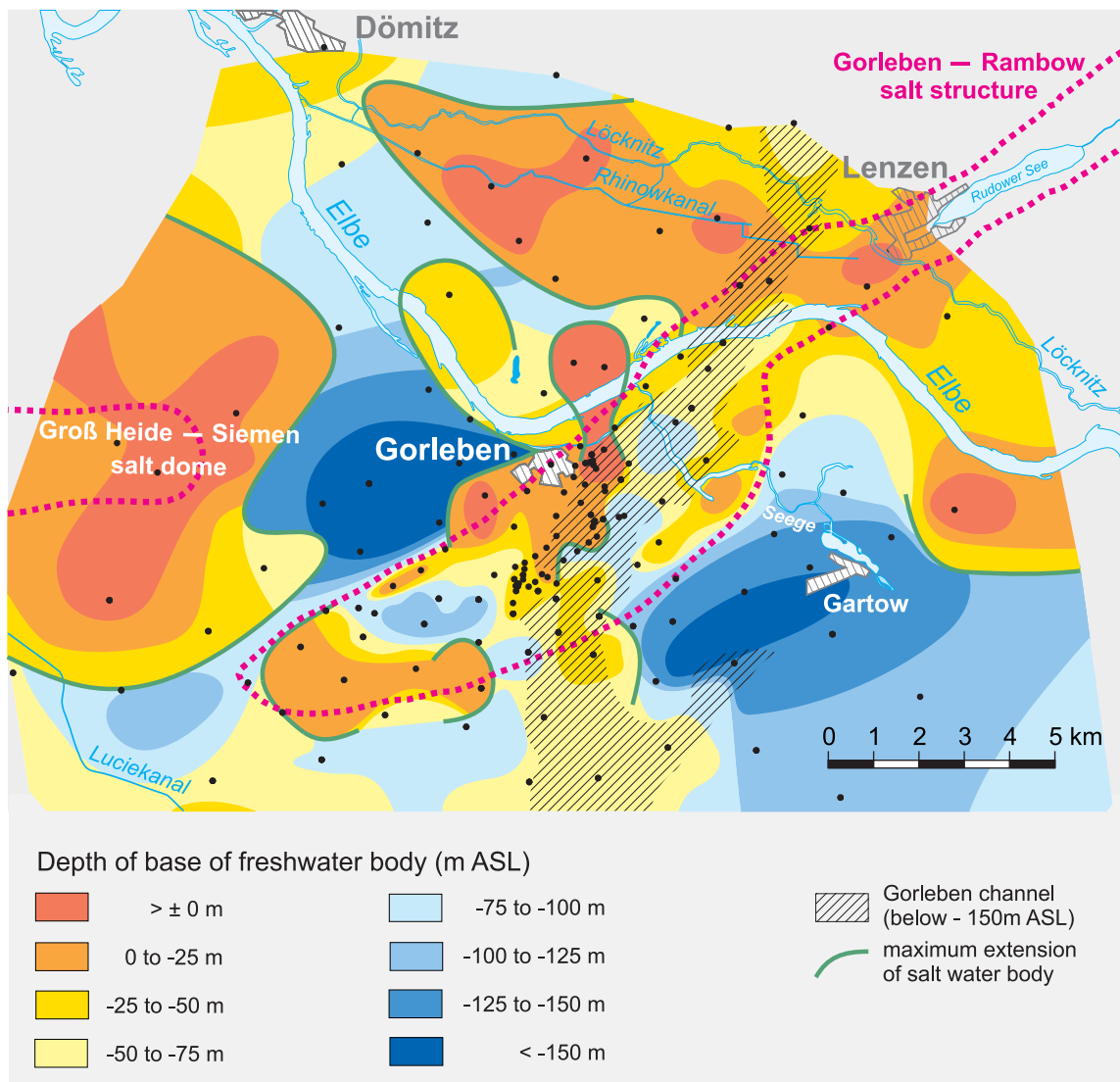


Figure 27: Depth of the base of the upper freshwater body

Significant salt water highs in which salt water partially fills up the whole system right up to the groundwater surface are present at the following locations:

1. Above the Groß Heide–Siemen salt dome at the western edge of the investigation area
2. In the Elbe river valley
3. Above the southwestern end of the Gorleben salt dome
4. At the western edge of the Gorleben channel above the Gorleben salt dome

1. Figure 27 shows a large salt water high surrounding the **Groß Heide–Siemen** salt dome. As part of a programme investigating the presence of shallow saline groundwater, an extensive salt water high with up to 2.7 g/l TDS was identified in the Lucie lowland to the south of this salt structure (BRÜHL & FABER 1983). Two wells drilled directly above the salt dome revealed a continuous increase in pore water TDS with depth (Appendix 1, vertical cross section A – A').
2. As already discussed, the upper freshwater body in the central part of the **Elbe-Löcknitz lowland** is very thin throughout. The thinnest freshwater thickness at between 10 m to a maximum of 30 m was encountered along the Rhinow canal as well as above the Gorleben–Rambow salt structure in the Löcknitz area. The thickness of this freshwater body increases considerably towards the north and south; the edges of the salt water high are marked by the presence of freshwater underlying the salt water or lateral interdigitation of freshwater and salt water. Another localised salt water high lies further downstream along the Elbe near Elbholz to the northeast of Gartow. Shallow groundwater with increased salt concentrations of up to 1.3 g/l TDS were measured in this area by BROSE (1991).
3. In the overburden above the Gorleben salt dome, the depth to base freshwater varies over short distances by up to 100 m. Two major salt water highs are located above the **southwestern salt dome edge** in the region of the ring wall as well as at the western edge of the Gorleben channel. In both of these areas, Saalian glacial till directly overlies Early Tertiary clays, which themselves directly overlie the Zechstein evaporites. As a result, the clays and glacial till are salt water bearing throughout, with the salt concentration in the pore water decreasing upwards (cf. vertical cross section A – A', borehole GoHy 920).

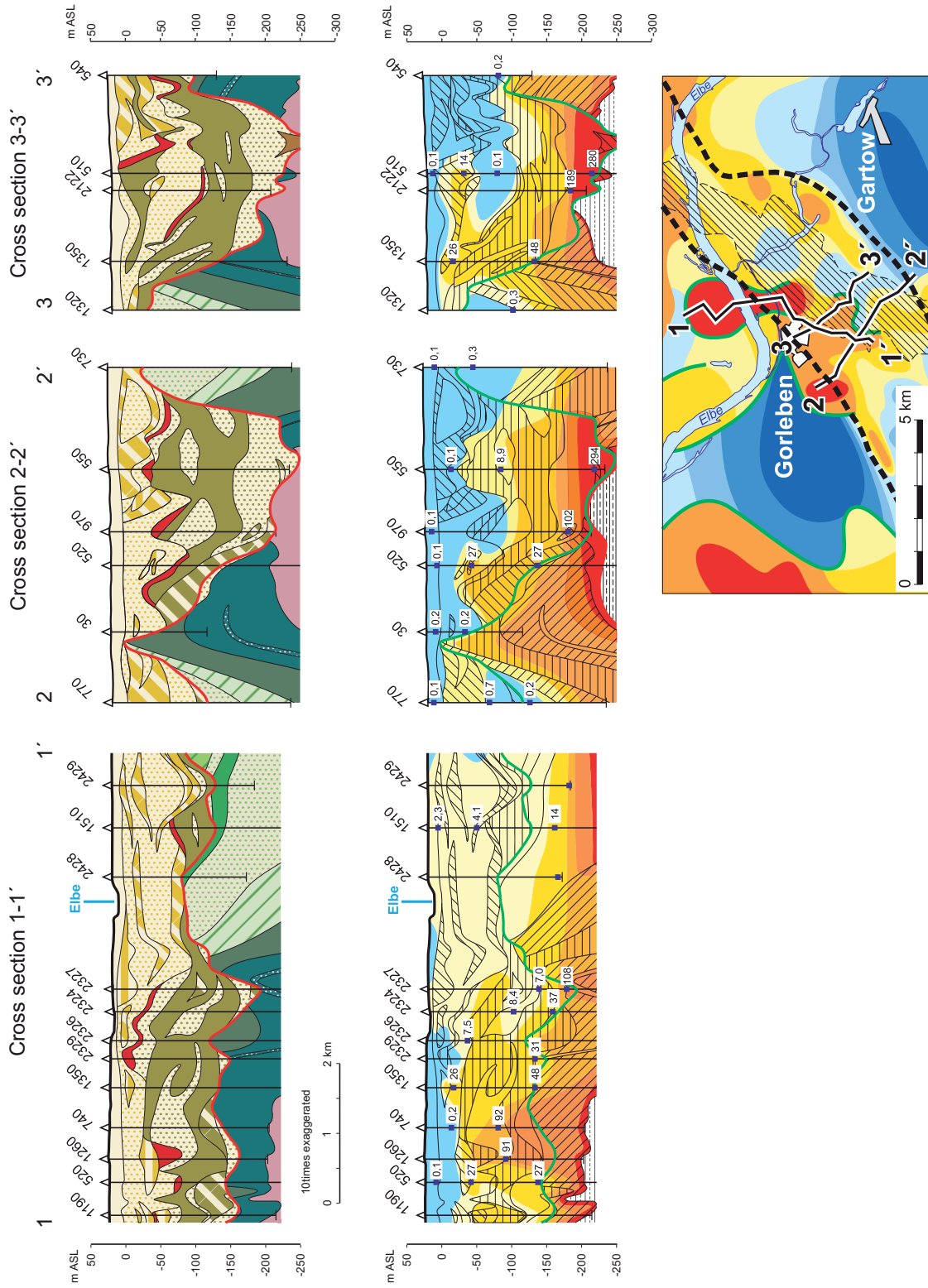


Figure 28: Hydrostratigraphic and hydrochemical vertical sections through the salt water high at the western edge of the Gorleben channel (legend see Appendix 1)

4. The second salt water high at the **western edge of the Gorleben channel** extends north-south over a length of around 6 km from the area to the south of Gorleben to the area to the north of the Elbe. Figure 28 shows the hydrogeological structure and the freshwater/salt water distribution around this high in a SSW-NNE cross section. Extremely high salinities of up to 90 g/l were measured in observation wells within the upper aquifer in the southern part of this high. High salt concentrations of this nature above the Gorleben salt dome are otherwise only encountered within the lower channel aquifer. The salt concentrations within the salt water high decrease to the north, with a parallel rise in the freshwater/salt water interface, which reaches the groundwater surface at the Elbe.

7.2 Chemical composition of the groundwater

From 1979 to 1991 and 1996 to 1999, around 1 400 chemical analyses were carried out on water samples from observation wells and production wells as part of the surface exploration of the Gorleben site. The diagrams in the following chapters are each based on a representative analysis per measuring site or well. These representative analyses were selected from the analyses with the lowest ion-balance errors.

7.2.1 Groundwater classification

The vertical subdivision into a freshwater and a salt water body corresponds to a similar vertical subdivision into chemical water types dependent on salinity. The following sequence reflects the main components of the water:

- Ca-SO₄ water
- Ca-HCO₃ water
- Na-HCO₃ water
- Na-Cl water

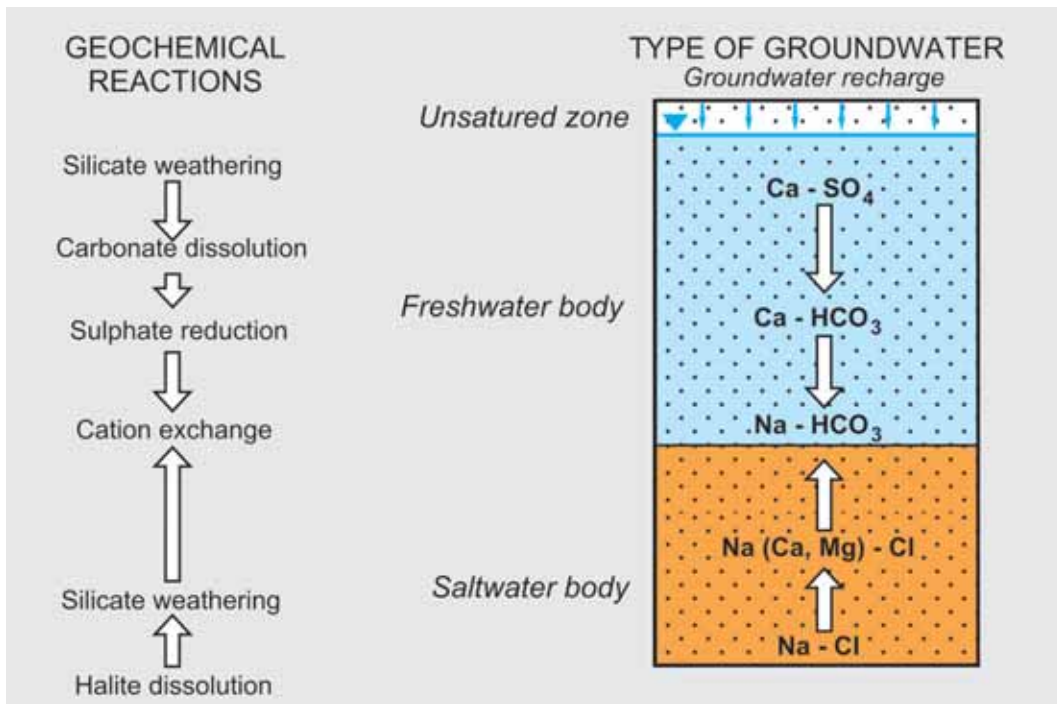


Figure 29: Schematic diagram of the vertical groundwater type zoning within the Gorleben study area

Figure 29 is a schematic diagram of the vertical zoning of groundwater types. **Ca-SO₄ waters** preferentially occur in the uppermost ten metres within the lime-free or decalcified sediments of the dune areas. The absence of lime in these sediments means that the water is undersaturated with calcite. The main weathering reaction in the soils is therefore the hydrolytic decomposition of feldspars. As a result of this, as well as the atmospheric deposition of sulphuric acid, the most frequent components in the percolating water by far are calcium and sulphate (Fig. 30). The average TDS of this very low mineralised water is 150 mg/l.

In the Elbe-Löcknitz lowland, and also in parts of the Elbe lowland to the south of the Elbe, some of the groundwater in the Lower Terrace sediments is also of this water type. However, with an average TDS of 660 mg/l, this water is much more highly mineralised than the Ca-SO₄ water in the dune areas.

These waters are the surface waters of the Elbe, which infiltrates into the shallow aquifer during floods as a result of water management measures. The anthropogenic contamination of this water also accounts for its higher TDS and raised sulphate levels (KLINGE et al. 2001).

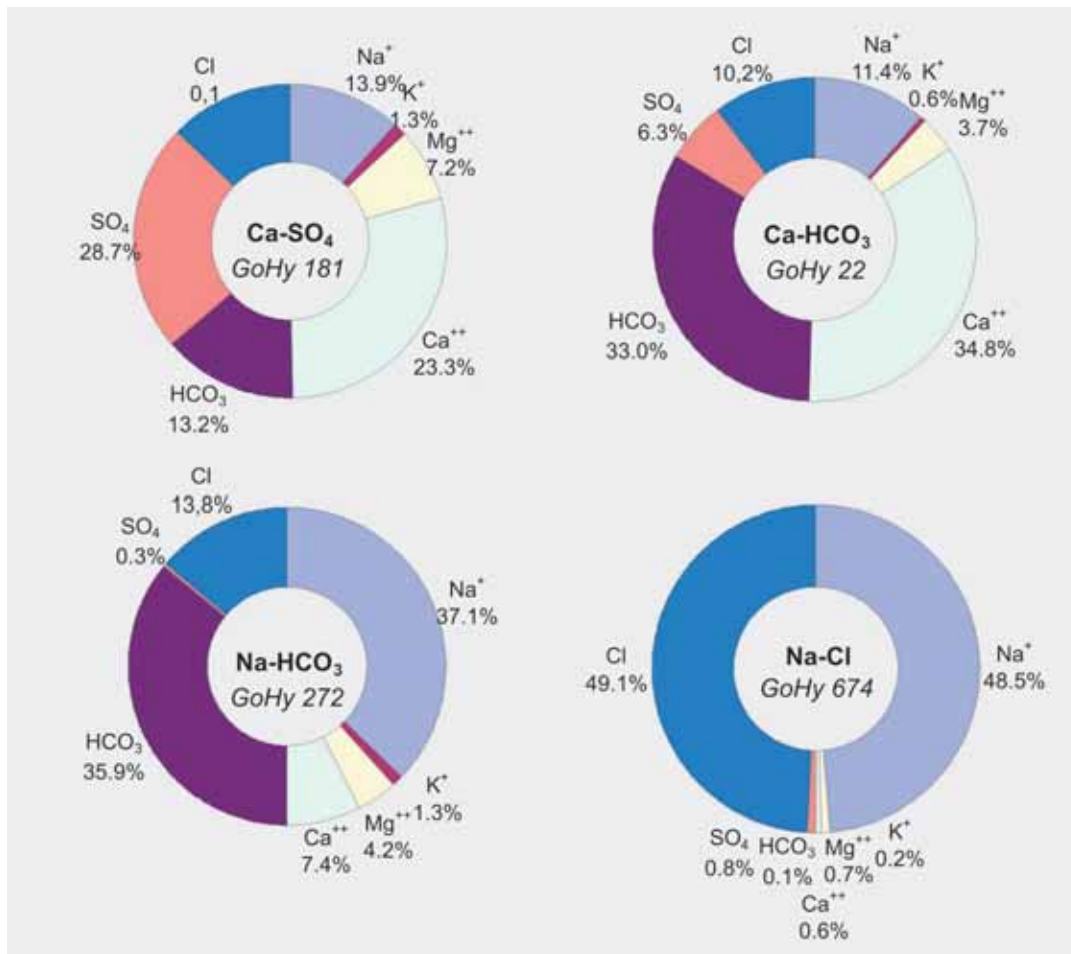


Figure 30: Chemical composition of various groundwater types within the study area

In the geest areas, the increasing lime content with depth in the sediments leads to higher Ca-HCO₃ concentrations within the groundwater. And because of the parallel decrease in sulphate concentration as a result of microbial sulphate reduction, which causes an additional increase in the Ca-HCO₃ concentration (cf. Chapter 7.2.2), **Ca-HCO₃ waters** are the dominant water type within the freshwater body at depths exceeding 25 m below ground level. The average TDS of this water is around 250 mg/l.

Na-HCO₃ waters occur locally within the freshwater body and form a third water type. This water is formed by freshwater intrusion into originally salt water-bearing aquifers. Ion exchange between sodium-bearing clay minerals and Ca-HCO₃ waters removes calcium ions from the groundwater to varying degrees and releases a proportionate amount of sodium into the water. These waters have slightly higher chloride contents than the Ca-HCO₃ waters, and, at approx. 490 mg/l, the average TDS is also higher compared to the Ca-HCO₃ waters.

The groundwater of the salt water body and the groundwater in the transition layer between the freshwater and the salt water bodies all belong to the **Na-Cl water** type, although the NaCl percentage varies from over 50 to more than 95 equivalent per cent depending on the TDS.

Figure 30 shows the composition of a salt-saturated brine from the evaporite/Quaternary sediment contact zone at the base of the Gorleben channel. The proportion of sodium and chloride in this highly mineralised water generally exceeds more than 90 equivalent per cent in each case, while the Ca-SO₄ proportion attributable to gypsum dissolution is around 2 %.

7.2.2 Geochemical interactions between groundwater and sediments

The original composition of the groundwater is subject to secondary modification by a number of geochemical interactions between the groundwater and rock minerals, as well as by microbial transformation.

The following reaction types occur:

1. Alkalisiation

The alkalisiation of groundwater is governed by ion exchange processes between groundwater and sodium-bearing clay minerals. These reactions lead to the enrichment of sodium in the groundwater and a corresponding reduction in calcium and magnesium concentrations. Only slightly mineralised groundwater is affected by alkalisiation. In extreme cases, alkalisiation leads to the formation of Na-HCO₃ waters. Na-HCO₃ waters preferentially occur around the freshwater/salt water interface, particularly when saline pore water has been displaced by freshwater as a result of a shift in the freshwater/salt water interface (cf. e.g. LÖHNERT 1970).

2. Alkali-earth alkalisiation

In salt water-bearing sediments, the chemical interactions between water and rock take place in a reverse direction: the contact of salt water with alkali earth-bearing minerals leads to the enrichment of the water in calcium and magnesium and corresponding depletion in sodium. In addition, feldspars and clay minerals become unstable through contact with saline water. Weathering reactions give rise to sodium-rich clay minerals and release of the alkali-earth elements calcium, magnesium and strontium. The highly saline waters therefore do not contain stoichiometric compositions of sodium and chloride, as would be expected in subsurface waters; instead, they have a sodium deficit with respect to chloride and associated excess alkali-earth elements.

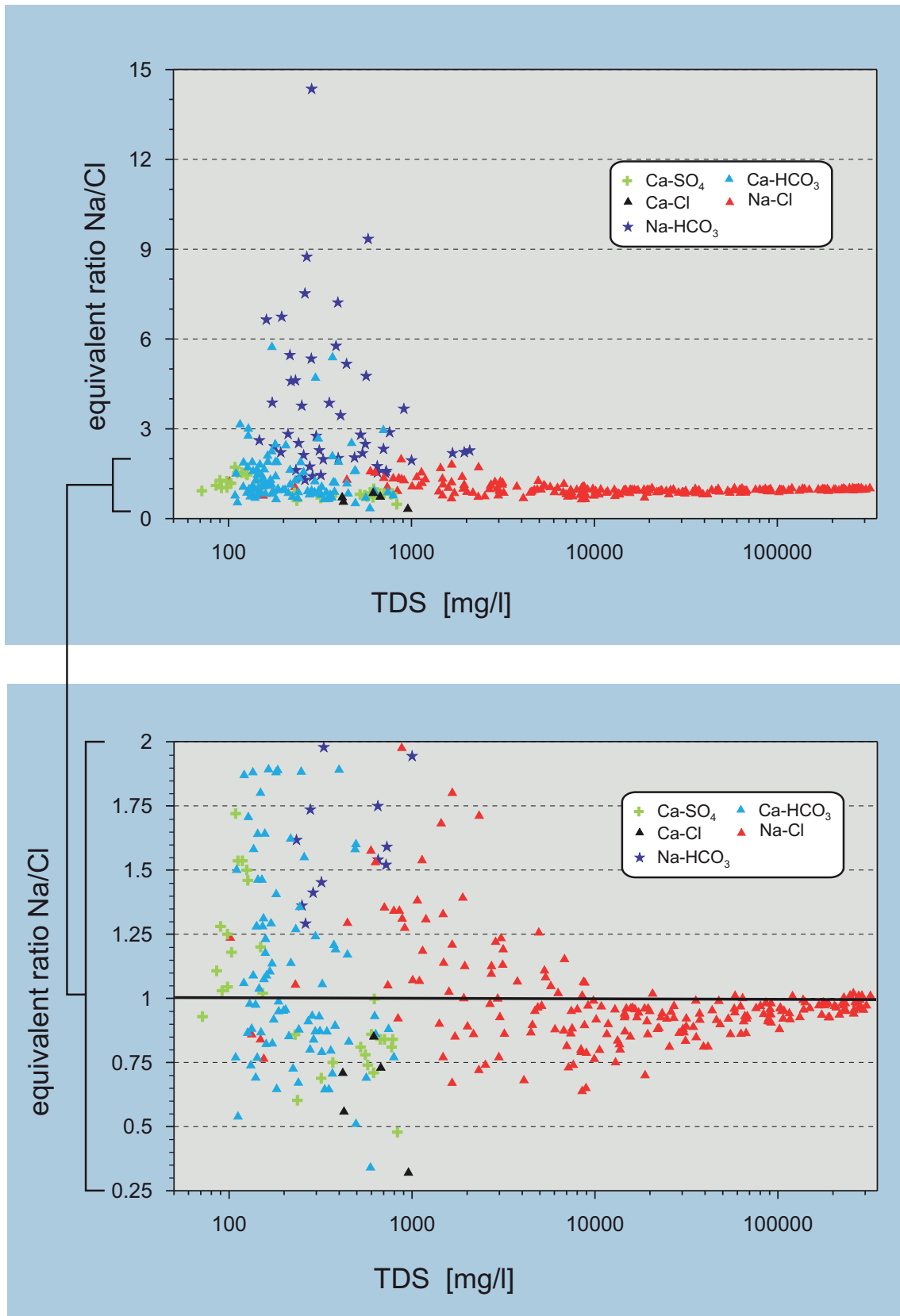


Figure 31: Na/Cl equivalent ratio in the groundwater versus TDS

3. Sulphate reduction

A large number of the deeper lying groundwaters in the freshwater body have strongly reduced sulphate concentrations compared to the shallow groundwaters. The lower sulphate concentrations are attributable to microbial sulphate reduction associated with the oxidation of organic material. Salty water, and water with medium salinities in particular, is also affected by microbial sulphate reduction.

The **alkalisation** and **alkali-earth alkalisiation** of the groundwater are demonstrated particularly clearly by the development of the Na/Cl equivalent ratio versus TDS (Fig. 31). In this and the following two diagrams, the salt concentration of the water is shown on the abscissa at a logarithmic scale to simplify the presentation. The size of the Na/Cl equivalent ratio shows the clear dependence of these reactions on the existing vertical subdivision into freshwater and salt water. A typical feature of the water in the **salt water body** – which should have a balanced Na/Cl equivalent ratio on account of its origin as subrosion water – is, as discussed, a more or less clear relative sodium deficit, arising from the aforementioned alkali-earth alkalisiation reactions. There is therefore no water within the salt water body with an Na/Cl equivalent ratio of > 1 .

The water in the **freshwater body**, i.e. groundwater with less than 1 000 mg/l TDS, has a much higher spread of Na/Cl ratios than the water in the salt water body. Waters with an Na/Cl equivalent ratio > 1 predominate, of which the group of Na-HCO₃ exchange waters has extremely high sodium concentrations. In addition, waters with considerable sodium deficits also occur within the freshwater bodies. These waters are primarily Ca-SO₄ waters from the topographic highs within the study area. In the decalcified sediments which occur here, the hydrolytic decomposition of silicates is more common than calcite dissolution. This leads to the preferential release of sodium relative to calcium.

Water samples from the transition zone between the freshwater and salt water bodies, which mineralisation changes from 1000 to 10 000 mg/l TDS, occupy an intermediate position. In general, these waters show a decline in the Na/Cl equivalent ratio from an average > 1 at the 1 g/l TDS level to values < 1 at the 10 g/l TDS level. This means that in the zone between 1 to 10 g/l TDS, there is a reversal of the water/rock exchange reactions from alkalisiation to the alkali-earth alkalisiation of the groundwater.

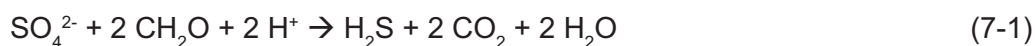
Na-HCO₃ exchange waters with extremely high Na/Cl equivalent ratios are frequently present within the lower aquifer in the Elbe-Löcknitz lowland as well as in the area south of the Elbe beneath the Gartower Tannen groundwater recharge area in the zone immediately above the freshwater/salt water interface.

No systematic relationship between the spatial positions of the observation wells is identifiable for the alkali-earth alkalisation of the salt water. However, there is a relationship with the stratigraphy of the aquifer, because salt water from Quaternary aquifers is more strongly altered as a result of alkali-earth alkalisation than waters from Tertiary aquifers. This is probably attributable to the different composition of the sediments: there are generally larger amounts of feldspar and clay minerals available in the Quaternary deposits for weathering and neogenic reactions. These give rise to higher exchange rates (KLINGE 1994).

The nature and extent of **microbial sulphate reductions** within the water is highlighted by Figures 32 and 33. The diagrams show the sulphate and bicarbonate concentrations of the groundwater versus TDS. Figure 32 also shows the calculated mixing line between a sulphate-rich saturated Na-Cl brine and a low mineralised shallow groundwater. This diagram shows that a considerable proportion of the waters in the 100 to 10 000 mg/l TDS concentration zone have very low sulphate concentrations, which cannot be genetically attributed to dilution by the mixing of highly concentrated brines with low mineralised groundwaters.

The lower sulphate concentrations are explained by microbial sulphate decomposition under anaerobic conditions with simultaneous oxidation of organic carbon.

The following formula is a typical example of this reaction:



If sulphate reduction takes place in calcareous aquifers, the CO_2 released by the reaction reacts with calcite to form bicarbonate. Figure 33 shows the influence of this calcite dissolution on the bicarbonate concentration of the groundwater: groundwaters with total dissolved solids of between 500 and 10 000 mg/l in particular have much higher bicarbonate concentrations compared to shallow waters and highly concentrated brines. On the basis of the bicarbonate content and determination of the sulphate isotope composition of the dissolved sulphate, it is possible to indirectly conclude that microbial sulphate reduction takes place up to a TDS of around 200 g/l (KLINGE 1994).

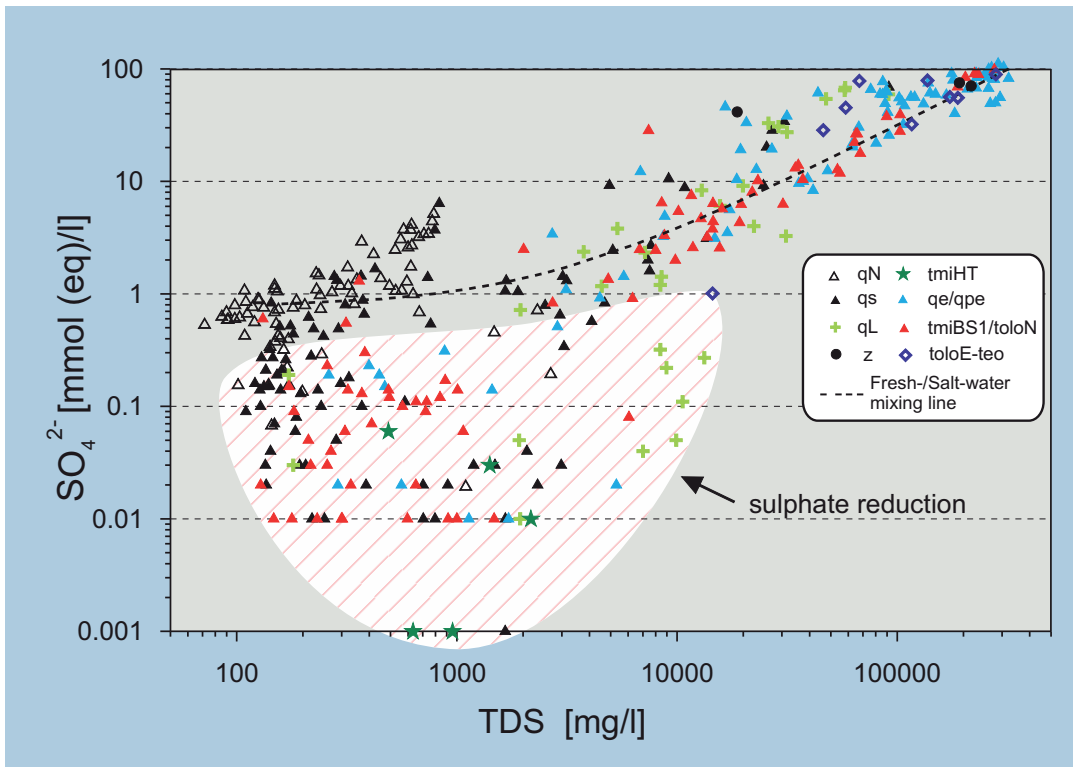


Figure 32: Sulphate concentrations of the groundwater versus TDS

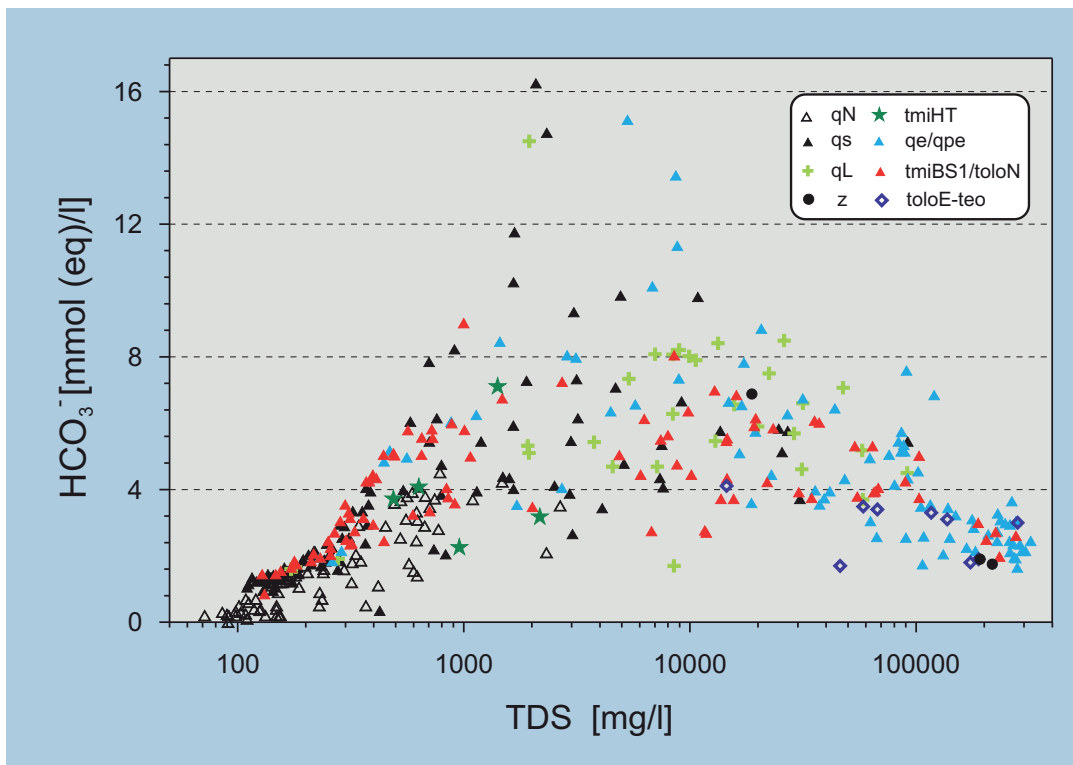


Figure 33: Bicarbonate concentrations of the groundwater versus TDS

Because practically all sediments have organic material in the form of lignite partings in the Untere Braunkohlensande, or contain finely dispersed detritus from reworked Braunkohlensande in the Quaternary sediments, sulphate reduction is largely dependent on the depth-dependent oxygen concentration within the groundwater. A general reduction in sulphate content with increasing depth is therefore observed within the freshwater body. A notable feature is the strong reduction in the range of sulphate concentrations at a depth of 20 to 30 m below ground level, which documents the start of sulphate reduction at this depth (KLINGE 1994).

7.3 Isotope-hydrological investigations

The main objective of the isotope-hydrological investigations was to date the groundwater with the help of tritium (^3H) and ^{14}C as well as the stable environmental isotopes ^{18}O and deuterium (^2H , D). In addition, the noble gas concentration in the groundwater was also analysed.

The analysis was carried out by the Institute of Environmental Physics of the University of Heidelberg, and in some cases by the Institute for Radiohydrometry at GSF/Neuherberg. In the area south of the Elbe, highly saline waters from the lower part of the Gorleben channel were preferentially sampled. Sampling and analysis took place in 1985 and in 1990/1991. Samples from some observation wells in the rim synclines were also analysed for comparative purposes. Overall, samples from 82 wells in the area south of the Elbe were analysed by the University of Heidelberg. In addition to these investigations, measurements of the ^{18}O content from samples from all observation wells were taken throughout the area. The results of this analysis were discussed by SUCKOW (1993).

In the area to the north of the Elbe, measurements of the environmental isotopes ^{18}O and deuterium (D), as well as the radioactive elements tritium and ^{14}C were carried out at all groundwater observation wells. These investigations were supplemented by the determination of noble gases He, Ne, Ar, Kr and Xe at 14 selected observation wells, as well as special investigations on core samples (RÜBEL 2000).

7.3.1 Tritium

Tritium occurs naturally, primarily in the upper atmosphere, as a result of the impact of cosmic radiation on nitrogen atoms. It decomposes with a half life of 12.4 years. The natural tritium concentration in precipitation in Central Europe is approx. 6 TU (tritium units). Because of the increased production of tritium as a consequence of nuclear weapon testing since 1952/53, dating requires additional information on the tritium

deposition function in groundwater, and the change in tritium concentration over time in the atmosphere. The tritium concentration then allows the age of the groundwater to be interpreted in relation to the maximum atmospheric tritium concentration in 1963/64. Groundwater recharged prior to this period is tritium-free.

Tritium measurements can also indirectly provide information on the tightness of groundwater observation wells: deeper wells in which tritium is detected despite the expected higher age of the water generally have leaks in the casing, which allow shallow tritium-bearing groundwater to intrude into the well during pumping.

Tritium concentration measurements have been carried out in Gorleben since the start of the isotope investigation programme. Up to 1985, the detectable limit was relatively high at 0.4 TU because of the measuring technique used. A change in measuring technique since 1990 has considerably reduced the detectable limit to 0.08 TU and in some cases 5 mTU. For this reason, Figure 34 only presents the results recorded since 1990.

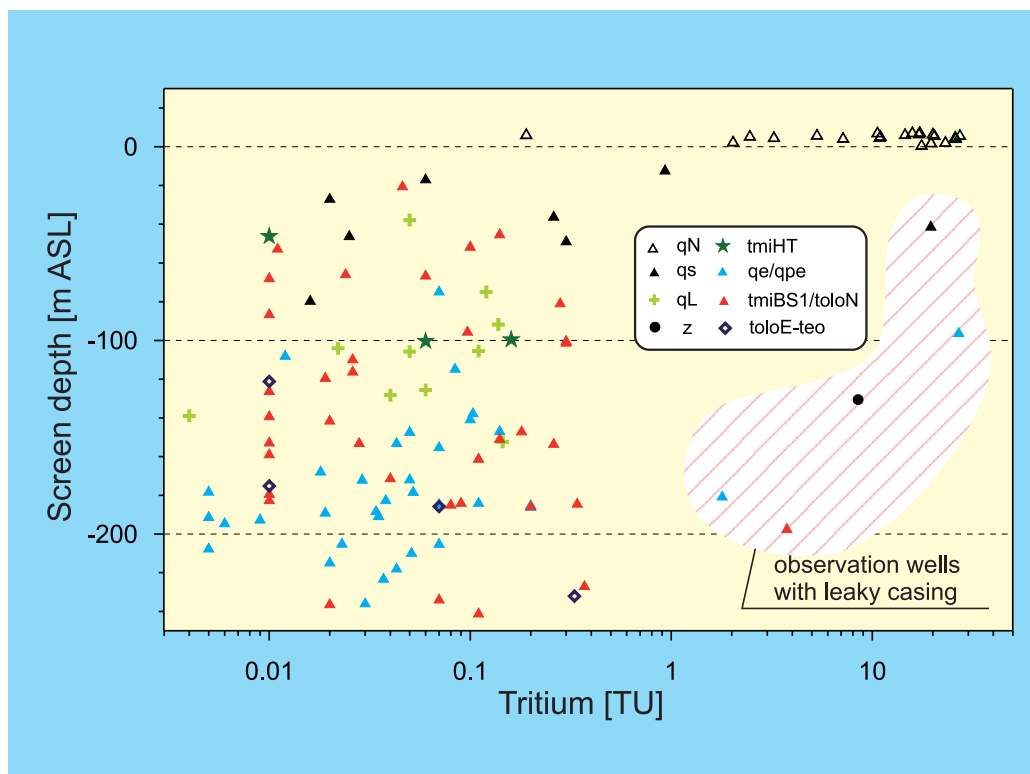


Figure 34: Depth profile of measured tritium concentrations in groundwater

As expected, significant tritium concentrations were only measured in shallow groundwater observation wells – with the exception of five other observation wells. The samples in all other observation wells have very low tritium concentrations, generally lower than 0.1 TU to a maximum of 0.5 TU. This value corresponds to the mixing in of 2 % precipitation from 1990. These samples can therefore be considered as practically tritium-free. The unusually high tritium concentrations in five deep groundwater observation wells clearly indicate leaky casings. Because of this clear demonstration of contamination by shallow groundwater, these samples were no longer included in the further analysis.

The tritium concentration in observation wells in the shallow aquifer (qN) varies between 5.3 and a maximum of 27.3 TU – with the exception of four samples – and the groundwater has thus been recharged since 1963/64. Four observation wells with much lower concentrations of 0.2 to 3.2 TU are located in the Elbe-Löcknitz lowland where the water regime influenced by the Rhinow canal favours the upwelling of older, relatively tritium-free groundwater (KLINGE et al. 2001).

7.3.2 Stable oxygen and hydrogen isotopes

In addition to the frequently occurring light oxygen and hydrogen isotopes ^{16}O and ^1H , the stable isotopes within natural waters also include the rarer heavy isotopes ^{18}O and ^2H (D). The isotope ratios of the stable hydrogen and oxygen isotopes are given as deviations (δ in ‰) from standard mean ocean water SMOW.

Various effects result in changes in the isotopic composition of precipitated water. Because of the different masses and vapour pressures of the isotopes, temperature-dependent isotope fractionation can occur at the transition from the liquid to the gaseous phase, and vice versa. Because heavier water molecules preferentially condense and precipitate, precipitation becomes isotopically lighter with lower ambient temperatures. This isotopic depletion is highlighted by the lower δ values of precipitation. Another fractionation effect is the isotopic depletion of precipitation with increasing distance from oceans as well as a rise in topography of the earth's surface.

According to CRAIG (1961), the concentrations in precipitation follow the “Global Meteoric Water Line” (GMWL) throughout the world according to the expression:

$$\delta\text{D} = 8 \times \delta^{18}\text{O} + 10 \quad (7-2)$$

When groundwater is recharged, information on the environmental conditions is stored in the isotopic composition of the water. The ratio of the ^{18}O to ^{16}O oxygen isotopes and the ^2H (Deuterium) to ^1H hydrogen isotopes therefore permit conclusions to be drawn on the ambient temperature of the groundwater at the time of recharge. In this way, groundwater formed during the Pleistocene glaciations has more negative values than groundwater generated during the Holocene.

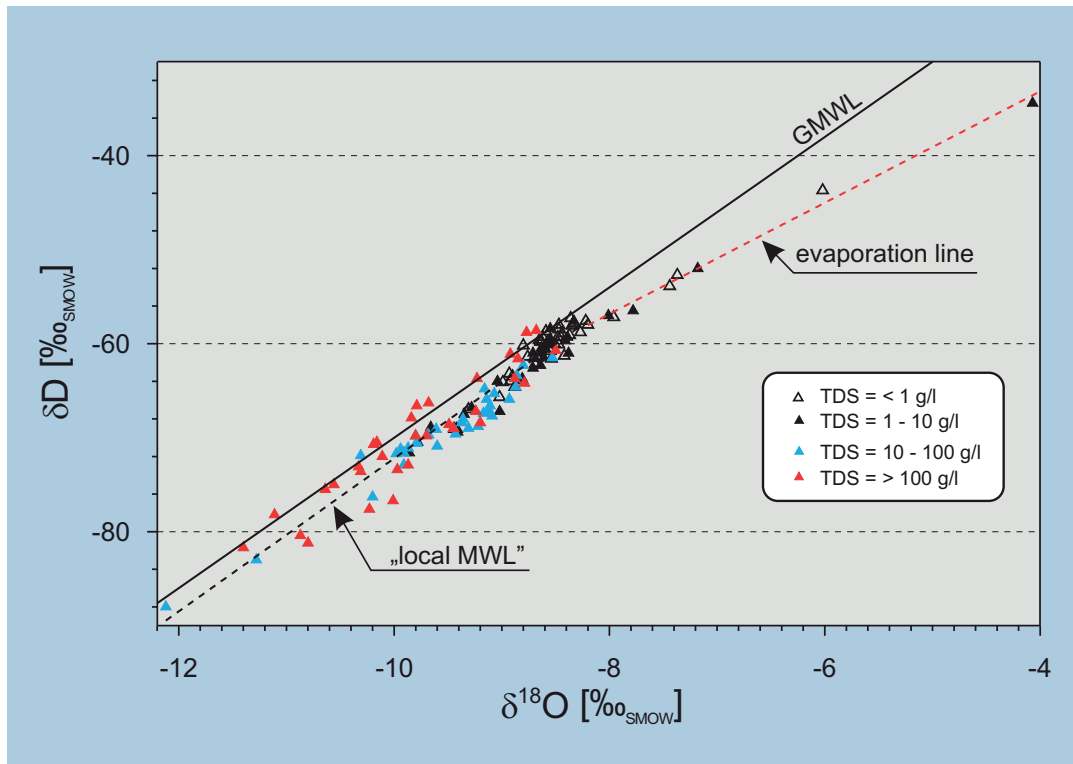


Figure 35: Correlation between $\delta^{18}\text{O}$ and δD

Figure 35 presents the $\delta^{18}\text{O}/\delta\text{D}$ ratio in the groundwater samples in the study area. The data points of the water in the diagram are represented by different symbols depending on their TDS. This diagram shows that most of the data points do not lie along the Global Meteoric Water Line, but are grouped along a regression line expressed by

$$\delta\text{D} = 8.1 \times \delta^{18}\text{O} + 9.1 \quad (7-3)$$

which lies beneath the GMWL. This can be considered as a local meteoric water line according to Suckow (1993).

A small group of nine samples differs from the remaining samples by their clear enrichment in ^{18}O and deuterium isotopes. With respect to the GMWL, the regression line for these data points has a shallower gradient ($\delta D = 5.9 \times \delta^{18}\text{O} - 9.5$). These are freshwater samples from shallow groundwater observation wells in the lowland between the Elbe and Lößnitz, and the Seege lowland south of Gartow. The shape of the regression lines is characteristic for isotope enrichment as a result of evaporation. This can be explained by the mixing in of partially evaporated surface water. Because of the shallow depth of the water table in the river valley, groundwater evaporation in a large part of this area exceeds groundwater recharge (Chapter 3.3).

With respect to the data points grouped along the local meteoric water line, the salty water samples are generally isotopically more negative than the freshwater samples. This indicates that the salt water was apparently formed under colder climatic conditions than the freshwater.

Figure 36 shows the $\delta^{18}\text{O}$ figures versus the groundwater TDS. This figure shows the relationship between TDS and the isotope values even more clearly:

- The **low mineralised shallow groundwaters** (< 1 g/l) of the Lower Terrace sediments (qN) form a uniform data group – with the exception of samples enriched by evaporation (zone I). The $\delta^{18}\text{O}$ values range from -8.1 to -9.1 ‰. The freshwater data points from the lower aquifer (qe, tmiBS1/tolo) also lie within the shallow freshwater data zone.
- With respect to the **saline waters** with salt concentrations between 1 g/l and around 100 g/l, the isotope composition tends to shift towards more negative values with increasing TDS. Waters with salt concentrations between 1 g/l and around 6 g/l are still classified as freshwater, whilst more saline water is mainly grouped to the left of this data zone, i.e. isotopically depleted.
- The **highly mineralised Na-Cl brines** with more than 200 g/l TDS form a data group with very variable $\delta^{18}\text{O}$ signatures which range from strongly depleted values of -12.1 ‰ to $\delta^{18}\text{O}$ signatures typical of shallow groundwater (-8.6 ‰). Most of the samples are from the lower aquifer in the Gorleben channel (qe) and the Untere Braunkohlensande (tmiBS1/toloN) in the centre of the northwestern rim syncline, as well as from the cap rock in the Gorleben channel area, and from Oligocene and Eocene aquifers in the ring wall area.

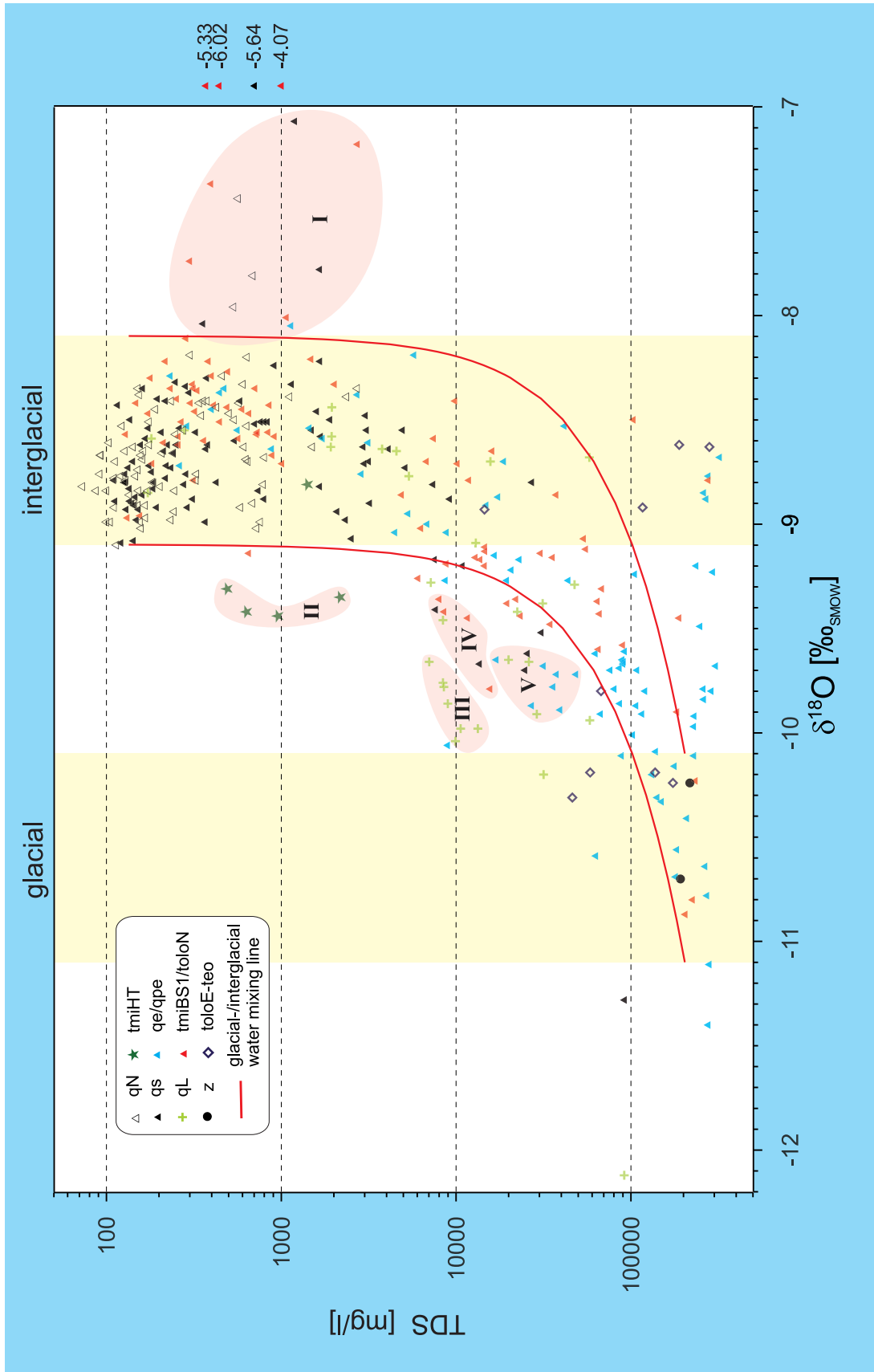


Figure 36: Relationship between $\delta^{18}\text{O}$ and groundwater TDS

In the case of the shallow freshwaters, these are certainly young waters only a few years or at most a few decades old. This is demonstrated by their tritium concentrations, etc. Even where the freshwater within the lower aquifer has no measurable tritium concentration, the $\delta^{18}\text{O}$ values of between -8 and -9 ‰ show that these groundwaters were also formed during interglacial climatic conditions. The oxygen and hydrogen isotope composition of both groups of freshwater therefore reflects interglacial recharge conditions. It can be assumed from the general understanding of climatic conditions during the Pleistocene and the isotopic composition of groundwater generated during Pleistocene glaciations, that the $\delta^{18}\text{O}$ values of these glacial waters are around 2 ‰ lower than the equivalent values for interglacial generated groundwater (KLINGE et al. 2000). This is also shown by the isotopic composition of the pore water in the Lauenburger-Ton-Komplex (qL) (cf. Chapter 7.3.4).

Figure 36 supports the conclusion that around 30 % of the brine samples were formed during glaciations. Two mixing lines are shown in the diagram, which represent the change in $\delta^{18}\text{O}$ values versus TDS for an assumed mixture of glacial brines and interglacial freshwaters. The end components of the mixing series are the upper and lower limits of the range of fluctuation of the $\delta^{18}\text{O}$ values of the freshwater, or the corresponding around 2 ‰ lower limiting values for the isotopically depleted salt water. The diagram shows that the data points of most of the salt water samples with lower salt concentrations lie in the area between the two mixing lines. It can therefore be concluded that these waters were generated by the mixing of glacial brines and Holocene freshwater generated under interglacial climatic conditions.

Around 50 % of the brines with > 200 g/l TDS, and the data points for the freshwaters enriched by evaporation (zone I), lie outside of this mixing zone. These waters are grouped to the right and below the mixing lines. Waters with a higher mixing isotope composition whose data points lie to the left or above the two mixing lines can be clustered as follows:

- Freshwater or low saline salt water samples from the Hamburg-Ton to the north of the Elbe, which are strongly isotopically depleted compared to the corresponding freshwaters in the upper and lower aquifers (zone II)
- Salt waters from sandy layers within the Lauenburger-Ton-Komplex from observation wells installed as part of the long-term pumping test within the Gorleben channel to the south of the Elbe (zone III)¹
- One small sub-group of salt waters from the Untere Braunkohlensande from observation wells at the northern edge of the northwestern rim syncline (zone IV), as well as a small sub-group of salt waters from the Elsterian channel sands at the edge of the Gorleben channel (zone V)

¹ To make things more comprehensible, the associated data zone is marked in each case in Figure 36. Individual data points which fall within neighbouring zones are also assigned to these data groups.

With all of these waters, the position of the data points supports the interpretation that the isotopically depleted salt water components of these waters mainly have lower TDS values than the brines in the centre of the Gorleben channel or the northwestern rim syncline.

As discussed earlier, the **highly mineralised Na-Cl brines** with more than 200 g/l TDS form a data group with a large range in $\delta^{18}\text{O}$ signatures, which cover the whole spectrum of glacial and interglacial isotope types. The waters occur within the Gorleben channel and the centre of the northwestern rim syncline – with the exception of four samples from the cap rock and Eocene aquifers. These waters were apparently generated from a mixture of glacial and interglacial brines.

Figure 37 shows the spatial distribution of these waters and their isotopic signatures. The diagram differentiates between glacial and interglacial waters, and waters with mixed isotopic signatures. The diagram reveals that the waters in the centre of the northwestern rim syncline are of glacial character throughout. Within the Gorleben channel, there is generally a rapid alternation of different water types, although brines with glacial signatures only occur in the southern and central sections of the channel, whilst waters with clear interglacial signatures occur in the central and northern parts of the channel. These interglacial brines occur mostly in the deepest parts of the channel aquifer, as do the glacial-type waters, whilst waters with mixed signatures dominate in the upper part of the aquifer.

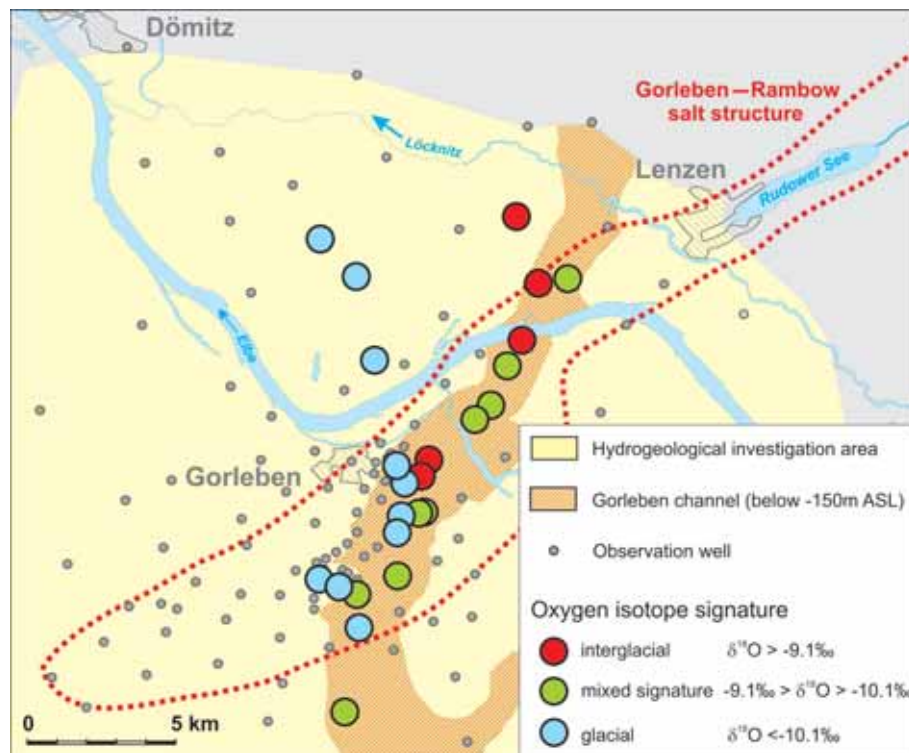


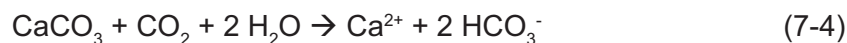
Figure 37: Oxygen isotopic signatures of salt water with > 200 g/l TDS

7.3.3 ¹⁴C age dating

Radiocarbon is continuously formed in the atmosphere from atmospheric nitrogen, by nuclear reactions. If carbon is removed from the atmospheric carbon cycle, the ¹⁴C concentration in sealed samples decreases with a half life of 5 730 years in accordance with the laws of radioactive decay.

The initial concentration of ¹⁴C in recent groundwater is mainly determined by the metabolism in the unsaturated soil zone. The ¹⁴C content of the dissolved CO₂ associated with the infiltrating water, is close to 100 pMC (per cent modern carbon). Because of the microbial decomposition of organic matter, the ¹⁴C content of soil air is normally also approx. 100 pMC.

Further changes in ¹⁴C concentration of the percolating rain water are influenced by the carbonate available in the aquifer. The dissolved CO₂ reacts with carbonates to form bicarbonate:



Ideally, this leads to a doubling of the dissolved inorganic carbon in the water. Because carbonate in the rock is generally ¹⁴C-free, the ¹⁴C concentration in the water drops to approx. 50 pMC. Young newly recharged groundwater would therefore generally have ¹⁴C concentrations of around 50 pMC. In reality, the ¹⁴C concentration is usually much higher, at around 85 pMC. The higher ¹⁴C concentrations are explained by the exchange of CO₂ between the soil air and the groundwater, i.e. groundwater and soil air form an open system. This exchange increases the initial concentration of ¹⁴C in the water. As a simplification, the initial concentration was therefore defined as 85 pMC by RÜBEL (2000) and SUCKOW (1994). In decalcified or largely decalcified sediments, which are widespread at shallow depths in the Gorleben area outside of the floodplains, the reaction described above does not lead to complete inversion of the dissolved carbon dioxide into bicarbonate. It can only proceed completely in deeper zones, where the sediments have higher calcite concentrations. However, in these closed systems, exchange with the soil air no longer takes place. The initial concentration of ¹⁴C in these waters therefore dropped down to around 50 pMC.

Redox reactions can cause other changes in the ¹⁴C content of the groundwater within the aquifers. In addition to iron and nitrate reduction, the ¹⁴C concentration is primarily influenced by microbial sulphate reduction. Oxidation of the dissolved organic matter in the groundwater generates additional carbon dioxide, which leads to calcite dissolution and thus to the formation of additional bicarbonate of organic and inorganic origin in

the groundwater (see above). This enrichment in bicarbonate leads to dilution, i.e. to a reduction in the ^{14}C concentration in the groundwater when fossil ^{14}C -free organic matter is reduced.

In principle, a correction can be made for the additional carbonate input resulting from microbial sulphate decomposition on the basis of the measured $\delta^{13}\text{C}$ values of the carbon if recent carbon has been oxidised. It is not, however, possible to correct for the decomposition of ^{14}C -free organic matter. Another possible limitation arises from the fact that all Quaternary deposits, including the shallow sediments of the Lower Terrace, contain finely dispersed lignitic detritus derived from reworked lignite partings in the Miocene Braunkohlensande. ^{14}C measurements of the dissolved organic carbon in samples from the Gorleben study area, undertaken as part of a research project, gave unrealistically high water ages of several thousand years for young shallow groundwaters (BUCKAU et al. 1993). It must be assumed that the low ^{14}C concentrations in the dissolved organic carbon is a result of the breakdown of ^{14}C -free lignitic material in the soil. For this reason, the initial concentrations of ^{14}C in such cases can lie well below 80 pMC.

As a consequence, dating the groundwater in the Gorleben area using the ^{14}C method generally involves major uncertainties. The significance of ^{14}C measurements is primarily that, in conjunction with measurements of the oxygen and hydrogen isotope composition, they enable the age of the water to be estimated within an order of magnitude, or enable these measurements to be validated. It can therefore be assumed for a ^{14}C value of > 25 pMC, that water was formed in the Holocene. Holocene formation is even probable with values of 12 pMC. Because of the uncertainties described here, this report generally avoids the conversion of ^{14}C measured data into model ages.

In Figure 38, the ^{14}C concentrations of the groundwater are presented at a double logarithmic scale versus TDS. For the majority of the waters with total dissolved solids up to a maximum of around 100 g/l, this diagram generally shows a decline in ^{14}C concentration with increasing TDS, which correlates with the described depletion in the stable deuterium and ^{18}O isotopes. By way of contrast, the ^{14}C concentrations of the highly saline waters with more than 200 g/l TDS vary over a wide range between the detection limit at around 1 pMC to a maximum of 30 pMC. The diagram again shows analogies here with the correlation diagram between $\delta^{18}\text{O}$ and TDS, whereby the five brines with an interglacial isotopic signature also have the highest ^{14}C concentrations within this data group.

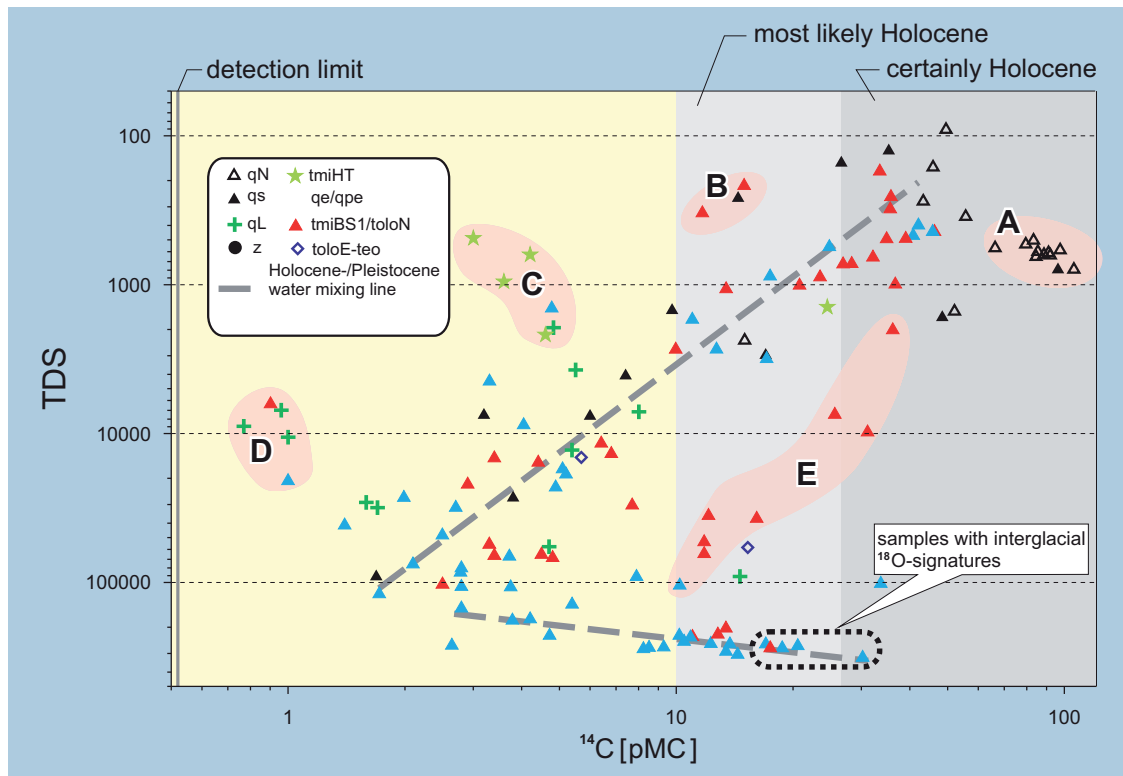


Figure 38: ^{14}C concentrations of groundwater versus TDS

As expected, the highest ^{14}C concentrations were found in the shallow groundwaters (qN). In detail, the relatively highly mineralised freshwaters in the Elbe-Löcknitz lowland (zone A in Figure 38) with around 70 pMC to 100 pMC, have much higher ^{14}C concentrations than the low mineralised waters in the geest areas to the south of the Elbe, with ^{14}C concentrations of around 30 to 40 pMC. Because of the uniform presence of tritium, all of these waters are very young groundwaters or mixed waters whose young components are only a few decades old at most.

The strong variations in ^{14}C concentrations in the waters reflect their different genesis. The groundwaters in the Elbe-Löcknitz lowland contain varying proportions of Elbe river water (KLINGE et al. 2001). As a result, the ^{14}C concentrations in the groundwater resemble the natural ^{14}C concentration in the atmosphere. The groundwater in the geest areas arises from the infiltration of precipitated water in the shallow, largely decalcified sands. Because of the reaction between infiltration waters and sediments described in the introduction, their ^{14}C concentrations are primarily only around half as high as in the groundwaters of the Elbe-Löcknitz lowland. This again highlights the fact that it does not make sense to convert ^{14}C concentrations into conventional ^{14}C ages for the waters in the study area.

In Figure 38, another four groups of waters are marked which deviate from the general trend because of their unusually low (zones B to D) or unusually high ^{14}C concentrations (zone E). The waters in zones C and D are samples from the Lauenburger-Ton-Komplex and Hamburger-Ton aquitards, whose $\delta^{18}\text{O}$ values are also lower than those from samples with comparable salt concentrations in the aquifers. This supports the thesis that these pore waters are of glacial character with low primary salt concentrations (cf. Chapter 7.3.2). In addition, the low sulphate concentrations and in some cases markedly high bicarbonate concentrations, as well as the ^{34}S isotope values (BERNER et al. 2001) show that these waters are strongly sulphate reduced in an analogous way to the samples in zone B, and that this has also lowered the ^{14}C concentrations.

The samples with unusually high ^{14}C concentrations in zone E are from salt water in the transition zone between the highly saline brines in the centre of the rim syncline and the overlying artesian freshwaters. These waters arose by the mixing of glacial brines with young freshwater within the lower aquifer. According to the ^{18}O values (Fig. 36), they contain 30 to 50 % Holocene water – which does not contradict the ^{14}C values. The salt concentration in the Pleistocene component must therefore have been just below 160 g/l according to Figure 36, and accounts for the downward shift observed in Figure 38.

In conclusion, the following deductions can be made from the ^{14}C concentrations of the water:

- The general reduction in ^{14}C concentrations with increasing TDS supports the interpretation of the oxygen and hydrogen isotope compositions that the salt water primarily arose through the mixture of young, Holocene interglacial freshwater with Pleistocene glacial salt water.
- The very high ^{14}C concentrations of up to 30 pMC in the NaCl brines with interglacial isotopic signatures within the Gorleben channel are an additional indication of the young age of this water. It is highly probably that this water is post-glacial infiltrated Holocene water which has become salty through contact with the Zechstein evaporite. The theoretically feasible formation of this water during the course of a Pleistocene Interglacial can be excluded with a high degree of certainty.

7.3.4 Analysis of core samples from the Hamburg-Ton and Lauenburger-Ton-Komplex

The whole thickness of the Hamburg-Ton and Lauenburger-Ton-Komplex aquitards was cored in 4 boreholes as part of the drilling programme in the Elbe-Löcknitz lowland. This core material was used to determine the isotopic composition of the pore water as well as the salt and noble gas concentrations. The sampling and analysis techniques are described in detail in RÜBEL (2000).

The investigations revealed a number of important new findings about the isotopic compositions of the pore water and the hydraulic properties of these aquitards. In addition, they generated new results, which allow conclusions to be drawn on the condition of the overall system during the Pleistocene glaciations. The results are discussed in the following, using two boreholes as examples.

Figure 39 shows the change in salt and helium concentration with depth, as well as the $\delta^{18}\text{O}$ and δD values measured in the pore waters of the Lauenburger-Ton-Komplex from the GoHy 1623 borehole. The borehole is located at the northern edge of the study area in the centre of the Gorleben channel. The 75 m thick Lauenburger-Ton-Komplex consists of thick, continuous clayey-silt units as well as a few thin sandy beds. The upper aquifer in the Saalian and Weichselian sediments is completely freshwater-bearing in the section penetrated by the borehole. Beneath the aquitard in the Elsterian channel sands, there is a thin freshwater body underlain by highly saline water. The pore waters in the Lauenburger-Ton-Komplex have largely constant, slightly raised salt concentrations in the order of around 3 g/l TDS.

Figure 39 is the depth section of the **$^4\text{helium excess}$** versus the solution equilibrium with the atmosphere (referred to below as $^4\text{He}_{\text{exc}}$). ^4He is generated by the radioactive breakdown of uranium and thorium. Because these elements are primarily bound to clay minerals, the in-situ production of ^4He is much higher in clays than in sands. And as a result of the longer residence time of pore water within the pores of aquitards, there is a significant enrichment in ^4He in such sediments. The concentration distribution of the helium allows conclusions to be drawn on the pore water flow and material transport in aquitards. And in principle, if information is available on $^4\text{helium}$ production rates, the $^4\text{helium}$ concentration can be used to estimate the age of pore water to the nearest order of magnitude.

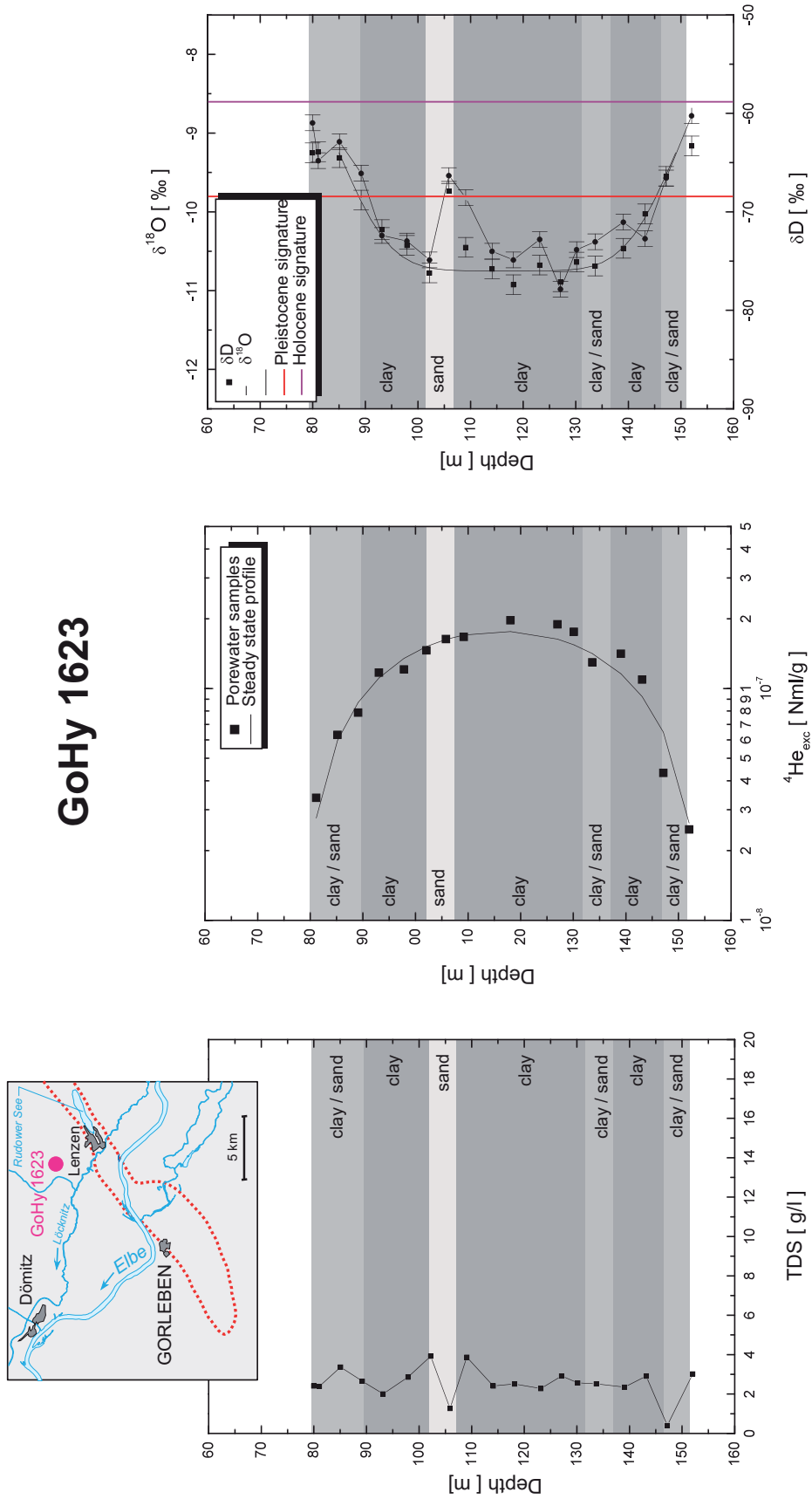


Figure 39: Depth section of salt concentration, $^4\text{He}_{\text{exc}}$ and $\delta^{18}\text{O}$ and δD measured values in the Lauenburger-Ton-Komplex pore water in the GoHy 1623 borehole

The $^4\text{He}_{\text{exc}}$ concentration profile in Figure 39 has a symmetrical parabolic curve with low $^4\text{He}_{\text{exc}}$ at the upper and lower edges and a maximum – approximately one order of magnitude higher – in the centre of the Lauenburger-Ton-Komplex. According to RÜBEL (2000), this profile can be explained by equilibrium between the in-situ production of helium in the clay, and the molecular diffusive loss into the overlying and underlying aquifers containing young pore waters with low helium concentrations. According to RÜBEL (2000), around 80 000 years are required for this diffusion profile to establish itself. This is a certain indicator that no significant advective vertical groundwater flow has taken place within the Lauenburger-Ton-Komplex

Another piece of supporting evidence for the lack of advective groundwater flow in this aquitard are the stable oxygen and hydrogen isotope profiles: the pore waters have glacial signatures throughout. The Pleistocene glacial pore waters are only successively displaced by younger interglacial Holocene groundwaters at the upper and lower margins of the aquitard. These younger glacial groundwaters circulate in the overlying and underlying freshwater-bearing aquifers. The low depth of penetration of these Holocene waters of only a few metres also indicates very minor or completely absent vertical pore water flow.

Figure 40 shows the depth section of the salt and helium concentration as well as the $\delta^{18}\text{O}$ and δD recorded values from the pore waters of the Hamburg-Ton in the GoHy 1674 borehole. This borehole lies at the centre of the Elbe-Löcknitz lowland in the distribution area of the Hamburg-Ton. The freshwater/salt water interface in the area penetrated by the borehole is only 20 m below ground level and lies within the upper Saalian aquifer. The lower sections of the upper aquifer as well as the Hamburg-Ton and the underlying Untere Braunkohlensande of the lower aquifer are salt water-bearing throughout. The salt concentrations at the base of the lower aquifer exceed 200 g/l TDS.

Unlike the Lauenburger-Ton-Komplex, the Hamburg-Ton is characterised by intensively interbedded sandy, silty and clayey layers. Compact massive clay layers only appear at the base of the sequence. The different properties of these lithologies are also strongly reflected in the helium concentration profiles of the pore water. The depth section of the helium concentration in the pore water shows a logarithmic increase with depth. It is probable that this exponential curve continues into the lower aquifer, because the values recorded in a deeper observation well at the base of the lower aquifer also lie on the continuation of this regression line. The $^4\text{He}_{\text{exc}}$ value in this well is around one order of magnitude higher than the corresponding value in the central part of the Lauenburger-Ton-Komplex.

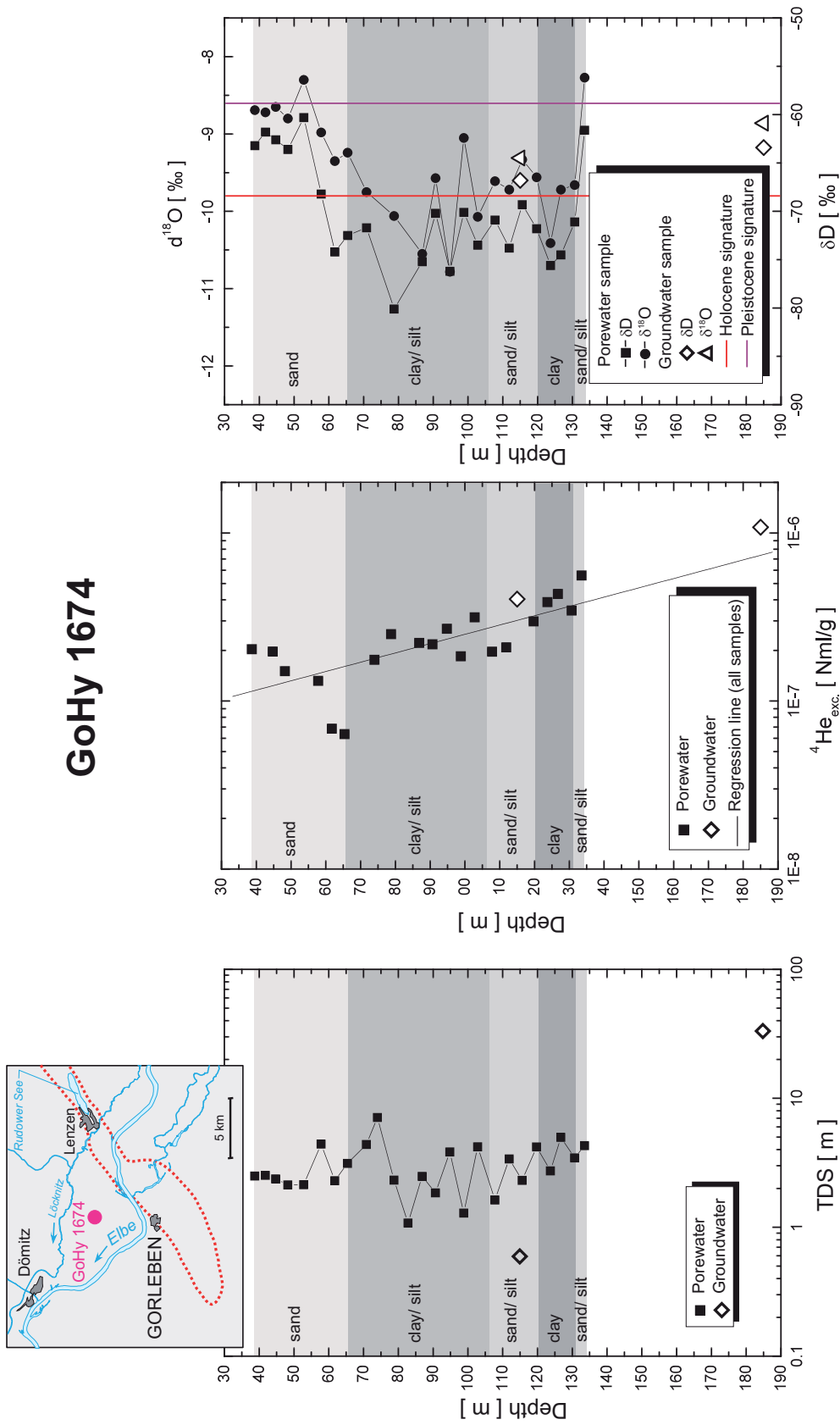


Figure 40: Depth section of salt concentration, the $^4\text{He}_{\text{exc}}$ and the $\delta^{18}\text{O}$ and δD recorded values in pore water from the Hamburg-Ton in the GoHy 1674 borehole

The exponential curve shows that a completely different helium transport mechanism must exist in the borehole within the Hamburg-Ton compared to the Lauenburger-Ton-Komplex. According to RÜBEL (2000), the profile in the Hamburg-Ton reflects the diffuse upward vertical flow of helium through the Hamburg-Ton giving rise to net helium transport into the upper aquifer. At the same time, the high helium concentrations in the highly saline groundwater at the base of the lower aquifer indicate long groundwater residence times.

The depth sections of the stable isotopes show a much stronger variation over a shorter distance compared to the GoHy 1623 profile. The isotopes are generally depleted in the interior of the formation and thus indicate generation of the pore waters during a glacial period. The waters tend to be less depleted within the mainly sandy-silty layers than within the clay sections. This points to the flow of younger Holocene water into the more permeable beds. The average difference between the deuterium values of around 5 ‰ indicates that the proportion of mixed-in younger Holocene water in the sandy beds could be around 25 %. In both boreholes, the pore waters in the sandy beds at the upper and lower edges of the formation have clear Holocene isotopic signatures.

Overall, the evidence indicates that the aquifer system in the Elbe-Löcknitz lowland was filled with salt water for long periods, at least during the last Pleistocene glaciation, so salt water with glacial signatures could diffuse into the aquitards from the surrounding aquifers. The relatively low salt concentrations of the pore water in the Lauenburger-Ton-Komplex in the GoHy 1623 borehole – sedimented under freshwater conditions – indicate that the salt water in the underlying and overlying beds of the aquitard have relatively low salt concentrations. The changed hydraulic conditions during the Holocene led to partial displacement of this salt water by freshwater in the lower aquifer, which influenced the pore water composition of the aquitards to varying degrees. Whilst the superimposition and displacement of the Pleistocene salty pore waters in the Lauenburger-Ton-Komplex was limited to the direct area of contact at the upper and lower edges of the aquitard, this process went further in the Hamburg-Ton because of its higher proportion of sandy and silty beds. The displacement and superimposition of the Pleistocene water took place preferentially here in the more permeable sandy beds (KLINGE et al. 2001).

8 Groundwater dynamics

8.1 Groundwater levels

Since the beginning of the investigation programme in 1979, water levels have been measured every two weeks in the study area south of the Elbe. The measuring network encompassing 324 groundwater observation wells was operated until mid 1994. On average, continuous measurements are available for 9 to a maximum of 15 years. The groundwater observation well network in the area north of the Elbe was completed until 1997 to 1998. A measurement programme was carried out here from this time until the end of 2000.

The groundwater level fluctuations are mainly controlled under natural conditions by the different degrees of groundwater recharge reflecting the weather conditions. Observation wells located in the lowlands near rivers were also affected by the water courses themselves. The influence of the water courses is intensified by the dikes because they give rise to higher river water levels than would be the case under natural conditions.

The effect of these two influencing factors is explained in the following on the basis of two observation well groups, GoHy 190 and GoHy 280.

The GoHy 190 observation well group is located in the geest high of the Gartower Tannen in the area underlain by the Gorleben channel. GoHy 191 is screened in Lower Terrace sands, GoHy 192 within the Lauenburger-Ton-Komplex at a depth of -103.7 m above sea level, and GoHy 193 at the base of the Elsterian channel sands. GoHy 193 contains brine with 115 g/l TDS, GoHy 191 has a low mineralised freshwater with 0.18 g/l TDS. GoHy 192 has 19.9 g/l TDS (Fig. 41).

The GoHy 280 observation well group lies immediately adjacent to the Elbe, to the northwest of Gorleben. The GoHy 281 and GoHy 283 observation wells are screened within the freshwater body of the Lower Terrace sediments and the sandy beds of the Hamburg-Ton at depths of +5.3 m and -118,7 m above sea level respectively. The GoHy 284 observation well is screened within the Untere Braunkohlensande and, similar to GoHy 193, contains brine with 103 g/l TDS (Fig. 42). Figure 42 also shows the hydrograph of the Elbe river level at Gorleben for the purposes of comparison.

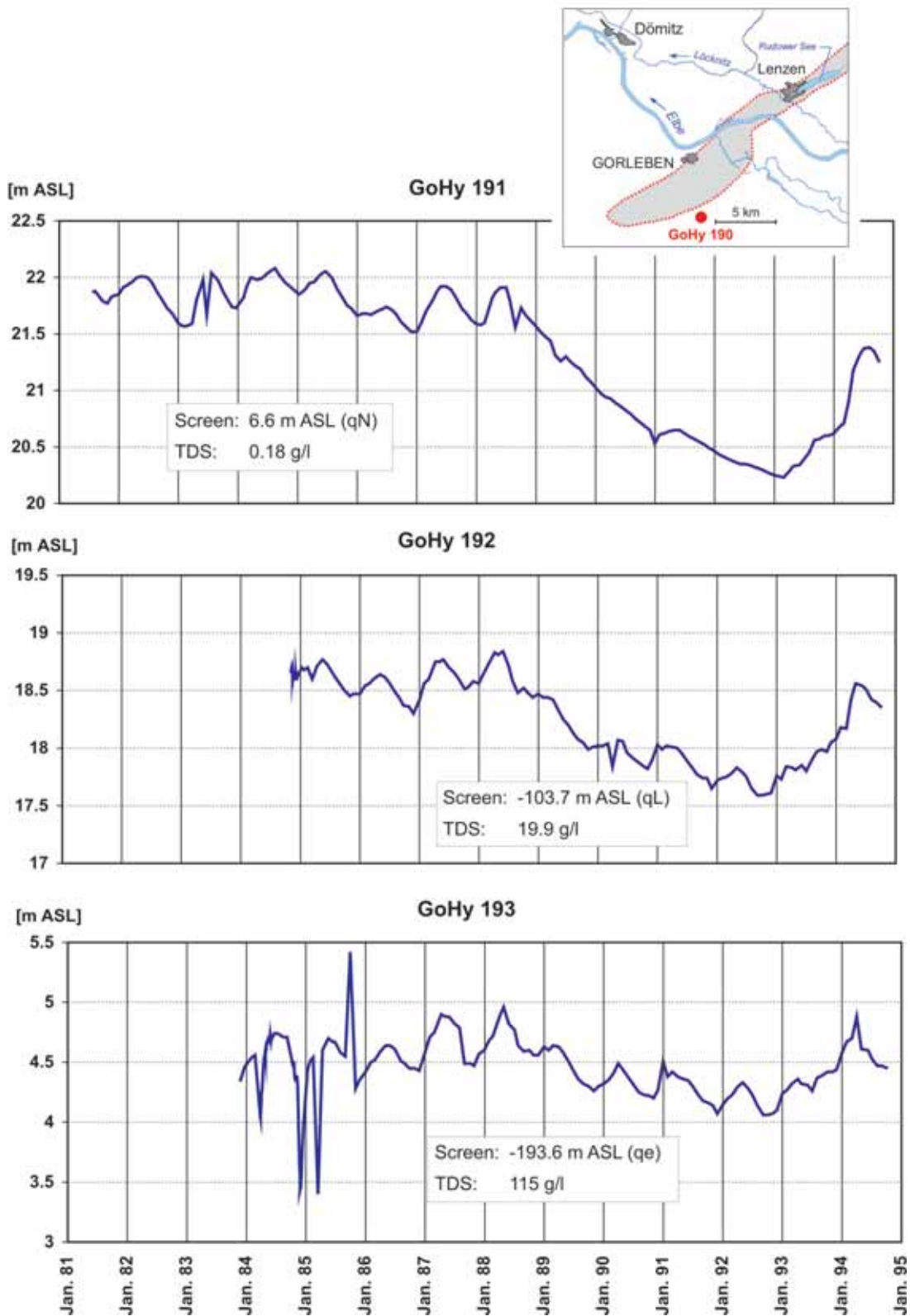


Figure 41: Hydrograph of the GoHy 190 observation well group

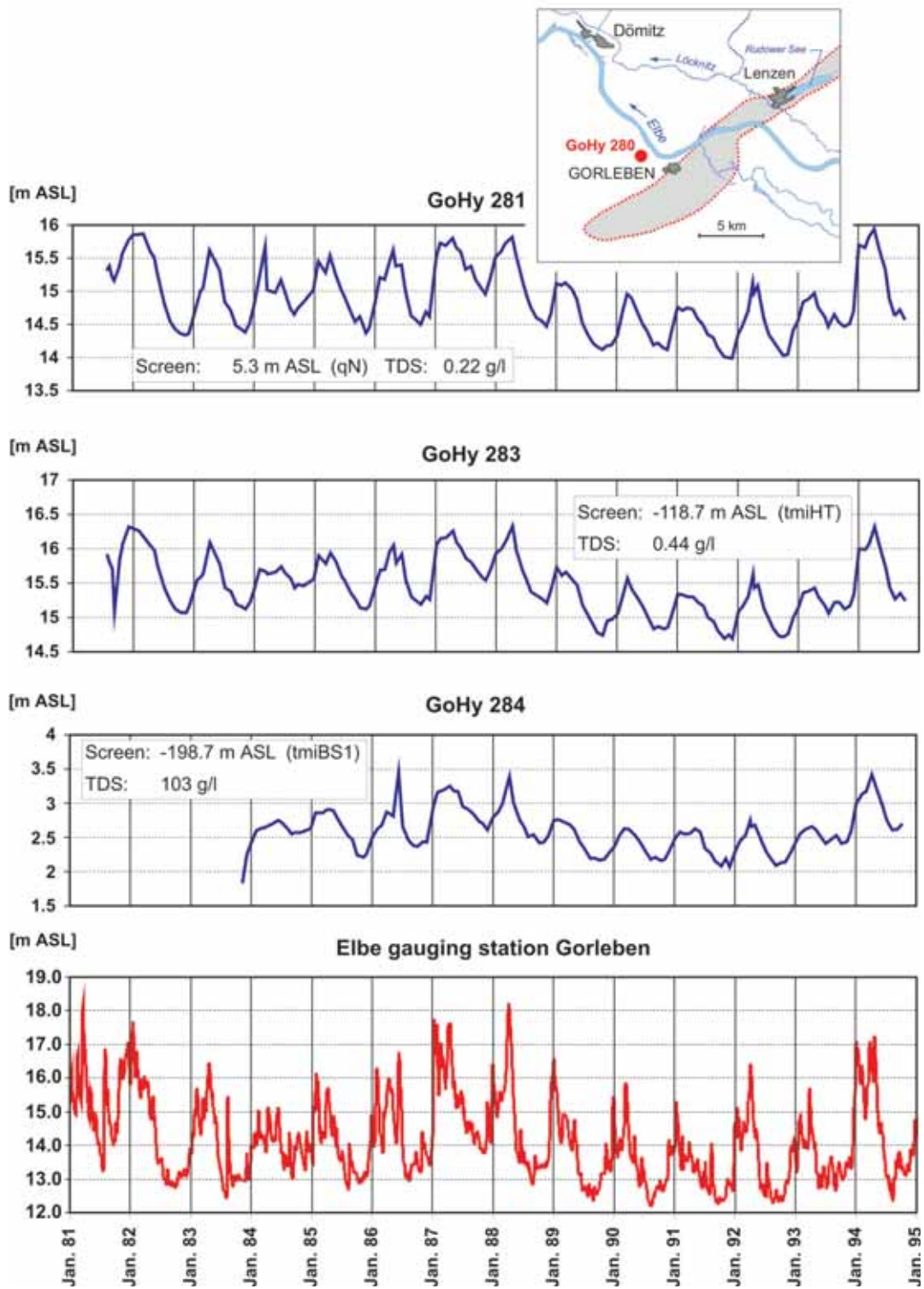


Figure 42: Comparison of the GoHy 280 observation well hydrograph and the Elbe river hydrograph at Gorleben

The shallow GoHy 191 observation well in the Gartower Tannen recharge area shows a marked seasonal variation over a period from 1982 to 1989. The water level maximum in April is followed by a decline until the beginning of winter and then a rise from December/January before reaching the maximum again. However, from 1989 to the end of 1992, a strong downwards trend took place with a completely absent or only partially recognisable seasonal trend. The groundwater level then rose again from 1993 until the end of recording in 1994. This long-term groundwater level trend is largely synchronous with the precipitation over the same period (cf. Fig. 3). The period up to 1988 is marked by high groundwater levels associated with years of high precipitation levels. This was followed by a dry period with unusually low precipitation levels in 1989 and 1991. The average precipitation levels in 1990 and 1992 had no impact on the strong downward trend in the groundwater level. The infiltrating precipitation water during this period was apparently largely exhausted by filling up the field capacity because of the relatively deep water table of around 6 m. As a result, there was no significant contribution to groundwater recharge during these times. There was no measurable rise again in the groundwater level until the above-average precipitation levels in 1993 and 1994.

In the deep groundwater observation wells at GoHy 192 and GoHy 193, the seasonal change in water levels to 1989 was largely synchronous with GoHy 191 and marked by simultaneous peaks and similar fluctuation amplitudes of around 40 – 50 cm in all observation wells. This also points to a simultaneous reaction to pressure changes in the lower aquifer in the Gorleben channel as a result of recharge effects. The long-term trend, with a decline in water levels after 1989 and a renewed rise in water levels after 1994, is also largely identical, although unlike in GoHy 191, the downward trend between 1989 and 1993 in GoHy 193 has a superimposed annual curve. A noticeable aspect is that the seasonal maximum in 1991 and 1992 was already reached in January and February. This indicates lateral influences within the lower aquifer (see below).

The curves of the GoHy 280 observation well group show a marked synchronous seasonal pattern in all observation wells. Compared to the GoHy 190 group, the amplitude at GoHy 280 is much higher, at around 1 m in the freshwater observation wells and around 60 cm in GoHy 284. A comparison with the Elbe river hydrograph at Gorleben shows that the high water peaks in the Elbe have an almost instant direct impact on the groundwater level. The high river levels, which mostly occur in January and February (e.g. 1982, 1987, 1989 and 1994), mean that the winter groundwater maxima occur two to three months earlier than in the geest highs.

In a similar way to GoHy 191 to 193, the curves also show a decline in groundwater levels from 1989 to 1993, although the marked seasonal fluctuation is retained here and the decline in water levels is much lower at around 30 cm. These seasonal fluctuations themselves correlate with the marked low water levels in the Elbe during the summer months and much lower winter high water levels. Overall, this shows that the groundwater levels around GoHy 280 are directly dependent on the water levels in the Elbe.

In principle, the speed with which the groundwater levels react to the high and low water levels in the Elbe depends on aquifer permeability and the distance of the observation wells from the river. In the area to the south of the Elbe, a correlation between the observation well hydrographs and the Elbe river levels shows that the area in which the groundwater levels are controlled by the water level in the Elbe is around 3 – 5 km wide (BOEHME 1993). As a consequence, the seasonal fluctuations in the GoHy 192 and 193 deep groundwater observation wells discussed above are associated with the high water periods in the Elbe. This is shown particularly clearly in the groundwater level peak in January 1991, which correlates with high water levels in the Elbe at the same time. The GoHy 190 observation well group is located around 5 km south of the Elbe.

8.2 *Groundwater dynamics in the freshwater body*

8.2.1 *Shallow groundwater*

The usual method of determining the potential gradient in freshwater-bearing groundwater systems is to compare the water levels between two gauges. This is the basic method for preparing a water table contour map. Figure 43 shows the water table contour map for the shallow groundwater based on 107 shallow groundwater observation wells measured between 20 and 28 April 1998.

The water table beneath the topographic high of the Gartower Tannen in the southeast of the study area lies just over 22 m above sea level at maximum groundwater height. This groundwater recharge area also has the deepest water table of the shallow groundwaters, with depths of more than 6 m. The groundwater flows almost radially from this groundwater high into the surrounding Seege and Elbe (and Lucie) lowlands, where the groundwater discharges into the water courses. The watershed of the shallow groundwater between the Seege and Elbe river systems in the east, and the canal systems in the Lucie lowland to the west which drain into the Jeetzel, runs NNW, from the centre of the recharge area in the southeast to the area directly adjacent to the Elbe to the northwest of Gorleben.

From here, the watershed runs SE-NW, parallel to the Elbe, along the Langendorfer geest ridge.

The regional water table gradient between the recharge area in the Gartower Tannen (> 22 m above sea level) and the rivers (14 to 15 m above sea level) is around 0.9 ‰ to the west and northwest towards the Jeetzel river system, and around 1.5 ‰ to the north and northeast towards the Elbe-Seege system. The H hbeck in the east and the Langendorfer geest ridge in the west have their own recharge areas, which also drain towards the Elbe and Jeetzel, and the Elbe and Seege respectively.

In the Elbe-L cknitz lowland in the north of the study area, the overall groundwater flow is parallel to the Elbe in an ESE-WNW direction. Because of the minor topographic differences, the groundwater gradient in the lowland between Lenzen and D mitz is only 0.2 ‰. At the northern edge of the study area, there is a southerly groundwater flow from the Mecklenburg-geest highs bordering the areas to the north – as clearly shown in the east-west running water table contours.

There is a strong anthropogenic influence on the groundwater flow in the Elbe-L cknitz lowland as a result of water management. Maintenance of the water level in the Rhinow canal by the Gaarz pump works leads to permanent drawdown of the water level of approx. 1 m in the central part of the lowland. Because of these water management measures, the groundwater flowing from the north out of the Mecklenburger geest not only drains into the L cknitz but also into the Rhinow canal. The influence of the Elbe on the shallow groundwater is strongly dependent on the water level in the river. During high water levels, there is massive infiltration into the shallow aquifer. Steep gradients develop orthogonal to the Elbe as a consequence. The associated groundwater flow mainly drains into the Rhinow canal. During low water level phases, the influence of the water management measures in the Rhinow canal extends as far as a system of drainage ditches around 2 – 3 km south. South of a watershed running approximately parallel to the Elbe (Fig. 43), the aquifer reinfilters until the next wave of high water in the Elbe. The hydrological balance in the Elbe-L cknitz lowland shows that the infiltration of shallow water into the aquifer is considerably higher than the volume of reinfiltration (KLINGE et al. 2001).

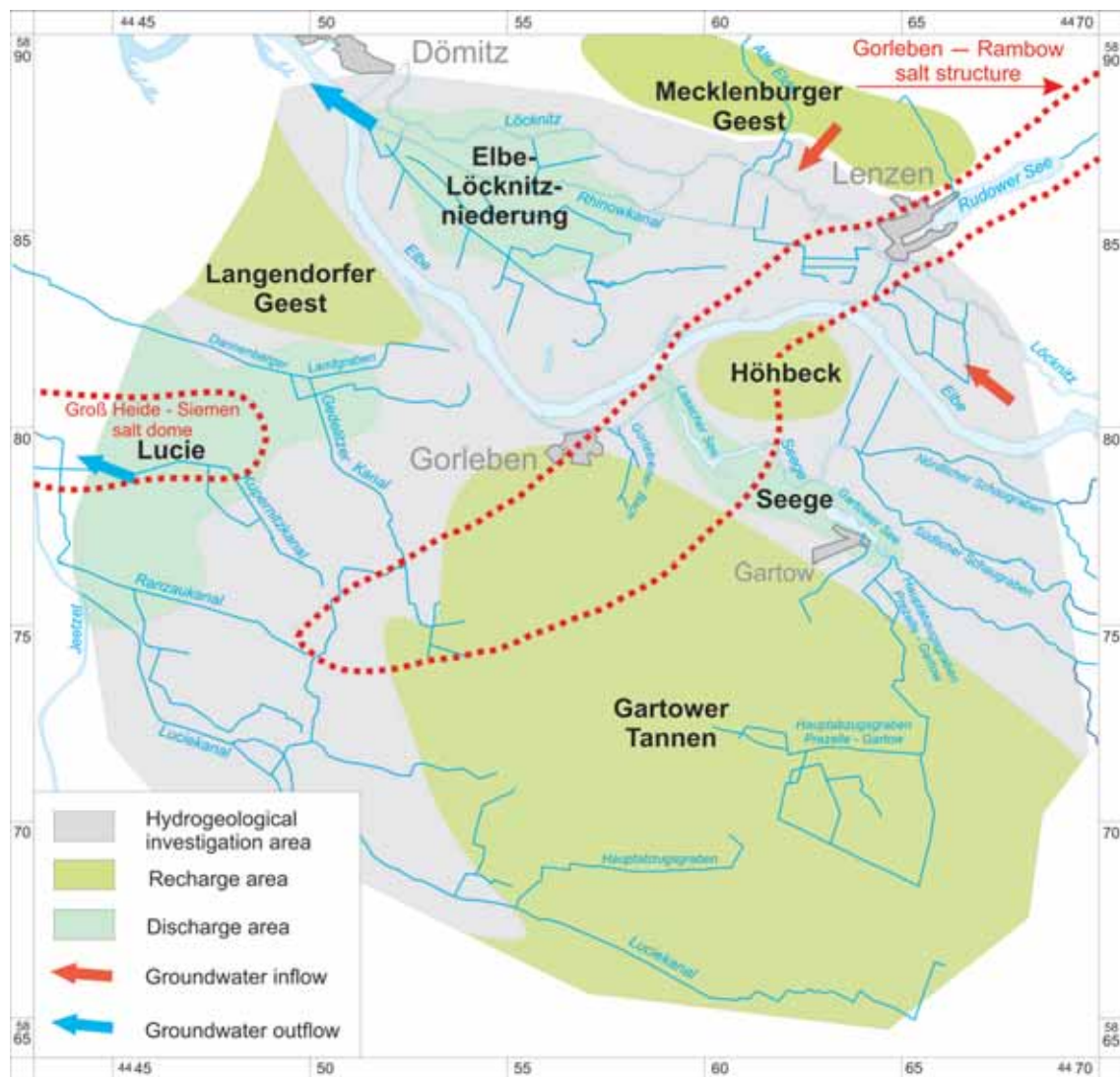


Figure 44: Schematic diagram of regions of groundwater recharge, groundwater discharge and groundwater inflow and outflow

Figure 44 again highlights the overall hydraulic picture in the shallow aquifer. It shows the following:

- three local **recharge areas** in the Gartower Tannen, Höhbeck and Langendorfer geest ridges
- the **discharge areas** of the groundwater in the lowlands of the Seege, the Elbe and Löcknitz, and the “Lucie” drainage ditch system
- two **inflowing areas**, in the north from the Mecklenburger geest, and in the east from the groundwater inflow to the Elbe lowland running parallel to the Elbe
- the **groundwater outflow** from the investigation area into the Elbe and Löcknitz river systems, and the Jeezel river system

8.2.2 The freshwater body of the lower aquifer in the Elbe-Löcknitz lowland

In the area to the south of the Elbe, a uniform freshwater body is present in the rim synclines – in particular where the Hamburg-Ton is absent – which encompasses the upper part of the lower aquifer. In the Elbe-Löcknitz lowland, where the Hamburg-Ton and Lauenburger-Ton-Komplex aquitards are present virtually throughout, a freshwater body is formed in the lower aquifer directly below the Hamburg-Ton and the Lauenburger-Ton-Komplex which stands under artesian pressure – as already discussed in Chapter 7.1.2. Gaps in the extension of the Lauenburger-Ton-Komplex (hydraulic windows) in the Mecklenburger geest highs bordering the area to the northeast, where the topography is 40 m on average above the level of the Elbe-Löcknitz lowland, lead to the inflow of freshwater into the lower aquifer as far as the Elbe-Löcknitz lowland and corresponding displacement of the original salt water.

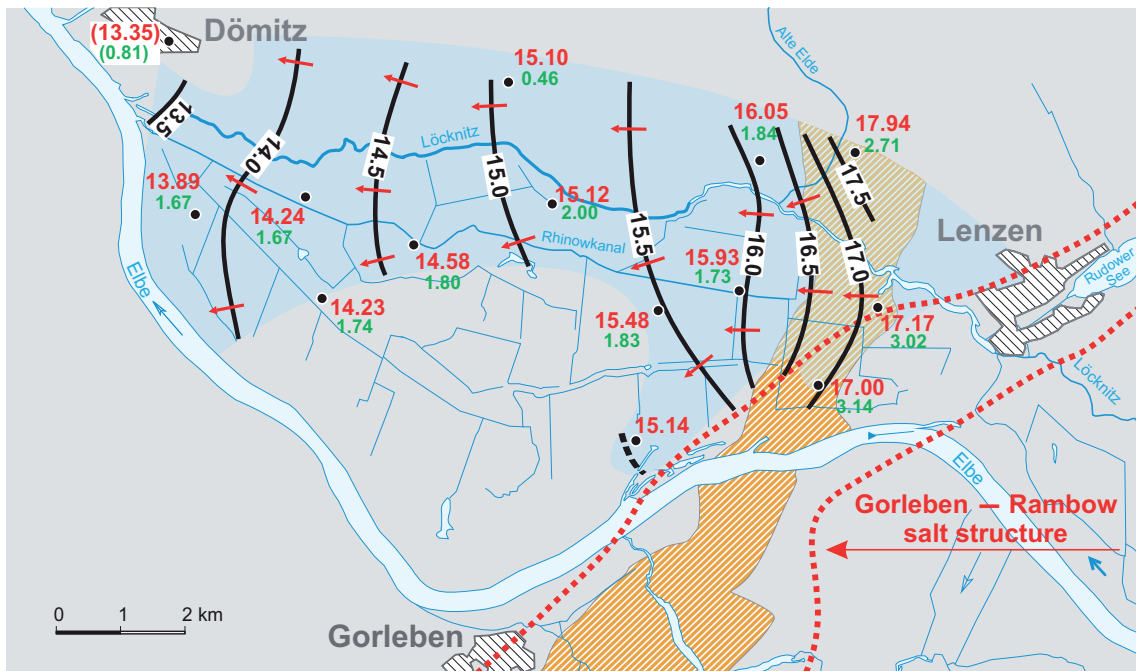


Figure 45: Potentiometric surface of the freshwater body within the lower aquifer

Figure 45 shows the potentiometric surface within the freshwater body based on the water levels recorded in September 1998. The diagram also shows additional information on the hydraulic head differences between the shallow free water table and the potentiometric surface within the deep freshwater body. The map reveals a general east-west oriented hydraulic head gradient with corresponding groundwater flow. Water flow is driven by the high hydraulic potential at the northeastern edge of the area represented by the GoHy 1622 observation well. ALBRECHT & ZWIRNER (1999) assume the existence of a vertical connection in a Quaternary channel between the upper and lower groundwater aquifer northwest of Dömitz. The possible associated reduction in pressure in the lower aquifers at the northwestern edge of the study area is the main reason for the overall east-west oriented water flow within the lower freshwater body.

The average pressure gradient within the freshwater body is 0.4 ‰. However, instead of a uniform pressure gradient, there are two zones with very different gradients. To the east of the 16 m pressure contour, the potential gradient is approx. 1 – 1.3 ‰. This zone is almost identical with the area of distribution of the Elsterian sands within the Gorleben channel. To the west of the Gorleben channel in the distribution area of the Untere Braunkohlensande, the gradient is very much lower at a uniform 0.25 ‰.

The pressure level differences between the shallow free water table and those in the lower freshwater body can also be divided into two regional units. The differences between the three observation well groups in the Gorleben channel lie between 2.71 and 3.14 m, whilst those in the adjacent area to the west are much lower at between 1.67 m and 2.00 m.

KLINGE et al. (2001) interpret the difference in hydraulic head levels as an indicator of higher vertical hydraulic permeabilities at the western edge of the channel forming a migration path for the freshwater flow upwards into the upper aquifer. The associated pressure drop in the lower aquifer can then lead to the described differences in pressure gradients.

8.3 Groundwater dynamics in the salt water body

Salty groundwater with increasing concentrations with depth is encountered around the Gorleben salt dome, and in the Gorleben channel and northwestern rim syncline in particular. This dissolved salt is mainly derived from subsrosion processes in the central part of the Gorleben channel, where the base of the Elsterian channel sands are in direct hydraulic contact with the Zechstein evaporites. Hydraulically induced groundwater flow and the associated mixing of shallow freshwater with underlying salty water accounts for today's distribution of freshwater and salt water around the salt dome.

Groundwater is influenced by the earth's gravity field and flows to establish a stable state with minimum potential energy. When a groundwater system contains waters with different salinities, the flow which takes place to establish equilibrium causes the deeper parts of the system to be occupied by salty water with higher densities. The shallower parts are occupied by fresher water with lower densities overlying the salty water. If the whole water system reaches equilibrium, and no salt is added or removed, layering develops with horizons of uniform water density and thus uniform salinity. Any disruption of this system, e.g. by local salt dissolution, generates turbulent correction currents aimed at re-establishing stable horizontal layering.

If freshwater in a homogeneous unpressurised aquifer with a constant water table gradient flows over a salt water body of constant density, the interface between the freshwater and salt water forms a surface dipping against the flow direction of the water. The gradient of this surface depends on the density of the water, the flow potential of the freshwater, as well as the flow of the salt water. If the salt water is flowing in the same direction as the freshwater, the interface surface only has a small gradient. If it flows in the opposite direction, a higher gradient develops (e.g. BEAR 1979).

Within a flow system, water flows from areas of higher hydraulic pressure to areas of lower hydraulic pressure. Detailed information on the pore water pressure and groundwater density distributions around the Gorleben salt dome would therefore support direct interpretation of the potential flow directions of the water. Moreover, additional precise information on the permeability distribution enables the speed of the water flow to be calculated using the generalised DARCY law. However, in practice, pore water pressure can only be measured at specific points within the filter sections of groundwater observation wells. Pressures in inaccessible parts of the aquifer can be interpreted using plausible assumptions in favourable cases by interpolating and extrapolating the local measurements.

The indirect determination of the hydraulic pressure, usually carried out in freshwater-bearing aquifers from the measurement of water levels in groundwater observation wells, assumes constant or at least accurately known water densities in the cased observation wells. However, as in the case of aquifers containing water of variable densities, this assumption is too inaccurate. Water pressure therefore has to be determined with a logging tool which directly measures the pressure in the filter zone of the groundwater observation well in question. Two pressures determined in this way are directly comparable when they are determined at two positions in the system lying at the same height with respect to sea level. Pressures measured at points of different heights need to be corrected to the same level, taking into consideration the different water densities and vertical flow components between the observation well and the reference level. This requires

information on the distribution of formation water density around each observation well. This can be continuously determined to the appropriate degree of accuracy from borehole resistivity logs (induction logs) and extrapolated onto vertical sections (cf. Chapter 7.1).

In the Gorleben study area, borehole logs were used to determine the electrical conductivity of the pore water. This information together with pore water pressure measurements was used to interpret the groundwater flow in the salt water-bearing part of the aquifer. This involved three steps:

1. Direct pressure measurements in the filter zones of the observation wells
2. Determination of the continuous vertical distribution of water density in the areas surrounding the boreholes with the help of induction logs
3. Correcting the measured pressures to a reference depth

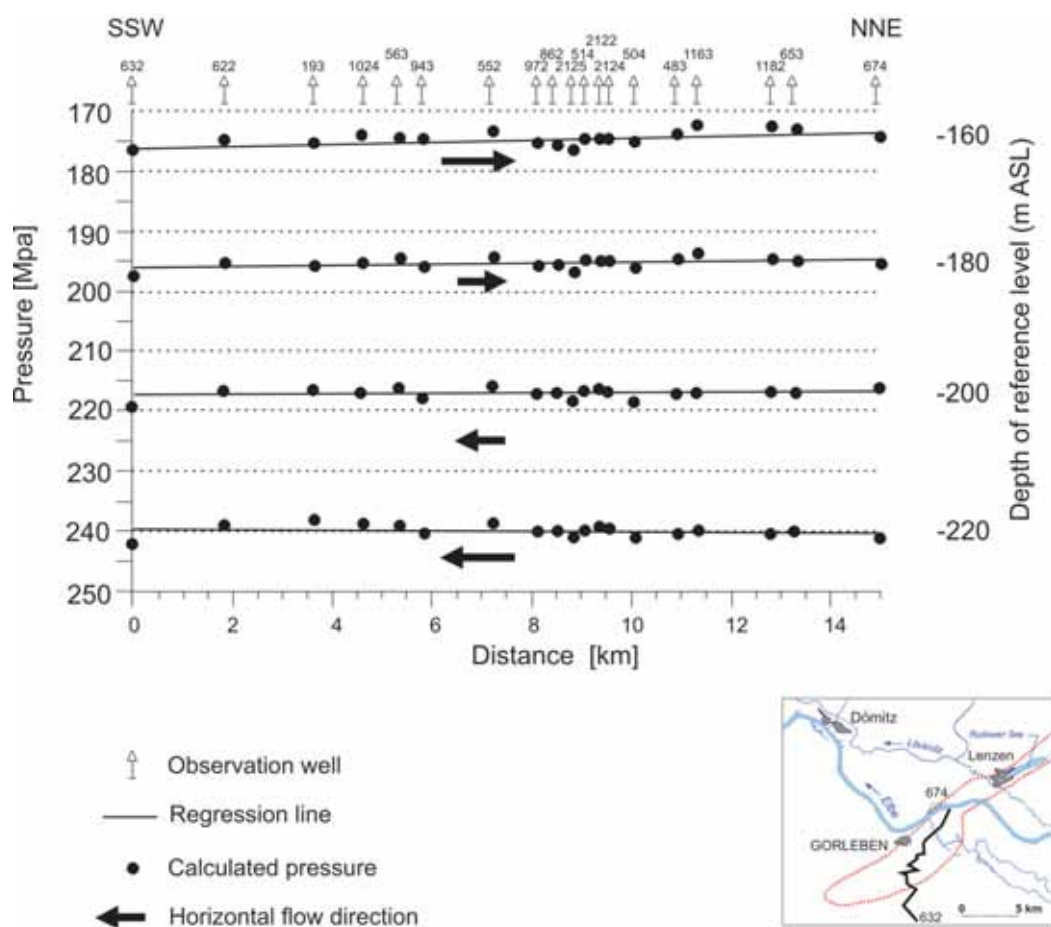


Figure 46: Calculated pore water pressures and flow directions in the Gorleben channel

Figure 46 is a calculation example which shows the change in water pressure in the lower Gorleben channel aquifer at four reference depths: -160 m, -180 m, -200 m and -220 m above sea level. This graph shows that the average gradients of the overall profile have strong superimposed local gradients with, in some cases, reversed directions between consecutive sections. This may be attributable to inaccuracies in the evaluation of the vertical salinity distribution. It could also be due to local salt subsidence, which would lead to an increase in hydraulic pressure and the formation of turbulent compensation currents. The average pressure gradient at -180 m above sea level is 1.0 Pa/m and points to the northeast – just as in the upper aquifer. However, it is less than one tenth of the pressure gradient observed above the channel in the freshwater body of the upper aquifer.

The pressure gradients at -200 and -220 m above sea level (e.g. approx. 0.8 Pa/m at -220 m above sea level) point to the south in the opposite direction of the freshwater flow. This indicates a deep flow of salt water towards the south in the lower part of the channel aquifer. This finding can be interpreted as indicating the presence of large-scale convection cells within the salt water body.

9 Numerical groundwater modelling

9.1 *Three-dimensional groundwater model with constant density*

Numerical groundwater models are used to incorporate hydrogeological findings with as few contradictions as possible within a complete quantitative picture of the flow processes within the groundwater. The results of this modelling forms the basis for the calculation of the effect of scenarios involving the transport of radioactive substances. In the event that these are released by the salt dome and enter the biosphere via groundwater flow through the overburden.

The overburden of the Gorleben salt dome consists of Quaternary and Tertiary sands and clays whose pores are filled with water. The groundwater or pore water is not stationary. Its flow is determined in extensive areas by the different heights of the water table in the lowlands and the topographic highs. When the ambient conditions remain constant (climate, topography), an approximate dynamic equilibrium is established in the long term between groundwater recharge on the highs, groundwater flow in the direction of the lowlands, and groundwater discharge in the floodplains. The groundwater flow generated in this way extends right down to the deep lying areas of the Miocene aquifers in the rim synclines, as well as the areas directly above the salt dome. Salt dissolution takes place above the salt dome, which increases the groundwater density and thus influences the flow system (DELISLE et al. 1985).

The consideration of a stable long-term meteorically controlled groundwater cycle and its exclusive incorporation in a numerical model formed a good approximation for the actual groundwater flow occurring within the overburden on the basis of the information available at the beginning of the investigation programme. The influence of pore water density associated with high salt concentrations could not be taken into consideration by the state-of-the-art of science and technology available at the time. A steady-state groundwater flow with constant pore water density over time and space was therefore assumed for the three-dimensional groundwater model.

The GS 4000 application was used for the preliminary model calculations (SCHMIDT 1991). The model is based on the DARCY filter law as well as the continuity equation for the steady-state case, which are solved using an integrated finite difference method. The model, its mathematical basis and the computing technique are described in more detail in SCHMIDT (1991).

The spatial distribution of topographic heights and lowlands was used to define the model area. The watersheds and flow lines which form the boundaries of the model are drawn vertically downwards from ground level to the Tertiary clay formation. The model boundaries to the west, southwest and south follow the main rivers. The Löcknitz forms the model boundary to the north (Fig. 47). The model simulations assume that no groundwater flow takes place through the vertical boundaries and the base of the model space formed by Tertiary clay layers or the salt dome itself, with the exception of inflow and outflow in the Elbe lowland. The groundwater flow in the model is therefore mainly maintained by the groundwater recharge at the upper boundary of the modelled area. This results in the same volume of groundwater outflow in the lowlands incorporated in the model.

This model area of approx. 350 km² was subdivided by discretisation into 380 cells of various sizes, depending on the information density, the significance of local structures and the level of accuracy required. The spatial subdivision involved 15 superimposed calculation levels between +15 m above sea level and -350 m above sea level. The spatial elements arising from the discretisation represent specific average hydrogeological properties. Each is assigned an average value for the vertical or horizontal hydraulic conductivity and the effective porosity. A differentiation is made between aquifers, aquicludes and aquitards².

When the model was developed, no reliable data were available on the lowland to the north of the Elbe, on the territory of the former GDR. As a conservative approach, the local absence of the Hamburg-Ton and Lauenburger-Ton-Komplex aquitards was therefore assumed at the northern boundary of the model.

² This reflects the subdivision used in this report: aquifer ($k_f > 10^{-5}$ m/s), aquitard ($10^{-7} < k_f \leq 10^{-5}$ m/s) and aquitard ($k_f \leq 10^{-7}$ m/s) as proposed by the Ad-hoc-Arbeitsgruppe Hydrogeologie (1997)

The model was easily calibrated. Down to a depth of approx. 150 m, there is a good correlation between the groundwater levels from natural observations and model calculations, taking into consideration the usual tolerance of 1 m used for large-scale flow models. There is also a good correlation of the exchange between groundwater and surface water. The infiltration and exfiltration areas in the model also correspond to their natural locations.

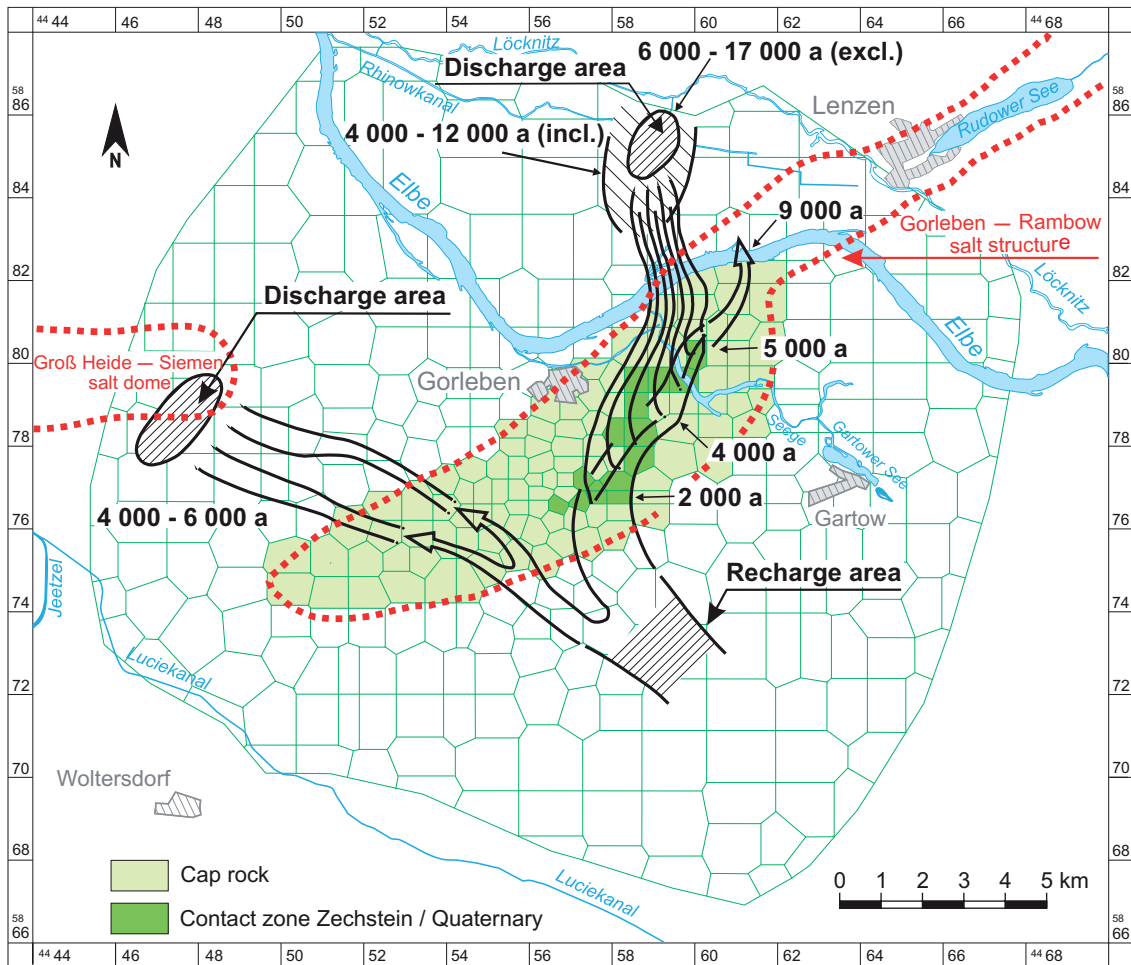


Figure 47: Model age of the groundwater in the channel area, and travel times from starting points at the base of the aquifer to the biosphere excluding (excl.) and including (incl.) consideration of the cap rock (from ALBRECHT et al. 1991)

The calculated travel times and flow paths are of particular interest, and special attention was given to the migration paths through the Gorleben channel and through the western part of the salt dome overburden. In the first case, travel times of several thousand years (4 000 – 17 000 years) are required for the pore water to reach the biosphere, depending on the particular starting point at the top of the salt dome. The discharge areas lie in the Elbe-Lössnitz depression to the north of the Elbe (Fig. 47). The same travel times are involved in flow from the recharge area of the Gartower Tannen to the starting points at

the top of the salt dome. Shorter travel times overall (4 000 – 6 000 years) were calculated for the flow paths over the western part of the salt dome from starting points up to 150 m below ground level.

As already discussed, this model approach is based on the basic simplification of constant pore water densities. This restrictive model assumption means that the model only approximately describes the hydraulic system in the salt water body below approx. 150 m.

9.2 Modelling of groundwater flow with variable densities

Numerical simulations of the groundwater flow started in 1989 taking into consideration variable water densities. Their aim was to assess the influence of salt concentration-dependent water densities on the flow field within the Gorleben study area. These investigations became necessary when calculations carried out by BGR, as well as the work of various international groups, revealed that completely different flow patterns usually occur in salt water/freshwater systems, and that there are lower flow velocities on average in the salt water zone, where convection cells often occur in some areas (SCHELKES et al. 1990; NEA & SKI 1988).

The two-dimensional model calculations were carried out on vertical sections reflecting the situation in the Gorleben channel. They were based on a generalised hydrogeological section running from the Gorlebener Tannen recharge area along the deepest part of the Gorleben channel through to the northwestern rim syncline (cf. Fig. 48). Pore water is almost saturated at the base of the channel above the salt dome. It was assumed that the salt concentrations were attributable to local direct contact between the pore water and the evaporite body. The modelling was aimed at clarifying whether the groundwater system in the region is in a steady state, and at identifying the hydrogeological and hydraulic parameter variations to which the system reacts sensitively.

The freshwater/salt water system modelling is based on the generalised form of the DARCY law, the continuity equation, and the transport equation, all linked by the variable density as a function of salt concentration. Viscosity is assumed to be constant. Calculations were carried out using the SUTRA program (Voss 1984). These model calculations proved to require an extremely large amount of computing time compared to model calculations with constant densities. Overall, modelling reached the limits of science and technology at the time, especially because there was then only very little international experience with the modelling of complex freshwater/salt water systems with large differences in TDS.

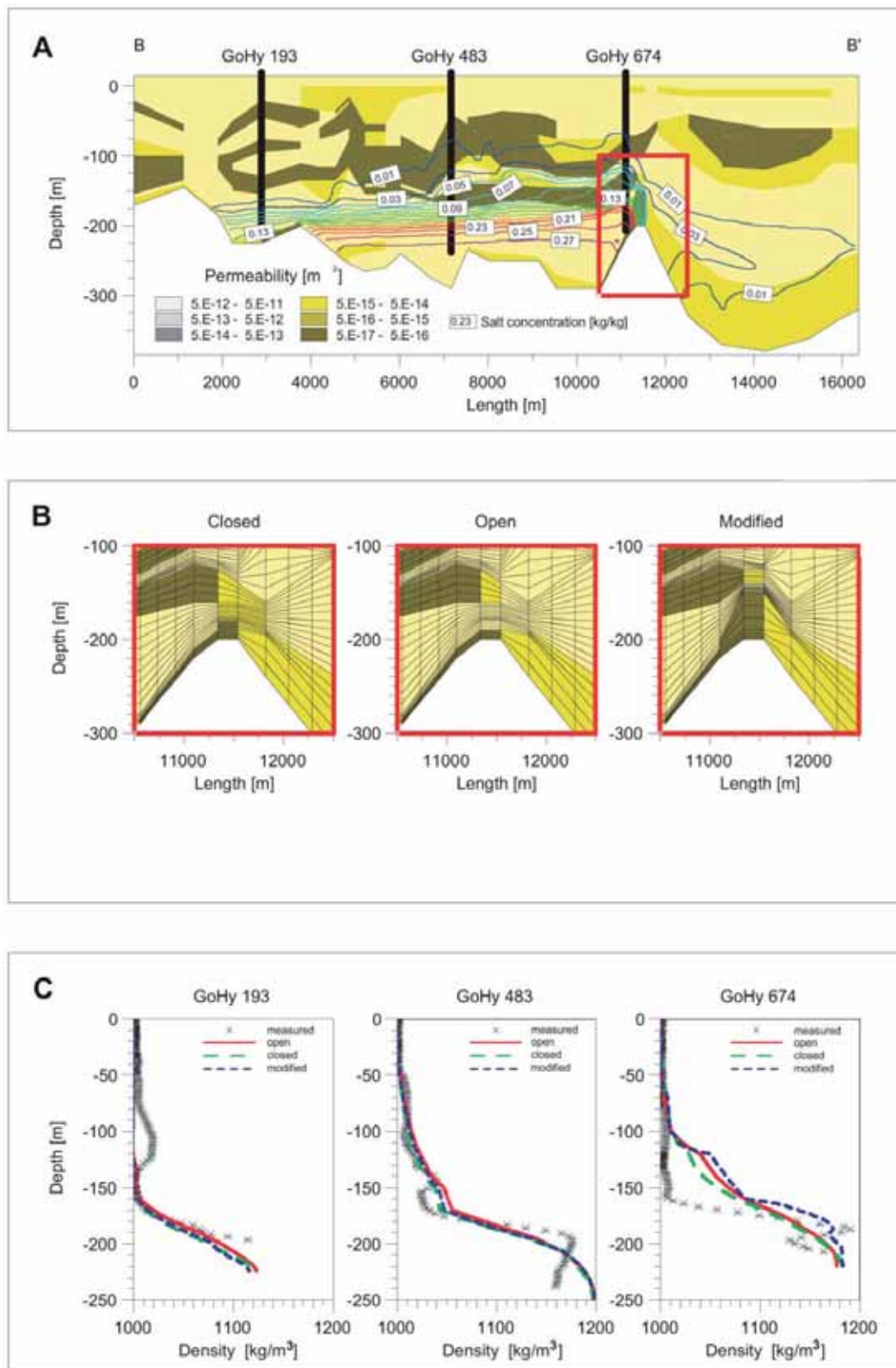
In the first calculations, which incorporated very simplified geometries of the geological structures in the model sections, the salinity distributions which established themselves during the modelled time periods reacted very sensitively to the geometrical arrangement of various permeable layers, the length of the contact zone with the underlying evaporite body where salt dissolution can take place, and to the size of the transverse dispersivity.

The longitudinal dispersion only had a minor influence on these model calculations (VOGEL & SCHELKES 1996). Other sensitivity factors were, however, the choice of initial distribution of salt concentrations and the length of the modelled geological time period.

Compared to field observations of the density distribution, the modelling results indicated that the salt water distribution in its current form and the associated flow system are not yet in a steady state (VOGEL et al. 1993). It was not possible for the forward modelling to even approximately develop a stable condition with a density distribution as observed. Even if the observed density distribution was used as the initial condition in the model calculations, the time-dependent calculations indicated an extension of the observed transition zone from highly saline to less saline waters in particular, with a trend to linear density distribution observable in some areas.

In the following calculations, the hydrogeological structures were modelled as realistically as possible. Gaps in the Lauenburger-Ton-Komplex were taken into consideration in the inflow areas by creating a connection between the shallow and the deep aquifers. The hydrogeological structure of the channel along the northwestern margin of the salt dome, and the role of possible gaps in the aquitards separating the upper and lower aquifers in the Elbe-Löcknitz lowland, were investigated in parameter variations. The modelling period was defined as 10 000 years based on the results of the previous studies. This approximately corresponds to the time since the end of the last ice age.

The modelling results revealed that gaps in the distribution of the aquitards in the Elbe-Löcknitz lowland had virtually no influence on flow within the lower aquifer. However, the hydrogeological shape of the channel at the northwestern edge of the salt dome (around GoHy 674 in Fig. 48), in combination with the selected initial density distribution conditions have a strong influence on the distribution of density distribution and thus the flow system at the end of the modelled period.



A: Hydrostratigraphic units and salt concentrations
B: Different shapes of channel outlet
C: Comparison of measured and calculated density logs

Figure 48: Model calculations of groundwater flow with variable densities (according to SCHELKES et al. 1990) – calculated salt concentrations

A characteristic bipartite vertical distribution divides the lower aquifer in the Gorleben channel into an upper gradient layer within which the salt concentrations of the waters increase almost logarithmically with depth, and a lower zone with highly saline to salt-saturated waters (cf. Chapter 7.1.2). The calculations achieved an acceptable match between the modelled density distributions and the field data (Fig. 48 C). The calculated flow velocities and flow directions shown in Figure 49 reveal northeastwards-pointing water flow in the upper gradient layer, whilst the lower zone contains turbulent flow patterns similar to eddies with reversed flow directions in some cases.

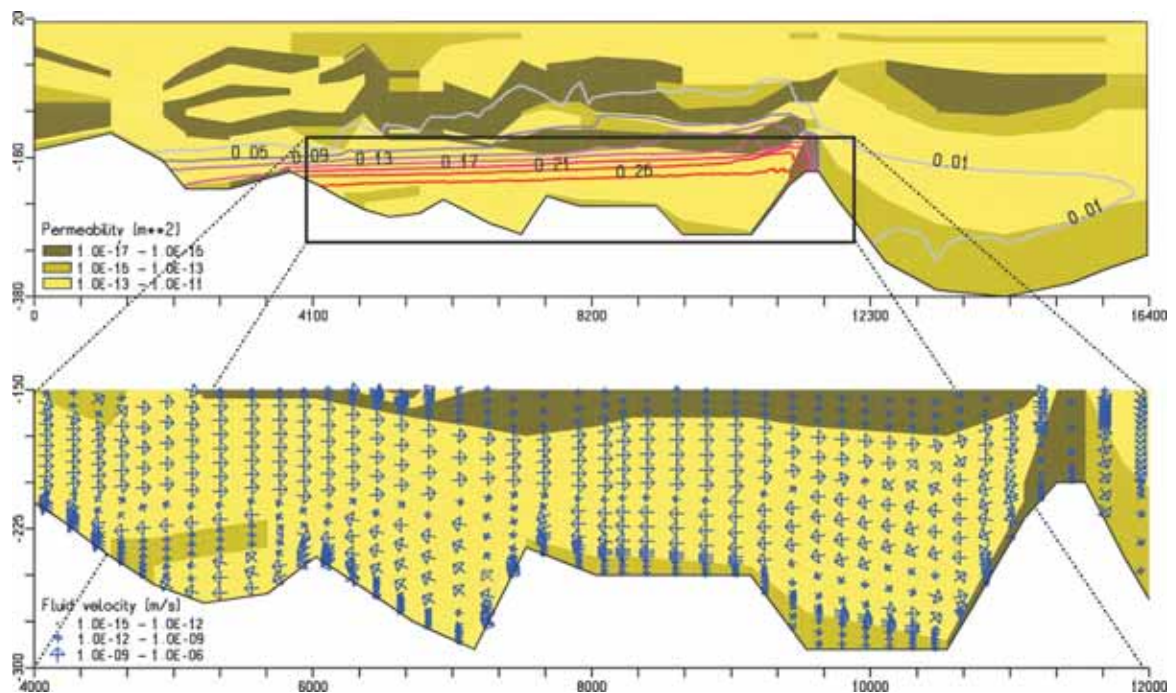


Figure 49: Model calculations of groundwater flow with variable density (according to SCHELKES et al. 1990) – calculated flow directions and velocities

In general, these model calculations have made a major contribution to understanding the flow and salt water transport mechanisms occurring within the Gorleben channel. Because of their research character, these model calculations cannot be used to derive reliable data for the quantification of salt water outflow or transport times. This is not least due to the two-dimensional approach, which means that all three-dimensional effects which can be expected in such a marked heterogeneous system such as the Gorleben study area have to be ignored.

9.3 *Paleohydrogeological investigations*

The two-dimensional salt water/freshwater calculations showed that, since the last ice age, the groundwater system in the Gorleben area has still not moved into equilibrium. The influence of glaciations on this system is shown in various ways including the isotopic composition of the water, the recharge age of Holocene to Pleistocene waters, and the mixing of these waters.

These results were in part responsible for work to look more closely at the system behaviour within a paleohydrogeological model and to gain information on its development up to the present day. The objective was to gain a better understanding of the long-term climatically-driven changes in the groundwater system during the last ice age (BOULTON et al. 2001).

This approach required the incorporation of the previous local model area within a regional model, which takes into consideration all sources having a potentially significant influence on the groundwater system and the associated salinity distribution. The boundaries of this study area, which is cut by the Elbe river, run approx. 110 km east-west and approx. 125 km north-south, and are formed by surface watersheds, flow lines and rivers (Fig. 50). In the southwest, it is bounded by the terminal moraine of the Warthe stage of the Saalian Glaciation, and in the northeast by the terminal moraine of the Weichselian Glaciation, which are both recharge areas because of their topographic height. The boundary to the southeast is the course of the Elbe river. Within the study area, the Elbe lowland is the drainage area, although up until the Holocene, probably no single river had actually cut down into the fluvial Weichselian sands. Groundwater flow was mainly from out of the highs into this lowland. The local Gorleben study area lies at the centre of this area.

One basis for the model calculations was provided by a profile that runs across the area from SSW to NNE (Fig. 51). The most important aquifers at this regional scale are also formed by Miocene, Untere Braunkohlensande and glacio-fluvial Quaternary sediments. These are interbedded with clay layers and thick glacial tills which influence the behaviour of the whole system as aquitards. The base is generally formed by Paleogene clays, and the Rupelton in particular. The profile was selected to follow the course of the channel over the Gorleben salt dome, and thus the profile described in Chapter 9.2 (Fig. 49). It is therefore also subject to the same conditions with respect to possible subsidence (KÖSTERS et al. 2000).

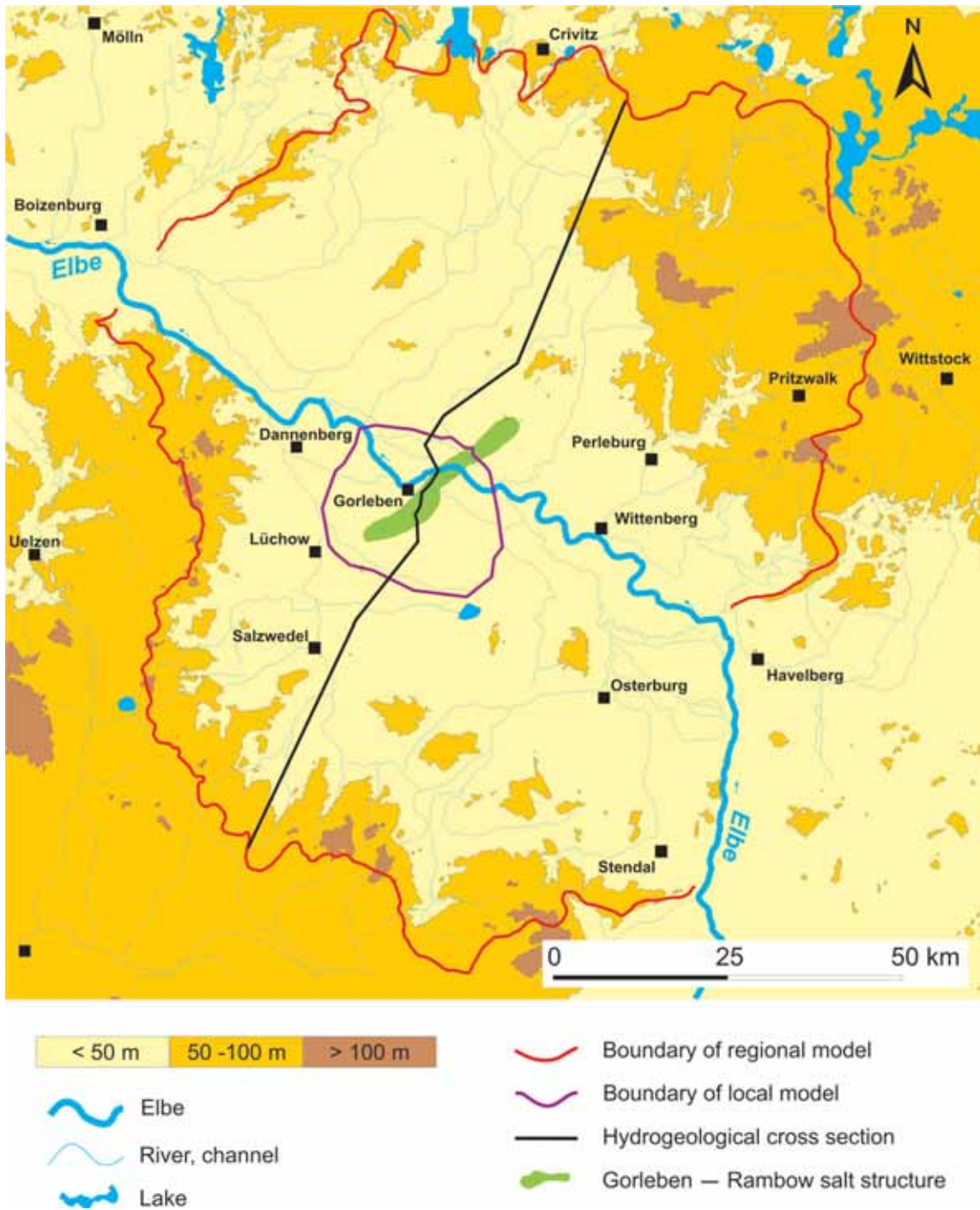


Figure 50: Geographical location of the regional paleohydrogeological study area

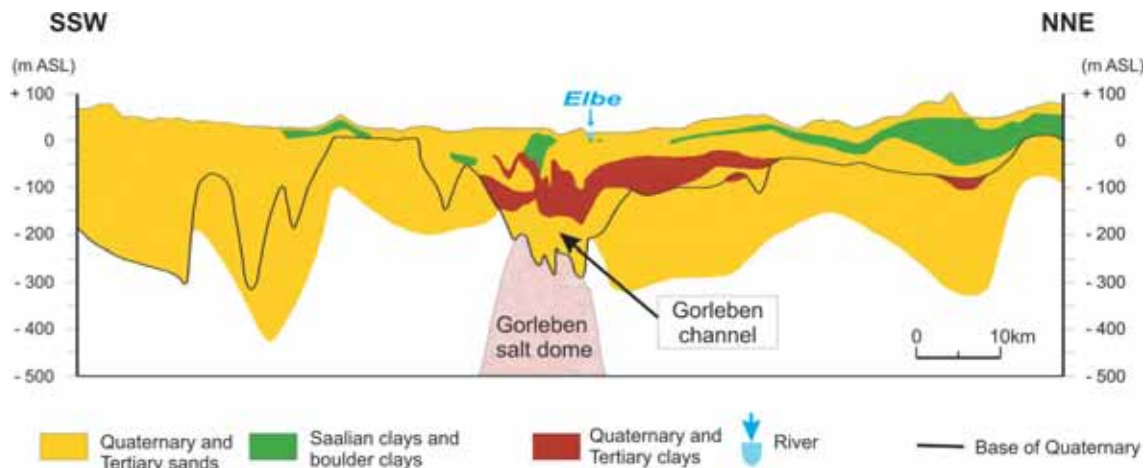


Figure 51: Simplified hydrogeological cross section (location of cross section, cf. Fig. 50)

Permafrost is one of the most important processes controlling groundwater flow. Its development and depth were calculated from climate development and the position of the surface waters (talik formation) (DELISLE 1998, DELISLE & BOULTON 2000). The results were used as input in the model calculations, where the frozen sediments were represented by very low permeable layers. These calculations were carried out using the SUTRA program.

A 120 000 year simulation period since the Eemian, the last interglacial, was selected for the modelling, and this period was divided up into a number of intervals with uniform precipitation and permafrost conditions (Fig. 52). The period from approx. 20 000 years ago turned out to be important, as it involved the maximum advance of the glaciers as far as the northern edge of the model, during which melt-water flowed into the model area under high pressure.

Generally, the model calculations showed that the presence of permafrost has a strong influence on the hydraulic system because it prevents groundwater recharge. When permafrost is present, the spatial distribution of groundwater discharge sites is determined by the position of rivers and lakes which are underlain by taliks. Because of the predefined pressure gradients at the surface, the groundwater generally flows from the northern and southern highs into the Elbe lowland. The flow of highly saline waters in the lower part of the Gorleben channel is linked to the paleoclimatic conditions. During the stadials, the water flowed northwards, during the interstadials, it flowed southwards (KÖSTERS et al. 2000). An example is shown in Figure 53.

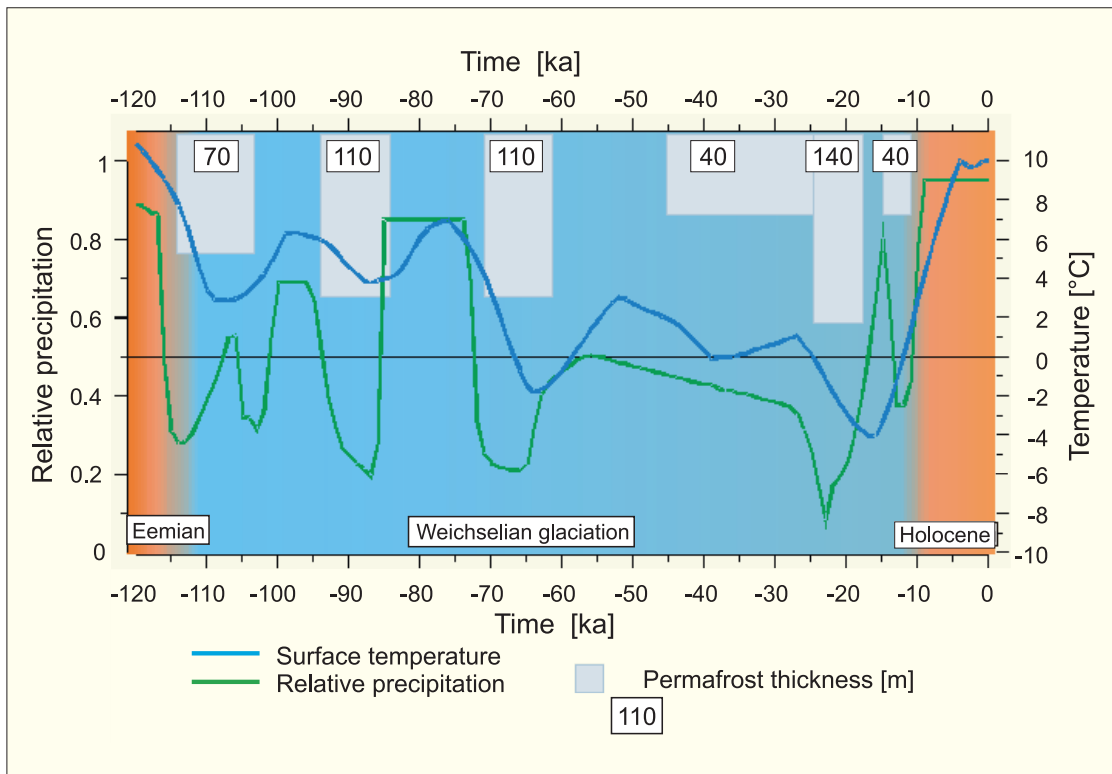


Figure 52: Calculated permafrost thicknesses in the model area within the Weichselian Glaciation

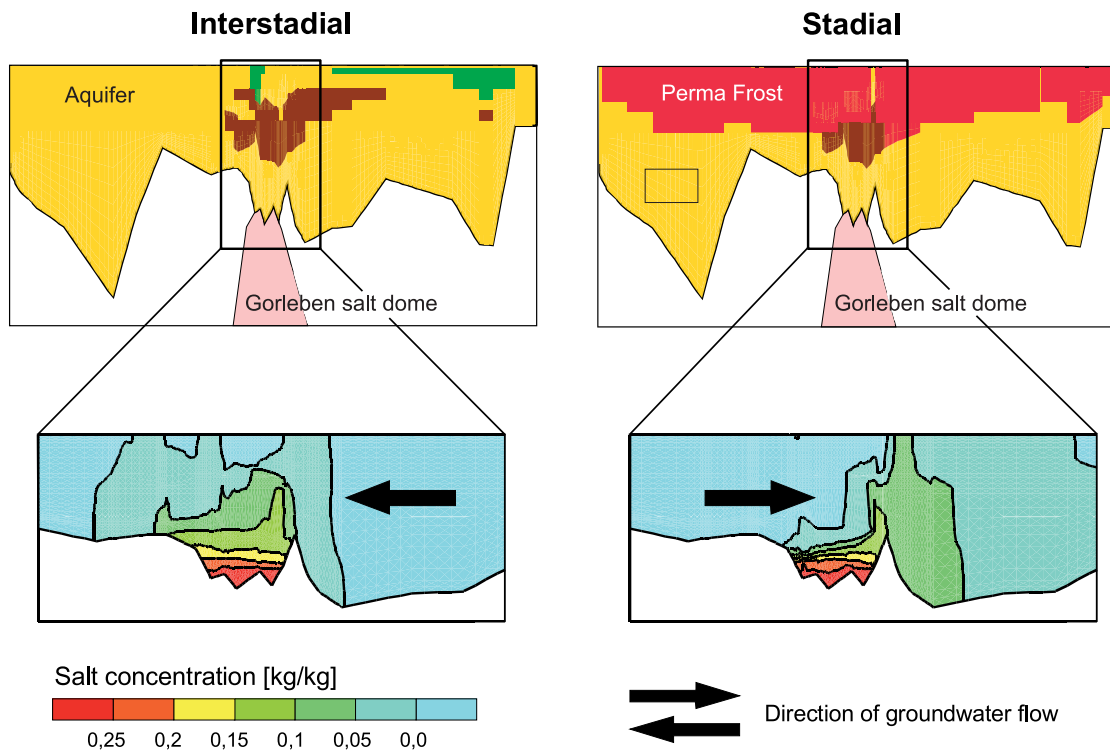


Figure 53: Salt concentration and flow direction of groundwater above the Gorleben salt dome during a typical stadial and interstadial

The position of the glacier front during the high phase of the last glaciation had the strongest influence on the groundwater system. The inflow of meltwater at the base of the ice sheet may have had a very strong influence on the size and direction of groundwater flow at a regional and local scale. Depending on the existence of a glacial lake in front of the ice sheet, the salt water present in the Gorleben channel could have been completely or only partially flushed out (BOULTON et al. 2001).

In either case, a freshwater/salt water distribution analogous to today's situation would have established itself in the intervening period. The model calculations showed that the hydraulic conditions after the high phase 20 000 years ago was critical for the status of today's groundwater system and the associated salinity distribution (KÖSTERS et al. 2001, VOGEL et al. 2001).

9.4 Conclusions from groundwater flow modelling

The numerical calculations on the salt water/freshwater regime showed overall that an accurate analysis of the groundwater system requires a three-dimensional model which takes into consideration variable densities. Time-dependent changes should be allowed for as part of an analysis of the paleohydrogeological system behaviour. The large-scale and hydraulically complicated system of the whole region around the Gorleben salt dome has not yet been completely simulated taking into consideration all of the main components. In a similar way to the further improvement of the technical side of the investigation, work continues on developing suitable flow and transport models for complex 3D modelling which make allowance for density effects.

The three-dimensional freshwater modelling carried out so far is, however, a reasonable approximation of the real situation within the freshwater body. The reverse is true for the density-influenced flow processes involving salt water in the Gorleben channel, where the realism of these models is limited. The two-dimensional freshwater/salt water modelling in the Gorleben channel shows that slower flow velocities and longer travel times can probably be expected in the salt water body compared to the freshwater body. The results of the three-dimensional freshwater models should therefore be considered conservative with respect to the flow velocities and travel times within the Gorleben channel.

10 Final discussion on freshwater/salt water dynamics within the overburden of the Gorleben salt dome

The previous chapters discuss the site-specific investigations on the spatial distribution and dynamics of the freshwater and salt water in the Gorleben area. They also evaluate the results of these investigations. This chapter again summarises these investigation results and provides a final overall evaluation. The focus is on the definition and evaluation of potential migration paths from the salt dome surface into the biosphere.

The site-specific investigations concentrated to a large extent on the Gorleben channel as highlighted by the borehole location map (Fig. 1). This channel contains Quaternary sediments covering an area of several square kilometres, which either lie directly on top of the cap rock or, in a few cases, are also in direct contact with the Zechstein evaporites. The results of the investigation within the channel, together with other findings, e.g. on groundwater dynamics, gave rise early on to the generalised qualitative assessment that “clayey sediments present over the central part of the Gorleben salt dome are neither thick enough nor continuous enough to be able to act as a permanent barrier protecting the biosphere from contamination” (PTB 1983).

It was therefore necessary to investigate and understand the hydraulic systems within the channel, and, as far as possible, quantify the flow processes acting in the channel by various means including the use of numerical groundwater models. Input for this was provided by the very comprehensive and detailed field investigations carried out in this study area.

The Gorleben channel can be hydrogeologically characterised as follows – as already described in the previous chapters:

- Above the salt dome, the channel-like trough in the Tertiary clays and cap rock reaches down to depths of below -290 m above sea level.
- In the central part, Quaternary sediments with good permeability are in direct local contact with easily soluble Zechstein evaporites.
- The Lauenburger-Ton-Komplex present throughout the channel functions as an aquitard separating the lower, highly permeable Elsterian aquifer (which is in contact with the Zechstein evaporite) from the upper regionally widespread aquifer system. However, the upper parts of the clay complex have been strongly disrupted by glacio-tectonics in some places so localised zones of higher vertical permeability have to be expected in the upper parts of the Lauenburger-Ton-Komplex.

- The lower channel aquifer is hydraulically connected to the Untere Braunkohlensande in the south and in the north. These sands are present throughout the rim synclines and form an important supra-regional aquifer.
- Hamburg-Ton, which overlies the Untere Braunkohlensande in the rim synclines and acts as an aquitard, is absent over large areas in the southeastern part of the salt dome. As a result, there is direct hydraulic contact between the upper and lower aquifers in some parts of the Gartower Tannen groundwater recharge area.
- In the northwestern rim syncline, both aquitards are continuous in the area of the Elbe. Small hydraulic windows are present to the northwest of Dömitz and to the south of the Elbe.

Hydraulically, the lower aquifer in the Gorleben channel can be described as a tubular structure because of the extensive distribution of the Lauenburger-Ton-Komplex within the channel. The southern end of this tube-like structure extends into the groundwater high beneath the Gartower Tannen, whilst to the north in the Elbe lowland it is connected with the lower aquifer of the northwestern rim syncline. The potential gradient between the Gartower Tannen and the Elbe lowland means that flow takes place from south to north in the lower aquifer parallel to the channel axis, if **freshwater conditions** are assumed.

Figure 54 shows the hydraulic situation in a generalised cross section running from the Gartower Tannen in the south, through the Gorleben channel, into the northwestern rim syncline in the Elbe-Löcknitz lowland, through to the area northwest of Dömitz. Because of the assumed hydraulic window to the northwest of Dömitz, it is expected that the groundwater flowing in from the Gorleben channel flows out here into the shallow aquifer – assuming freshwater conditions.

Numeric flow modelling under freshwater conditions gave rise to flow times through the channel of a few thousand to a few ten thousand years because of the good permeability of the channel sediments (cf. Chapter 9.1). This modelling was carried out before the investigation programme was initiated in the Elbe-Löcknitz lowland. Because there was no information available on the hydrogeological structure and groundwater hydraulics in the Elbe-Löcknitz lowland, it was assumed that a hydraulic window is located in the depression immediately to the north of the Elbe – this assumption was made at the time as part of a “conservative” approach. When the investigation in the Elbe-Löcknitz lowland was actually carried out later, it revealed that the aquitard separating the two aquifers was continuous in this area.

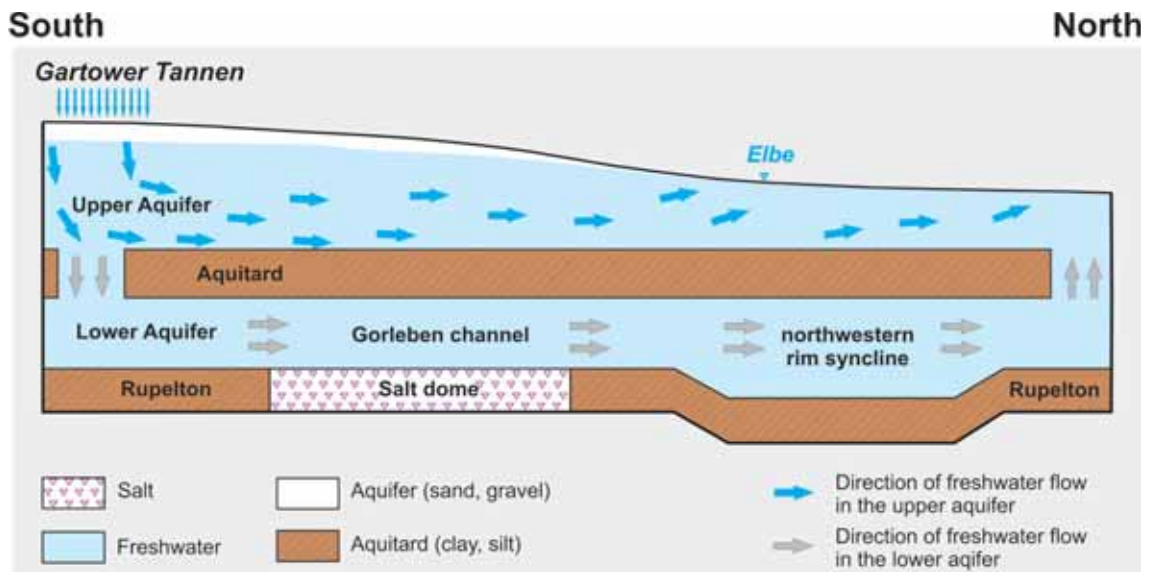


Figure 54: Generalised conceptual model of water flow in the lower aquifer under freshwater conditions (location of schematic cross section, cf. Fig. 59).

However, because, as discussed earlier, such windows probably exist in the area northwest of Dömitz and in the neighbouring area to the south of the Elbe, any new hydraulic modelling carried out in future, which takes into account all of the up-to-date information on the hydrogeological structure of the northwestern rim syncline, would probably not produce any fundamental differences to the migration paths and travel times already determined, as long as freshwater conditions are assumed.

The waters in the Gorleben channel have very high salt concentrations throughout because of dissolution of rock salt in the contact zone between the Zechstein evaporites and the channel aquifer. A characteristic vertical salinity distribution has developed here typified by salt water of a moderate salinity in the upper part of the aquifer and highly saline to salt-saturated waters in the lower part of the aquifer below a transition zone (cf. Chapter 7.1.2).

The observed vertical distribution of salt concentrations in the channel, combined with pressure measurements and theoretical considerations on the effects of hydraulic gradients on groundwater with varying densities, gave rise to the model discussed in Chapter 8.3, where the pressure gradient existing in the Gorleben channel results in a northeastwards groundwater flow of the less mineralised waters in the upper part of the lower channel aquifer. This pressure gradient is reflected to a lesser degree in the highly saline waters at the base of the channel. Convection cells can develop here, leading to reverse flow in parts, and this tendency can be locally strengthened by salt dissolution. Figure 55 shows this hydraulic situation, again in a generalised cross section.

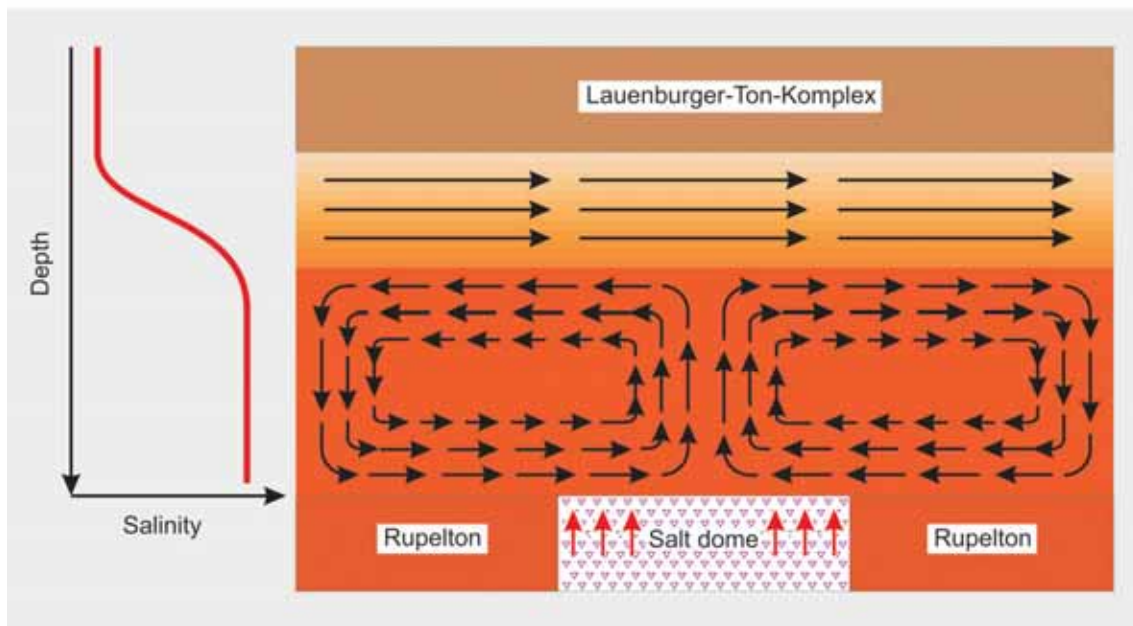


Figure 55: Generalised conceptual model of salt water flow in the lower aquifer in the Gorleben channel

In a scenario involving the release of radionuclides from a repository in the salt dome, longer travel times would be expected for salt water at the base of the channel compared to freshwater conditions. 2D freshwater/salt water modelling in a vertical cross section through the Gorleben channel reveals – for the simplified assumptions used in these model calculations (e.g. homogeneous isotropic aquifers) – that the fastest flow would occur in the uppermost part of the lower channel aquifer, that the velocities would tend to decrease downwards, and that their flow directions could reverse (cf. Chapter 9.2).

The model of salt water flow in the Gorleben channel outlined here was developed at a time when the hydrogeological structure of the area to the north of the Elbe was either only slightly known or completely unknown. At the time, the conservative approach was to assume an upward flow of salt water from the Gorleben channel into the shallow aquifers of the Elbe-Löcknitz lowland. The results of the investigation programme in the Elbe-Löcknitz lowland have now helped provide the information required to make a viable assessment of this previously open question.

The evaluation of the borehole geophysical logs and the chemical analysis of water samples revealed that a salt water body with more than 200 g/l TDS exists in the lower aquifer in the central part of the “basin-shaped” trough structure in the northwestern rim syncline. The chemical composition of this water indicates that this is typical halite subsurface water. The surface of this salt water body is almost horizontal, whilst its base follows the basal shape of the aquifer and reflects the basin-shaped trough structure. A

characteristic salinity profile determined from all of the boreholes drilled into this salt water body showed that the pore waters of the aquitards underlying the aquifer have much lower salt concentrations. This almost certainly excludes vertical upwelling of saline water from deep Mesozoic aquifers as the source of this salt water. Their origin can be determined on the basis of their spatial distribution.

In the distribution area of the Untere Braunkohlensande, the total dissolved solids in the water reduce continuously towards the structural highs in the north, northwest and southeast. A corresponding decline in salt concentration also takes place to the north within the Gorleben channel, whilst the zone of high salt concentrations of > 200 g/l TDS continue south in this channel. Brines therefore originated in the Gorleben channel to the south of the Elbe, where they were formed by dissolution of salt of the Zechstein evaporite body.

The potential inflow of salty water from the north or northeast can be just as much excluded by the salinity distribution described above, as the existence of subsidence in the Gorleben–Rambow salt structure in the area between the Elbe and the Lößnitz. Pore waters in the aquitards surrounding the Zechstein evaporite have much lower salt concentrations here than the brines of the lower aquifer.

As already discussed, the northwestern rim syncline forms a closed basin-shaped trough structure which is cut to the west of Lenzen by the north-south running Gorleben channel. The base of the lower aquifer in the Untere Braunkohlensande is located in the centre of this rim syncline at a depth of -330 m above sea level, but lies at a much higher level of around -150 m above sea level at the edges. The base of the aquifer in the Gorleben channel lies to the north of the Elbe at around -220 m to -230 m above sea level. There is therefore a height difference of around 100 m between the base of the lower aquifer in the Gorleben channel and the centre of the rim syncline (Fig. 8). The characteristic structure and distribution of the salt water body in the lower aquifer, i.e. its largely flat surface and its convex base, are a direct copy of this structure. It is also due to the 15 % to max 20 % higher density of the salt water compared to freshwater. Salt water flowing from the Gorleben channel south of the Elbe towards the north does not follow the northerly course of the Gorleben channel. Instead, it is diverted to the northwest into the centre of the rim syncline by the gradient of the base of the aquifer. Because of its higher density, the salt water collects here at the base of the aquifer. A marked temperature anomaly in the Gorleben channel to the north of the salt dome and the pore water pressure distribution in the salt water body provide evidence for the recent continuous outflow of salt water from the Gorleben channel into the northwestern rim syncline.

The **isotope-hydrological investigations** on the salt water in the Gorleben channel and the northwestern rim syncline reveal a much more complex picture than shown by the borehole temperatures. There is a rapid alternation in the Gorleben channel between Pleistocene brines and brines with mixed Pleistocene and Holocene signatures. In addition, some specific salt waters have clearly been dated as Holocene. These Holocene brines preferentially occur at the base of the aquifer. However, the highly saline waters in the northwestern rim syncline in the distribution area of the Untere Braunkohlensande have Pleistocene glaciation ages throughout.

The distribution pattern of the isotopic signatures in the Gorleben channel also supports the idea that the recent groundwater flow system also affects the lower salt water-filled channel aquifer above the salt dome. It seems clear that the Holocene waters flowing in from the south displace or mix together with the original Pleistocene waters. The partial displacement of Pleistocene brines by younger Holocene salt waters has so far been restricted to the Gorleben channel and/or the immediate neighbouring areas. Most of the waters in the northwestern rim syncline, however, are of Pleistocene age. This indicates that there was only very low water flow overall through the channel aquifer in the Holocene. This finding is consistent with the assumption in the model that taking the salinity of the water into consideration compared to a freshwater system, will tend to give rise to longer travel times.

In addition, a rough estimate indicates that the volume of salt water stored in the northwestern rim syncline is around three times that in the Gorleben channel (Table 4). The larger volume of salt water in the rim syncline and its ubiquitous Pleistocene glacial isotopic signature indicate that the rim syncline was already largely filled with saline groundwater at the beginning of the Holocene. The main outflow of salt water from the Gorleben channel must therefore have taken place during the last Pleistocene glaciation.

Table 4: Comparison of the salt water volume in the Gorleben channel and the northwestern rim syncline

		Gorleben channel	Northwestern rim syncline
Area of the salt water body (TDS > 200 g/l)	[km ²]	14	30
Average thickness	[m]	25	35
Volume of salt water-bearing aquifer	[m ³]	3.5 x 10 ⁸	1 x 10 ⁹
Salt water volume (assuming 30 % porosity)	[m ³]	1 x 10 ⁸	3 x 10 ⁸

According to the model outlined above of south to north directed salt water flow with decreasing flow velocities with depth and some reverse flow directions, Holocene waters should preferentially be encountered in the upper less-mineralised part of the aquifer, whilst Pleistocene waters should be expected at the base of the aquifer. In fact, brines clearly dated as Holocene preferentially occur in the highly saline part at the base of the channel. There is no simple explanation for this fact. Two models are outlined in the following which could explain the presence of Holocene brines at the base of the channel:

A salt table high overlain by a cap rock high with a relatively thin cover of Tertiary clays was penetrated by a well drilled in the transition zone between the Elsterian subsidence trough and the Gorleben channel (GoHy 850 borehole shown in vertical cross section D – D', Appendix 1). The salt table in the drilled section is more than 100 m higher than the base of the neighbouring Gorleben channel. The distance from the borehole to the centre of the channel at this location is only 700 m, i.e. there is an average gradient of around 15 % between the salt table high and the base of the channel. It is therefore possible in principle that salt-saturated brines at the salt table high tend to flow down the topographic gradient into the Gorleben channel because of its density – possibly flowing through hydraulic migration paths such as fractures in the cap rock.

If one also assumes that zones of increased hydraulic permeability exist in the Tertiary overburden around the salt table high, this would support the following model: salt-saturated brines from salt table highs flow down into the Gorleben channel and spread out at its base. They are replaced by Holocene waters of lower brine concentration or freshwaters from the overlying Quaternary aquifer system which reach the salt table in the same way, become saturated, and also flow down into the channel. During the Holocene, this could have led to underlayering of the glacial water in the Gorleben channel by salt-saturated younger Holocene water. This model is demonstrated in Figure 56 on the basis of part of the vertical cross section D – D'.

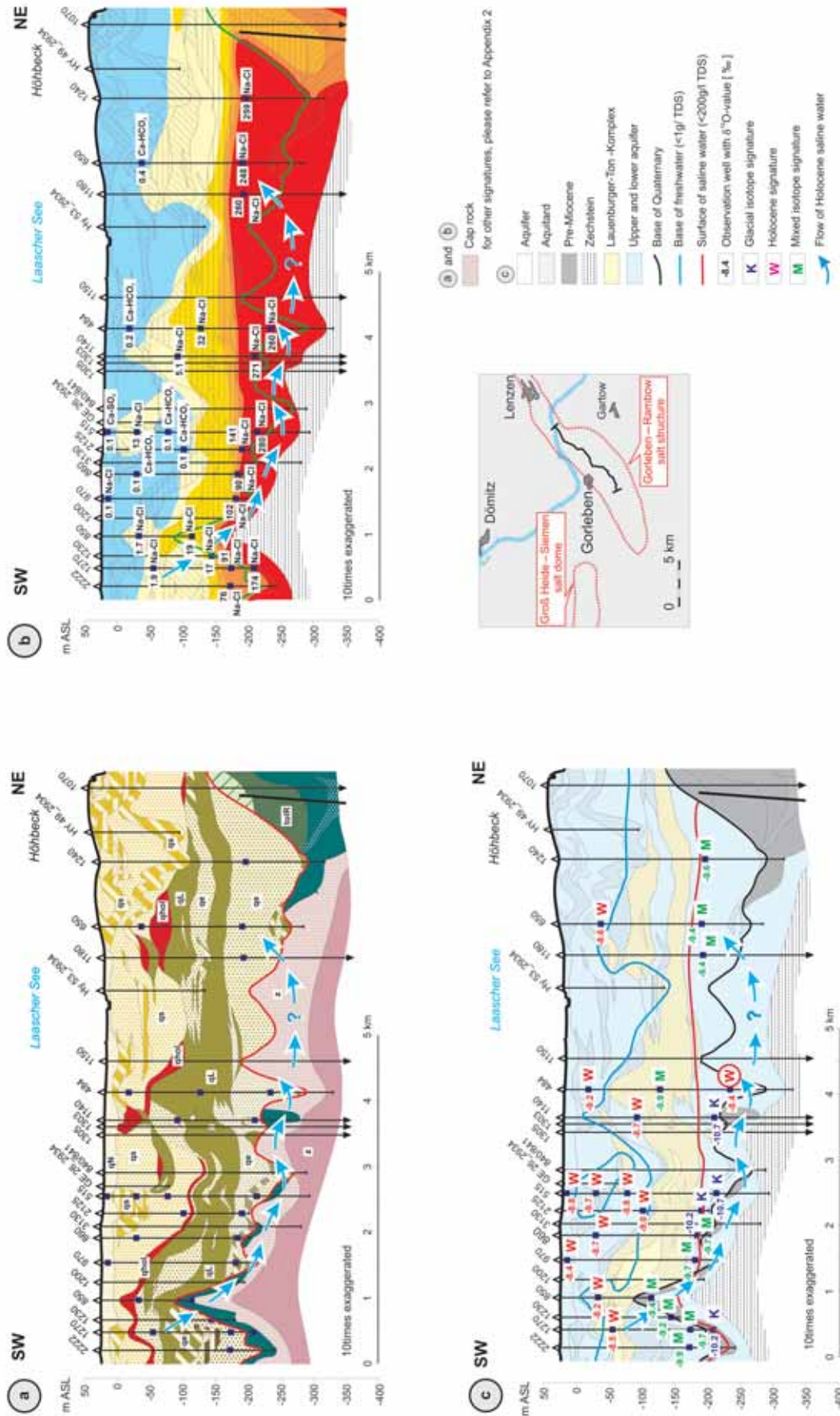


Figure 56: Conceptual model I to explain the presence of Holocene brines at the base of the Gorleben channel

Another model to explain this situation leads to the basic question of how far the freshwater/salt water flow system in the study area during the Pleistocene glacial period differed from the recent flow system. Indications of a different freshwater/salt water distribution during the Pleistocene arose from the investigations carried out by RÜBEL (2000) on pore waters within the Lauenburger-Ton-Komplex. These investigations reveal that the aquifer system in the Elbe-Löcknitz lowland, including the upper aquifer, was filled with salt water for a long period during the Pleistocene so salt water with glacial signatures diffused out of the aquifers overlying and underlying the Lauenburger-Ton-Komplex into the aquitard. Because of a change in hydraulic conditions at the beginning of the Holocene in the upper and lower aquifers, salt water was displaced by freshwater from the highs in the Mecklenburger geest, whilst the salt water with Pleistocene signatures in the Lauenburger-Ton-Komplex remained behind as relicts because of the low permeability of the aquitard (cf. Chapter 7.3.4). The chemical composition of the freshwater within the lower aquifer also reflects this displacement process: the freshwater is primarily NaHCO_3 -exchange water generally thought to have arisen as a result of cation exchange processes associated with the displacement of salt water by freshwater (cf. Chapter 7.2.2).

Corresponding NaHCO_3 -exchange waters also occur within the lower aquifer south of the Elbe under the Gartower Tannen groundwater recharge area, as well as in the pre-Elsterian subsrosion trough above the western part of the salt dome – in other words, in those areas where the upper freshwater body today has major thicknesses exceeding 100 m. The aforementioned evidence suggests that the lower aquifer in the study area was largely filled with salt water during the last Weichselian Glaciation at least and/or that the salt water/freshwater interface was higher overall at that time than today.

According to the present understanding of the climatic conditions during the Weichselian Glaciation, it can be assumed that a more or less complete permafrost cover existed in the Gorleben investigation area at the time (cf. Chapter 9.3). Because this permafrost cover prevented groundwater recharge, this probably brought the local groundwater flow systems to a stop, leading to a rise in the freshwater/salt water interface beneath topographic highs. When the permafrost soils melted as the climate warmed at the beginning of the Holocene, and groundwater recharge restarted, the downward flow of groundwater beneath the topographic highs led to the displacement of the Pleistocene salt water by Holocene freshwater.

The freshwater potentials of the Gartower Tannen in the south and the Mecklenburger geest in the north of the channel structure determine the recent hydraulic system. The pressure potential at the Gartower Tannen, which lies at around 22 m above sea level in the shallow aquifer, induces northward salt water transport in the channel aquifer above the salt dome into the Elbe-Löcknitz lowland. Further transport to the north is countered by the pressure potential of the Mecklenburger geest, which lies in the channel aquifer at around 18 m above sea level at the northern edge of the study area. This causes the southward flow of freshwater into the Elbe-Löcknitz lowland in the lower channel aquifer. The southern edge of this freshwater body currently lies within the Gorleben channel immediately to the north of the Elbe.

The topographically high position of the Gartower Tannen was formed by relatively young aeolian sand deposits laid down during the Holocene – unlike the Saalian highs of the Mecklenburger geest (KÖTHE et al. 2004). It is therefore feasible that the absence of this counteracting potential during the Early Holocene allowed the freshwater body in the lower aquifer to extend further south to the contact zone between the evaporite and the channel aquifer above the salt dome, to displace the original Pleistocene brines further to the south. Dissolution of salt of the contact zone gave rise to Holocene brines. As the dunes developed in the Gartower Tannen, the increasing pressure potential in the south then led to successive displacement of the freshwater/salt water interface to the north and to the overriding of Holocene brines by less saline Pleistocene salt waters or by less saline mixed waters (cf. Fig. 57).

As discussed earlier, the distribution of salt water in the lower aquifer suggests that the subsidence water flows out of the Gorleben channel into the northwestern rim syncline. With a view to defining potential migration paths out of the salt dome, it is important to clarify the extent to which this salt water enters the shallow aquifer. The characteristic shape of the brine body in the lower aquifer in the northwestern rim syncline suggests that this salt water probably collected in the rim syncline trough at the base of the lower aquifer with no significant transport of salt water into the shallow aquifer. On the other hand, in the area of the Elbe-Löcknitz lowland, there is a marked salt water high overlying this brine body, causing the salt water body to reach up close to the groundwater surface in the vicinity of the Rhinow canal in particular (Fig. 24).

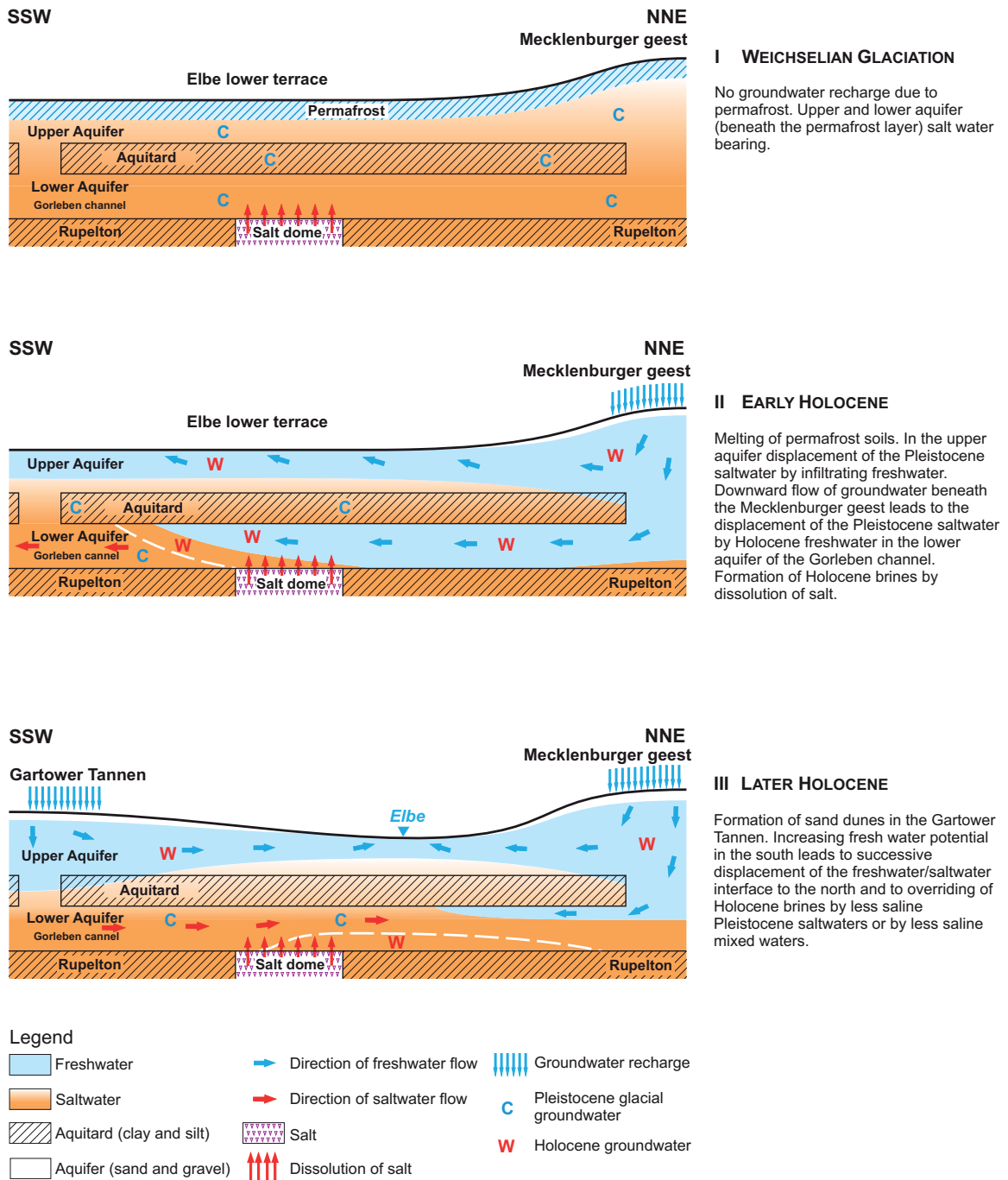


Figure 57: Conceptual model II to explain the presence of Holocene brines at the base of the Gorleben channel

The continuous presence of aquitards separating the two aquifers in the Elbe-Löcknitz lowland is evidence against the vertical rise of salt water. Investigations carried out by RÜBEL (2000) show that extensive vertical water flow can be largely excluded for the Lauenburger-Ton-Komplex at least. However, the Hamburg-Ton has much higher permeability than the Lauenburger-Ton-Komplex. Furthermore, it is possible in principle that there are patches at the edges of the Gorleben channel where both aquitards are either absent or have higher vertical hydraulic permeabilities. Nevertheless, recent connection between the brines of the lower aquifer and the shallow salt waters in the centre of the lowland can be excluded in principle for other reasons: the raised pressure potential in the artesian freshwater body which lies in the lower aquifer directly beneath the base of the aquitard is evidence against the vertical rise of salt water. The water flow within this salt water body itself is towards the Dömitz area, where direct hydraulic contact between the upper and lower aquifers is expected in the zone around a presumed Quaternary channel structure (KÖTHE et al. 2004). It is possible that there is minor exfiltration of salt water into the shallow system here as a result of mixing of freshwater and salt water in the transition zone between the freshwater body and the underlying brine. The shallow depth of the freshwater/salt water interface in the Dömitz area supports this theory (cf. vertical cross section C – C').

The presence of shallow salt water in the Elbe-Löcknitz lowland is associated with the Gorleben–Rambow salt structure, which crosses the valley of the Elbe in a NE-SW direction. The thickness of the aquifers is considerably reduced above the salt structure, and in some parts there is direct hydraulic contact between the upper and lower aquifers. The salt structure acts as a type of barrier on the regional groundwater flow of the Elbe lowland. This causes the water in the lower aquifer to be forced upwards. This could enable salt waters from the lower aquifer, which are encountered at greater depths to the east of the salt dome, to rise up into the upper aquifer via hydraulic windows in the area of the salt dome. The shallow groundwater flowing in the direction of the Elbe can then transport these salt waters in diluted form into the lowland around the Rhinow canal (Fig. 58).

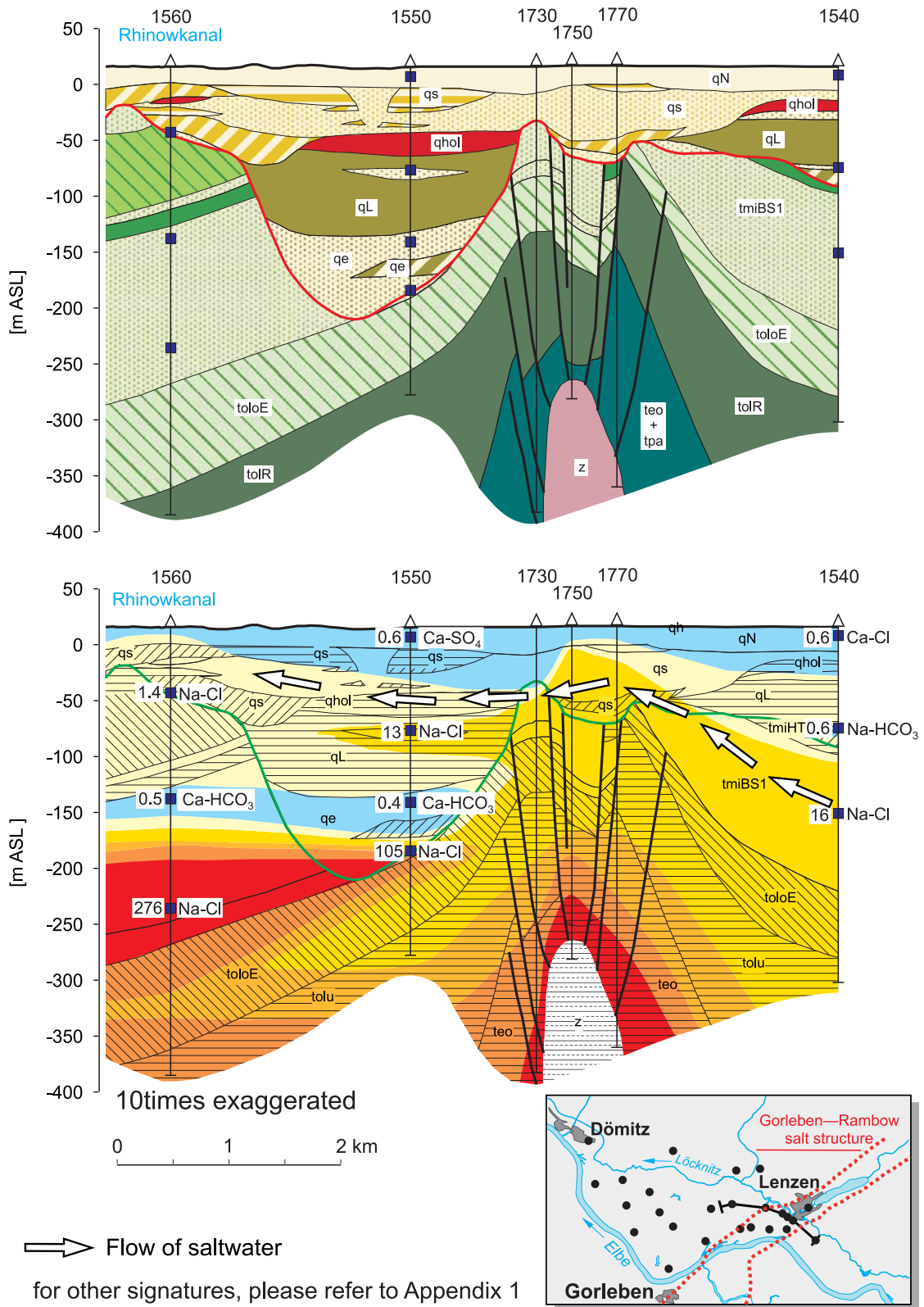


Figure 58: Hydrostratigraphic and hydrochemical vertical cross section through the Gorleben-Rambow salt structure around the Elbe-Löcknitz lowland (modified according to KLINGE et al. 2001)

In addition to this salt water high in the Elbe-Löcknitz lowland, two other salt water highs also exist in the study area (Chapter 7.1.2). The first involves the salination area in the broad region around the Groß Heide–Siemen salt dome. This most probably involves subrosion water from this salt dome, which rises to shallow depths in the groundwater exfiltration areas of the depression.

Another high at the western edge of the Gorleben channel is important with respect to salt water transport from the Gorleben channel. This high extends for around 6 km north-south in the direction of the local groundwater flow from directly north of the shafts of the exploration mine to the northern bank of the Elbe. In the southern part of this high, an extremely narrow zone of very high salt concentrations of up to approx. 90 g/l TDS was encountered in the upper aquifer. The presence of this higher salt concentration alone indicates the probable direct connection to the lower channel aquifer, even though continuous Lauenburger-Ton of varying thickness was encountered in the exploration boreholes. The freshwater/salt water interface that rises from south to north at the Elbe, is accompanied by the parallel reduction in groundwater salt concentrations to values of around 2 g/l TDS. Taken together, these facts suggest that highly saline water in the lower channel aquifer flows via a localised vertical hydraulic connection at the western edge of the channel into the upper Saalian aquifer, and then spreads out in the direction of the groundwater flow towards the Elbe. Vertical connection could be attributable to the strong glacio-tectonic overprinting of the primary stratification during the Saalian Glaciation phase (KÖTHE et al. 2004).

The three-dimensional numerical freshwater flow models at the time focused preferentially on the travel times and flow paths through the Gorleben channel and in the western part of the salt dome overburden. This produced relatively short travel times of 4 000 to 6 000 years overall for the flow paths over the western part of the salt dome (cf. Chapter 9.1). Unlike in the Gorleben channel, the Zechstein evaporite here is extensively covered by pre-Miocene clays, although of varying thickness and with some disturbed bedding as a consequence of subrosion. Despite the presence of a clay cover, a subrosion trough developed in the early Quaternary (Chapter 4.2). Cap rock thicknesses averaging 20 – 40 m also support relatively high subrosion rates. A Comparison of the current freshwater/salt water distribution over the western salt dome and in the Gorleben channel reveals large differences between these two areas:

The freshwater body above the western salt dome in the area of the pre-Elsterian subrosion trough is very thin throughout, and the aquifer is in some cases filled with freshwater right down to its base. As mentioned previously, the salt waters above most of the subrosion trough have relatively low mineralisation levels of less than 20 g/l TDS, which

is comparable to the waters in the southwestern rim syncline. These findings are very probably attributable to the groundwater dynamics in this area: in the area of the western salt dome, the salt water body has downward pointing gradients which could be due to larger freshwater thicknesses and more intensive flow through the freshwater body overall compared to the rim synclines. Nevertheless, low salt concentrations, in particular in the salt waters support the conclusion that the low permeable Tertiary sediments covering the Zechstein evaporites form an effective barrier between the Zechstein salts and the Quaternary aquifer which strongly inhibits the entry of salt into the groundwater. This is also remarkable because the Tertiary deposits are in some cases only a few tens of metres thick, and because it is likely that their bedding has been disturbed by the upward movement of the salt dome. Obviously the viscoplastic consistency of the clays prevents the formation of hydraulically active faults.

Overall, the existing freshwater/salt water distribution allows clear deductions to be made on the transport of salt water out of the Gorleben channel, and thus the definition of two different potential migration paths from the salt dome surface into the aquifer systems.

These two migration paths are shown in a schematic diagram in Figure 59:

- Salt water transport out of the Gorleben channel into the rim syncline in the northwest of the salt dome. Because of the higher density of highly concentrated brine compared to freshwater, brine collects at the base of the closed trough structure in the northwestern rim syncline, without any significant direct vertical further transport into the shallow aquifer. It is possible that diluted salt water migrates into the shallow system via a presumed hydraulic window located further downstream along the Elbe to the west of Dömitz.
- Probable direct vertical upwelling of salt water in the upper aquifer in the area of a localised hydraulic window at the western edge of the Gorleben channel. Salt water spreads towards the north along the regional groundwater flow and reaches the water surface in diluted form in the groundwater discharge areas of the Elbe depression.

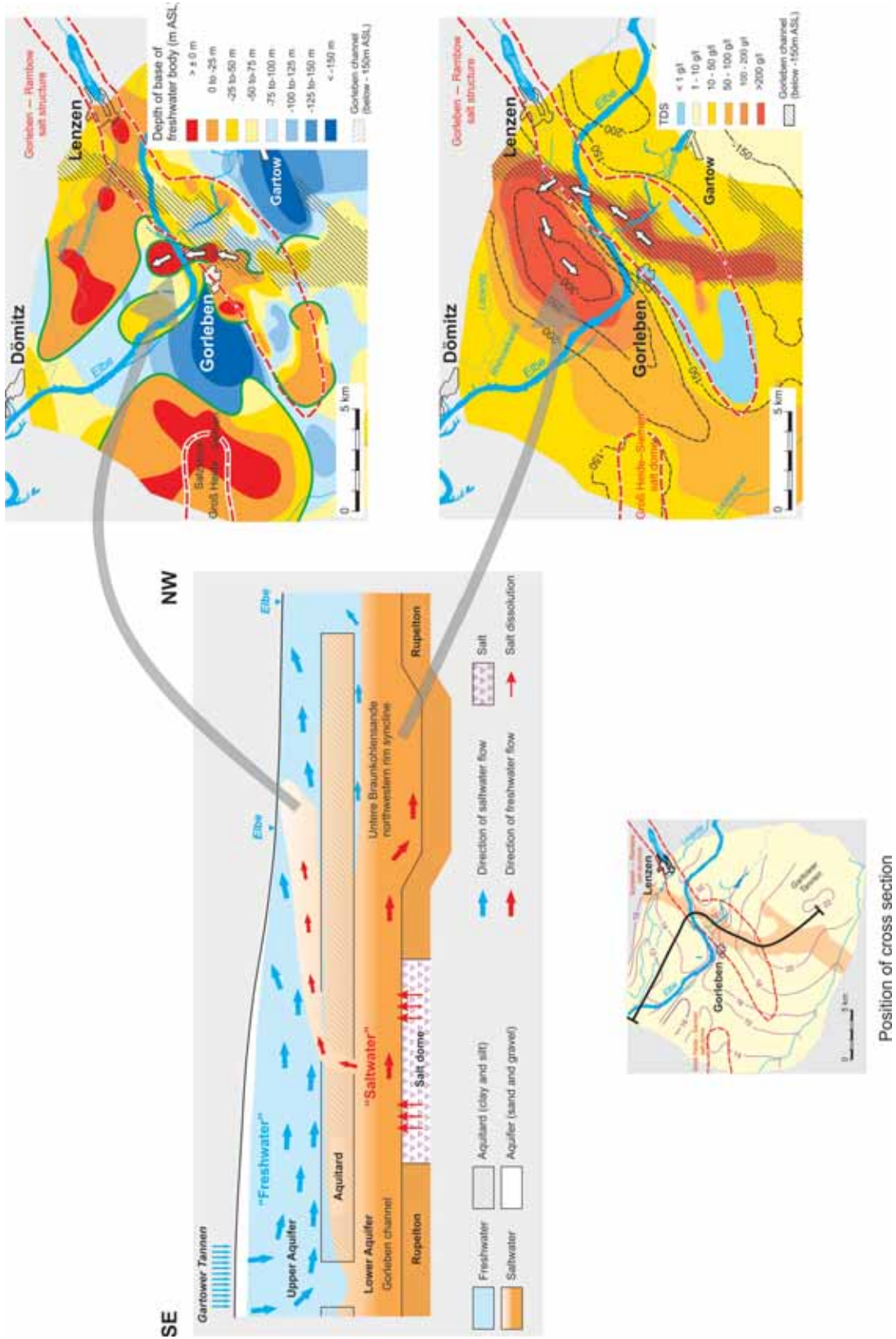


Figure 59: Schematic diagram of salt water transport out of the Gorleben channel

Quantifying the salt water transport, i.e. defining salt water transport rates and flow velocities, is a much more difficult task. The three dimensional freshwater flow models presented here reveal travel times of around 10 000 years for migration paths in the lower aquifer. Direct vertical migration of water out of the lower channel aquifer into the upper aquifer via localised vertical hydraulic windows in the Lauenburger-Ton-Komplex have not so far been taken into consideration in these model calculations. Empirically, such freshwater models generally lead to comparatively shorter travel times but only reflect to a very limited degree the strongly density-influenced flow processes taking place in reality in the salt waters in the Gorleben channel. Two-dimensional freshwater/salt water model calculations through the Gorleben channel show that slower flow velocities and water transport rates should be expected (cf. Chapter 9.2).

These results are in line with the isotopic signatures of the salt waters in the Gorleben channel. The fact that the salt waters still have glacial signatures in part even around 10 000 years after the end of the last Pleistocene glaciation, and therefore still contain glacial water, suggests that flow through the channel is less overall than would be the case under freshwater conditions. The results of the three-dimensional freshwater models can therefore be considered as conservative with respect to the flow velocities and transport rates out of the Gorleben channel. A more detailed quantification of salt water transport rates and flow velocities requires the use of more realistic three-dimensional flow models which take into consideration the locally variable density of the groundwater.

References

- Ad-Hoc-Arbeitsgruppe Hydrogeologie (1997): Hydrogeologische Kartieranleitung.– Geol. Jb., Reihe G, Heft 2. Hannover.
- ALBRECHT, H., BOEHME, J., BORNEMANN, O., DELISLE, G., EISENBURGER, D., FABER, E., FIELITZ, K., FISCHBECK, R., FRITSCH, J., GERLING, P., GIESEL, W., HOLLMANN, A. (BfS), HUNSCHE, U., JARITZ, W., KOPIETZ, J., LEYDECKER, G., LUDWIG, R., NICKEL, H., NIPP, H.-K., PLISCHKE, I., SCHELKES, K., SCHMIDT, G., SCHULZE, O., STREBEL, O., TITTEL, G. (BfS) & ZIRNGAST, M. (1991): Übertägige geowissenschaftliche Erkundung des Standortes Gorleben.– Zusammenfassender Bericht / Stand 01.01.1990.– Unveröff. Ber., BGR, Archiv-Nr. 108 880; Hannover.
- ASSMANN, W., PICKEL, H. J., SCHELKES, K. & VIERHUFF, H. (1983): Tiefe Grundwassermessstellen im Lockergestein, Erfahrungen und Weiterentwicklung.– bbr. 34 (2), 45-50, Köln.
- ALBRECHT, H. & ZWIRNER, H. (1999): Ergebnisdokumentation Känozoikum – Geologie des Deckgebirges im Untersuchungsgebiet Dömitz-Lenzen.– Unveröff. Ber., BGR, Archiv-Nr. 117 861; Hannover
- BEAR, J. (1979): Hydraulics of Groundwater, McGraw Hill, New York.
- BERNER, Z. A., STÜBEN, D., LEOSON, M. A. & KLINGE, H. (2002): S- and O-isotopic character of dissolved sulphate in the overburden aquifers of a Zechstein salt dome.– Applied Geochemistry 17 (2002), pp. 1515-1528.
- BESENECKER, H., KRIEGER, K. & NEUSS, M. (1983): Zur Regeneration eines Aquifersystems im Bereich quartärer Stauchzonen (Höhbeck/NE-Nieder-sachsen).– Z. dt. geol. Ges. 134, pp. 735-754; Hannover.
- BEYER, W. (1964): Zur Bestimmung der Wasserdurchlässigkeit von Kiesen und Sanden aus der Kornverteilung.– Wasserwirtschaft-Wassertechnik (WWT), pp. 165-169, Ost-Berlin.
- BOEHME, J., (1993): Grundwasserstandsdaten aus dem Bereich des Salzstockes Gorleben/ Teil V/ Auswertung.– Unveröff. Ber. BGR, Arch.-Nr. 111 673; Hannover.
- BORNEMANN, O. (1991): Zur Geologie des Salzstocks Gorleben nach den Bohrergebnissen.– BfS-Schriften, 4/91; Salzgitter.

- BORNEMANN, O., BEHLAU, J., FISCHBECK, R., HAMMER, J., JARITZ, W., KELLER, S., MINGERZAHN, G. & SCHRAMM, M. (2008): Standortbeschreibung Gorleben, Teil 3: Ergebnisse der über- und untertägigen Erkundung des Salinars.– Geol. Jb. C 73, pp. 5-211, 50 Abb., 7 Tab., 5 Anl., Hannover.
- BOEHME, J., FIELITZ, K., V. HOYER, M., KLINGE, H., KOPIETZ, J., LUDWIG, R., OCHMANN, N., SCHELKES, K., SÖFNER, B., & WERNICKE, W. (1995): Standortbeschreibung Gorleben-Süd – Hydrogeologie des Deckgebirges.– Unveröff. Ber., BGR, Archiv-Nr. 112693; Hannover.
- BOULTON, G., GUSTAFSON, G., SCHELKES, K., CASANOVA, J. & MOREN, L. (2001): Palaeohydrogeology and geoforecasting for performance assessment in geosphere repositories for radioactive waste disposal (Pagepa).– EUR 19874, Final report, Nuclear science and technology series, European Commission, Brussels, 147 pp.
- BRÄUER, V.; EICKEMEIER, R.; EISENBURGER, D.; GRISSEMANN, C; HESSER, J.; HEUSERMANN, S.; KAISER, D.; NIPP, H.-K., NOWAK, T.; PLISCHKE, I.; SCHNIER, H.; SCHULZE, O.; SÖNNKE, J. & WEBER, J.-R. (in preparation): Standortbeschreibung Gorleben, Teil 4: Geotechnische Erkundung.
- Bundesamt für Strahlenschutz (BfS) (1990): Fortschreibung der zusammenfassenden Zwischenberichtes über bisherige Ergebnisse der Standortuntersuchung Gorleben vom Mai 1983, Salzgitter.
- BROSE, F. (1991): Untersuchungen zum Auftreten örtlicher Versalzungen im oberflächennahen Grundwasser in der Umgebung des Salzstockes von Gorleben.– Dissertation, FU Berlin.
- BRÜHL, H. & FABER, P. (1983): Salzkonzentrationen im oberflächennahen Grundwasser des Kreises Lüchow-Dannenberg und ihre Verteilung.– PSE-interner Arbeitsbericht Nr. 83/1B, FU Berlin.
- BUCKAU, G., ARTINGER, R., GEYER, S., WOLF, M., FRITZ, P. & KIM, J.I. (2000): ¹⁴C dating of Gorleben groundwater.– Appl. Geochem. 15, pp. 583-597.
- CHIANG, W. H. & KINZELBACH, W. (1991): Processing Modflow (PM) Pre- and postprocessors for the simulation of flow and contaminant transport in groundwater systems with MODFLOW, MODPATH, and MT3D.– Handbuch zum Programm, Selbstverlag (Hamburg, Heidelberg).

- CRAIG, H. (1961): Isotopic variations in meteoric waters.– Science 133, p. 1702.
- DELISLE, G. (1980): Berechnungen zur raumzeitlichen Entwicklung des Temperaturfeldes um ein Endlager für mittel- und hochradioaktive Abfälle in einer Salzformation.– Z. dt. geol. Ges. 131, pp. 461-482; Hannover.
- DELISLE, G. (1998): Numerical Simulation of Permafrost Growth and Decay. – Journal of Quaternary Science, 13 (4), pp. 325-333.
- DELISLE, G., FIELITZ, K., GIESEL, W., SCHELKES, K., SCHMIDT, G., BOEHME, J., KELLER, S., LUDWIG, R. & VIERHUFF, H. (1985): Grundwasserbewegung im Deckgebirge über dem Salzstock Gorleben – Datenermittlung, Interpretation und Modellrechnungen.– Fachband 17 des Abschlußberichtes “Projekt Sicherheitsstudien Entsorgung”, 125 pp., Berlin.
- DELISLE, G. & BOULTON, G. (2000): A Numerical Model on the Weichselian Permafrost Aggradation/Degradation in Central and Northern Europe.– Proc. European Geophysical Society, XXV General Assembly, Nice, France, 24-29 April 2000.
- FIELITZ, K. & GIESEL, W. (1991): Evaluation of groundwater salinity from well logs and conclusions on flow velocities of saline water. In: De Breuck (Ed.), Hydrogeology of Salt Water Intrusion, Verlag H. Heise; Hannover.
- Geo-Data (2000): Großpumpversuch Dömitz-Lenzen, Bericht und Dokumentation GPV.– Geo-Data GmbH, Unveröff. Ber., erstellt im Auftrage des BfS.
- Geo-Data (2001): Großpumpversuch Dömitz-Lenzen, modellhafte Betrachtungen zum GPV.– Geo-Data GmbH, Unveröff. Ber., erstellt im Auftrage des BfS.
- HÄNEL, R. (Editor) (1998): Atlas of Subsurface Temperatures in the European Communities.– 36 pp., 43 plates; Commission of the European Communities, Directorate for Research, Sciences and Education; Hannover.
- HAZEN, A. (1893): Some physical properties of sand and Ggravel with special reference to their use in filtration.– Ann. Rep. Mass. State Bd. Health 24: pp. 541-556; Boston.
- HENNINGS, V. & DUIJNISVELD, W.H.M. (1997): Bodenkundliche Kartierung und flächendifferenzierte Berechnung der Sickerwasserrate aus dem Boden im Projektgebiet Dömitz-Lenzen.– Unveröff. Ber., BGR, Archiv-Nr. 116 001; Hannover.

- HOFFMANN, B. & RADELFAHR, H. (1986): Pumpversuche. Planung und Auswertung der Pumpversuche im Raum Gorleben. Teil 7.– Unveröff. Ber., Inst. f. Wasserwirtsch., Hydrologie u. landwirtschaftl. Wasserbau der Univ. Hannover; Hannover.
- KLINGE, H. (1994): Zusammenfassende Bearbeitung der chemischen und isotope-geochemischen Zusammensetzung der Grundwässer im Deckgebirge des Salzstockes Gorleben und seiner Randsenken – Projektgebiet Gorleben-Süd.– Unveröff. Ber., BGR, Archiv-Nr. 111 699; Hannover.
- KLINGE, H., RÜBEL, A., SUCKOW, A. & BEUSHAUSEN, M. (2000): Isotope hydrological studies on the salt water flow above the Gorleben salt dome.– Proc. SWIM 16, Nicholas Copernicus Univ., Vol. 80 (2000): pp. 95-102; Turon.
- KLINGE, H., KÖTHE, A., LUDWIG, R.R. & ZWIRNER, R. (2002): Geologie und Hydrogeologie des Deckgebirges über dem Salzstock Gorleben.– Z. Angew. Geol. (2/2002), pp. 7-15, Hannover.
- KLINGE, H., BOEHME, J., GRISSEMANN, C., HOUBEN, G., LUDWIG, R.R., SCHELKES, K. & SCHILDKNECHT, F. (2004): Standortbeschreibung Gorleben, Teil II, Deckgebirge Hydrogeologie.– Unveröff. Ber., BGR, Hannover.
- KÖSTERS, E., VOGEL, P. & SCHELKES, K. (2000): A Palaeohydrogeological Approach to Regional Density-Dependent Groundwater Modeling: A Case Study in Northern Germany.– Proc. SWIM 16, Nicholas Copernicus University, Vol. 80 (2000), pp. 103-110; Turon.
- KÖTHE, A., ZIRNGAST, M. & ZWIRNER, R. (2004): Projekt Gorleben, Standortbeschreibung Gorleben, Teil I, Deckgebirge Geologie.– Unveröff. Ber., BGR; Hannover.
- KÖTHE, A., HOFFMANN, N., KRULL, P., ZIRNGAST, M. & ZWIRNER, R. (2007): Standortbeschreibung Gorleben, Teil 2: Die Geologie des Deck- und Nebengebirges des Salzstocks Gorleben.– Geol. Jb., C 72, pp. 5-201, 42 Abb., 19 Tab., Hannover.
- KRÖHN, K.-P. (1991): Simulation von Transportvorgängen im klüftigen Gestein mit der Methode der Finiten Elemente.– Bericht Nr. 29/1991, Institut für Strömungsmechanik und Elektronisches Rechnen im Bauwesen, Universität Hannover.
- LANDDOLT-BÖRNSTEIN (1967): Zahlenwerte und Funktionen.– Bd. 2; 6. Ausg.; Springer Verlag, Berlin.

- LÖHNERT, E. (1970): Grundwasserchemismus und Kationentausch im norddeutschen Flachland.– Z. deutsch. geol. Ges., Sonderh. Hydrogeol. Hydrochem., pp. 139-159; Hannover.
- LUDWIG, R., SCHELKES, K., VOGEL, P. & WOLLRATH, J. (2001): Implications of large-scale heterogeneities for hydraulic model studies at the potential site of a radioactive waste repository at Gorleben, Germany.– Engineering Geology 61, p. 119-130; Amsterdam – Oxford – New York.
- MARGANE, A., MRUGALLA, S., SCHELKES, K. & SÖFNER, B. (2001): Hydrogeologie des Untersuchungsgebietes Dömitz-Lenzen.– Unveröff. Ber., BGR; Hannover.
- NEA & SKI (Ed.) (1988): The International HYDROCOIN Project Level 1: Code Verification.– OECD Publ., 198 pp.; Paris.
- OCHMANN, N. (1993): Auswertung der elektromagnetischen Messdaten aus der Überfliegung des Raumes Gorleben.– Unveröff. Ber., BGR, Archiv-Nr. 111398; Hannover.
- Physikalisch-Technische Bundesanstalt (PTB) (1983): Zusammenfassender Zwischenbericht über bisherige Ergebnisse der Standortuntersuchung in Gorleben.– Braunschweig.
- PORTMANN, F. & MENDEL, H.-G. (1999): Hydrologisches Untersuchungsprogramm Gorleben – Wasserhaushaltsbericht 1984-1997.– Unveröff. Ber., Bundesanstalt für Gewässerkunde; Koblenz.
- PREUSS, H. & VINKEN, R. & VOSS, H.H. (1991): Symbolschlüssel Geologie – Symbole für die Dokumentation und automatische Datenverarbeitung geologischer Feld- und Aufschlußdaten.– 328 pp., Niedersächs. Landesamt für Bodenforschung, Hannover.
- PREUSS, M. & WESSOLEK, G. (1990): Auswirkungen der Grundwasserabsenkungen und Nutzungsänderungen auf die Grundwasserneubildung.– Mitt. Inst. für Wasserwesen, Bundeswehr-Hochschule München, Band 38 B, pp. 295-305.
- RÜBEL, A. P. (2000): Stofftransport in undurchlässigen Gesteinsschichten. Isotopenuntersuchungen im Grund- und Porenwasser.– ISBN 3934366376, Der Andere Verlag, Osnabrück.

- SCHELKES, K. & VIERHUFF, H. (1983): Über den Einfluß undichter Aufsatzverrohrungen bei Grundwasser-Meßstellen auf hydrogeologische Untersuchungen.– Z. dt. geol. Ges., 134, pp. 789-805; Hannover.
- SCHELKES, K., VOGEL, P., KLINGE, H. & KNOOP, R.M. (1990): Modelling of variable-density groundwater flow with respect to planned radioactive waste disposal sites in West Germany – Validation activities and first results.— In: Proc. GEOVAL-1990, Symp. on Validation of Geosphere Flow and Transport Models, pp. 328-335, OECD 1991; Paris.
- SCHMIDT, G. (1987): Die Bewegung des Grundwassers im Deckgebirge über dem Salzstock Gorleben – Untersuchungen mit einem numerischen Modell.– Unveröff. Ber., BGR, Archiv-Nr. 102 396; Hannover.
- SCHMIDT, G. (1991): GS4000 – Ein dreidimensionales Modell zur Simulation der Grundwasserbewegung im porösen Medium.– Unveröff. Ber., BGR, Archiv-Nr. 108083; Hannover.
- SPONAGEL, H. & STREBEL, O. (1981): Ermittlung von boden- und nutzungsspezifischen Jahreswerten der Grundwasserneubildung mit Hilfe von Boden- und Klimadaten sowie deren flächenhafte Darstellung für den Raum Lüchow-Gartow-Schnackenburg.– Unveröff. Ber., BGR, Archiv Nr. 89714; Hannover.
- STRELTSOVA, T. (1988): Well Testing in Heterogeneous Formations.– 1. Aufl., J. Wiley and Sons; New York.
- SUCKOW, A. (1993): Isotopenhydrologische und Edelgaspaläotemperatur-untersuchungen im Deckgebirge des Salzstocks Gorleben.– Dissertation, Universität Heidelberg.
- THEIS, C. V. (1935): The relations between the lowering of the piezometric surface and the rate and duration of discharge of a well using ground-water storage.– Trans. Am. Geophys. Union, pt. 2: pp. 519-524; Washington D.C.
- VOGEL, P., SCHELKES, K. & GIESEL, W. (1993): Modelling of variable-density flow in an aquifer crossing a salt dome - first results.– In: Custodio, E.; Galofré, A. (Eds.): Study and Modelling of Salt water Intrusion into Aquifers (Proceedings 12th Salt water Intrusion Meeting, Barcelona November 1992), pp. 359-369, CINME, Barcelona.

- VOGEL, P. & SCHELKES, K. (1996): Influence of initial conditions and hydrogeological setting on variable density flow in an aquifer above a salt dome.– In: Calibration and Reliability in Groundwater Modelling (Proceedings of the ModelCARE 96 Conference held at Golden, Colorado, September 1996), pp. 373-381.
- VOGEL, P., KÖSTERS, E. & SCHELKES, K. (2001): A conceptual approach to long-term climatically driven groundwater variations in a freshwater/salt water system.– Proc. XXXI International Association of Hydrogeologists Congress Munich, 10 – 14 Sept. 2001, pp. 425-429.
- Voss, C. I. (1984): SUTRA: A finite-element simulation model for saturated unsaturated, fluid-sensitivity-dependant ground-water flow with energy transport or chemically-reactive species solute transport.– USGS Water Resour. Invest. Rep., 84-4369.
- WOLLRATH, J. & ARENS, G. (1992): INTRAVAL Phase 2: Investigations into the influence of the density stratification on groundwater flow by the example of pumping test “Weisses Moor”.– ET-Berichte 16/92; Salzgitter (BfS).
- ZIESCHANG, J. (1961): Zur zulässigen Höchstbelastung eines Brunnens.– Z. Angew. Geol., 7, pp. 580-582; Berlin.

Abbreviations

a	Year
ASL	Above mean sea level
BfG	Bundesanstalt für Gewässerkunde
BfS	Bundesamt für Strahlenschutz
BGR	Bundesanstalt für Geowissenschaften und Rohstoffe
BGL	Below ground level
¹³ C	Carbon 13 isotope
¹⁴ C	Carbon 14 isotope
D	Deuterium (² H)
d ₆₀	Grain size of the 60 % fraction of the cumulative grain size curve
d ₁₀	Grain size of the 10 % fraction of the cumulative grain size curve
DBE	Deutsche Gesellschaft zum Bau und Betrieb von Endlagern für Abfallstoffe mbH
Ec	Specific electrical conductivity of water [μ S/cm]
GoHy	Gorleben hydrogeology, prefix of boreholes in the hydrogeological investigation programme
² H	Deuterium (D)
³ H	Tritium
⁴ He _{exc}	Helium 4 excess concentration in water (measured value minus equilibrium)
K	Kelvin
k _f	Coefficient of hydraulic conductivity [m/s]
kf	Compression factor
¹⁸ O	Oxygen-18 isotope
¹⁶ O	Oxygen-16 isotope
pMC	Per cent modern carbon
q	Heat flow density in [W/m ²]

S	Storage coefficient [dimensionless]
SMOW	Standard Mean Ocean Water, standard for comparing oxygen and hydrogen isotope determinations
T	Transmissivity in [m ² /s]
T ₀	Annual average temperature at the earth's surface [°C]
T _i	Temperature in the i-th layer in [°C]
grad T _i	Temperature gradient in the i-th layer in [K/m]
TDS	Total dissolved solids
TU	Tritium unit, 1 TU = 1 tritium atom to 10 ¹⁸ hydrogen atoms
U	Degree of irregularity of the grain size composition of the sediment; $U = d_{60}/d_{10}$
V _{wa} , V _{to} , V _{sa}	Relative volume proportions of water, clay and sand
WD	(Test to determine) water permeability
δ ¹⁸ O	Difference between the 18O/16O isotope ratio of a sample and sea water
δ ¹³ C	Difference between the 13C/12C isotope ratio of a sample and the PDB standard (<u>P</u> ee <u>D</u> ee <u>B</u> elemnite limestone)
δD	Difference between the D/H isotope ratio of a sample and seawater

Note:

Stratigraphic and petrographic abbreviations reflect the Geology Symbol Legend (PREUSS et al. 1991). Standard measuring units, abbreviations and chemical symbols are not listed.

List of tables	Page
Table 1: Technical data on the long-term pumping tests	33
Table 2: Pumping test results: hydraulic parameters	35
Table 3: Thermal conductivities for the sedimentary components clay, quartz sand and water used in the calculations	46
Table 4: Comparison of the salt water volume in the Gorleben channel and the northwestern rim syncline	121

List of figures	Page
Figure 1: Location map of the exploration boreholes and observation wells for the hydrogeological investigation programme	12
Figure 2: Location and morphology of the Gorleben study area	14
Figure 3: Annual precipitation for 1984 – 1997 hydrologic years (according to PORTMANN & MENDEL 1999)	17
Figure 4: Groundwater recharge calculated from the soil water balance (percolation water rate in mm/year)	19
Figure 5: Simplified geological cross section through the Gorleben salt dome (according to ZIRNGAST in ALBRECHT et al. 1991)	21
Figure 6: Summary of the hydrostratigraphic structural units of the overburden in the Gorleben study area.	22
Figure 7: Aquifer subdivision in the overburden of the Gorleben salt dome	26
Figure 8: Base of the lower aquifer (according to KÖTHE et al. 2004)	27
Figure 9: Distribution of the Hamburg-Ton and Lauenburger-Ton-Komplex aquitards (according to Köthe et al. 2004)	29
Figure 10: Location of the long-term pumping test sites	33
Figure 11: Drawdown at the end of the pumping test phase – Weißes Moor 1 pumping test	36
Figure 12: Drawdown at the end of the pumping test phase – Weißes Moor 2 pumping test	37
Figure 13: Drawdown at the end of the pumping test phase – Meetschow pumping test	38
Figure 14: Drawdown at the end of the pumping test phase – Gorlebener Tannen pumping test	38
Figure 15: Drawdown at the end of the pumping test phase – Dömitz-Lenzen pumping test	40
Figure 16: Hydraulic conductivity coefficients from pumping tests and laboratory tests	42
Figure 17: Groundwater temperature distribution at -150 m above sea level	45
Figure 18: Measured and calculated temperature and thermal conductivity logs in the GoHy 1092 and GoHy 1534 groundwater observation wells	47
Figure 19: Heat flow density map	49
Figure 20: Groundwater temperatures and advective differential temperatures along the Gorleben channel (cf. Fig. 17 for cross section location).	51
Figure 21: Distribution of advective temperature differences in the northwestern rim syncline at -180 m above sea level	54

Figure 22: Correlation between total dissolved solids in the water sample from observation wells and the formation resistivities derived from induction logs	57
Figure 23: Distribution and total dissolved solids of the lower freshwater body in the Elbe-Löcknitz lowland	58
Figure 24: Vertical change in pore water conductivity in GoHy 1590 exploration well	60
Figure 25: Vertical density distribution of groundwater at the GoHy 1163 observation well on the basis of induction log interpretations.	61
Figure 26: Groundwater TDS at the base of the lower aquifer	62
Figure 27: Depth of the base of the upper freshwater body	63
Figure 28: Hydrostratigraphic and hydrochemical vertical sections through the salt water high at the western edge of the Gorleben channel (legend see Appendix 1)	65
Figure 29: Schematic diagram of the vertical groundwater type zoning within the Gorleben study area	67
Figure 30: Chemical composition of various groundwater types within the study area	68
Figure 31: Na/Cl equivalent ratio in the groundwater versus TDS	70
Figure 32: Sulphate concentrations of the groundwater versus TDS	73
Figure 33: Bicarbonate concentrations of the groundwater versus TDS	73
Figure 34: Depth profile of measured tritium concentrations in groundwater	75
Figure 35: Correlation between $\delta^{18}\text{O}$ and δD	77
Figure 36: Relationship between $\delta^{18}\text{O}$ and groundwater TDS	79
Figure 37: Oxygen isotopic signatures of salt water with > 200 g/l TDS	81
Figure 38: ^{14}C concentrations of groundwater versus TDS	84
Figure 39: Depth section of salt concentration, $^4\text{He}_{\text{exc}}$ and $\delta^{18}\text{O}$ and δD measured values in the Lauenburger-Ton-Komplex pore water in the GoHy 1623 borehole	87
Figure 40: Depth section of salt concentration, the $^4\text{He}_{\text{exc}}$ and the $\delta^{18}\text{O}$ and δD recorded values in pore water from the Hamburg-Ton in the GoHy 1674 borehole	89
Figure 41: Hydrograph of the GoHy 190 observation well group	92
Figure 42: Comparison of the GoHy 280 observation well hydrograph and the Elbe river hydrograph at Gorleben	93
Figure 43: Water table contours of the shallow groundwater	96
Figure 44: Schematic diagram of regions of groundwater recharge, groundwater discharge and groundwater inflow and outflow	98

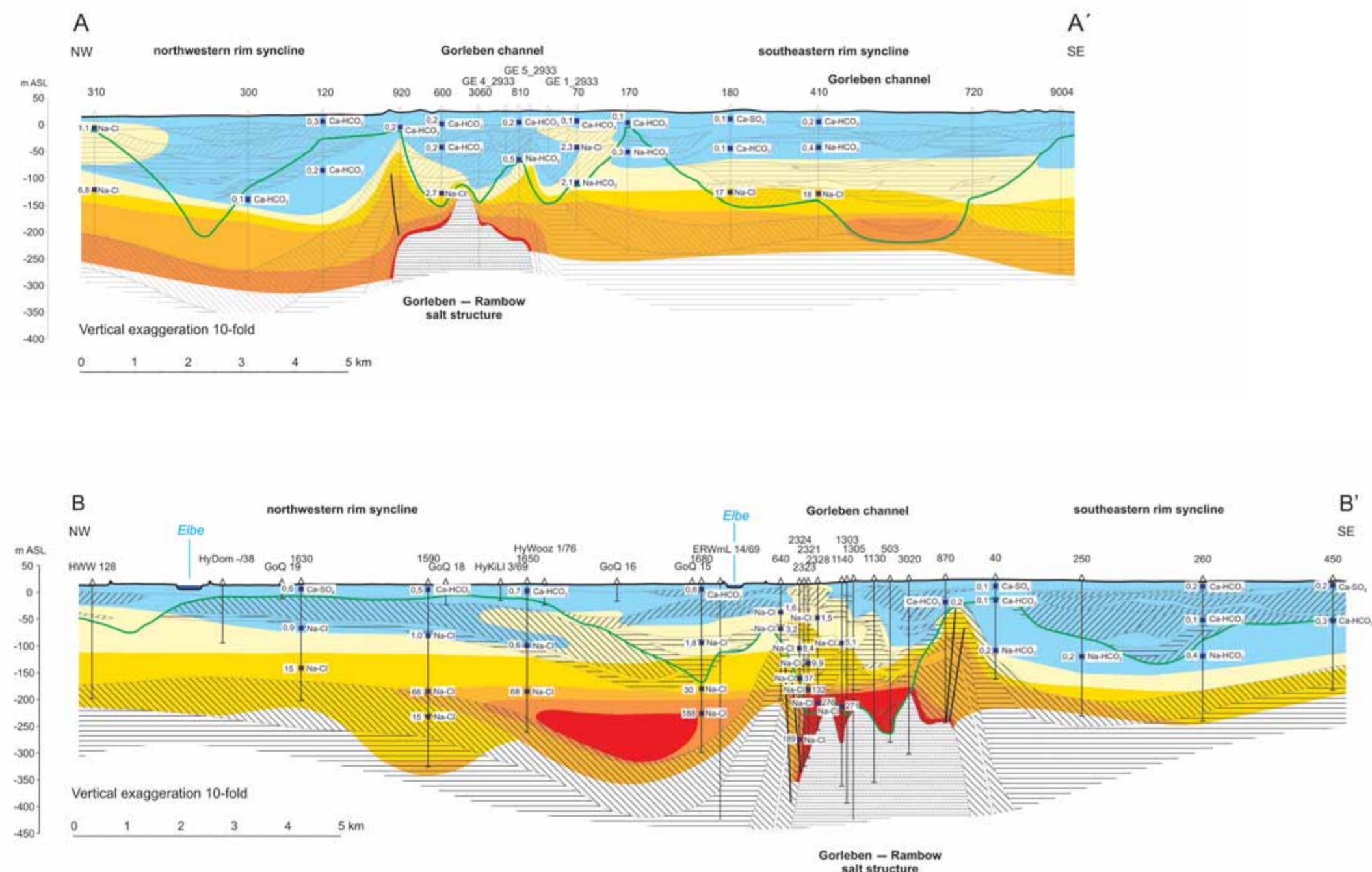
Figure 45: Potentiometric surface of the freshwater body within the lower aquifer	99
Figure 46: Calculated pore water pressures and flow directions in the Gorleben channel	102
Figure 47: Model age of the groundwater in the channel area, and travel times from starting points at the base of the aquifer to the biosphere excluding (excl.) and including (incl.) consideration of the cap rock (from ALBRECHT et al. 1991)	105
Figure 48: Model calculations of groundwater flow with variable densities (according to SCHELKES et al. 1990) – calculated salt concentrations	108
Figure 49: Model calculations of groundwater flow with variable density (according to SCHELKES et al. 1990) – calculated flow directions and velocities	109
Figure 50: Geographical location of the regional paleohydrogeological study area	111
Figure 51: Simplified hydrogeological cross section (location of cross section, cf. Fig. 50)	112
Figure 52: Calculated permafrost thicknesses in the model area within the Weichselian glaciation	113
Figure 53: Salt concentration and flow direction of groundwater above the Gorleben salt dome during a typical stadial and interstadial	113
Figure 54: Generalised conceptual model of water flow in the lower aquifer under freshwater conditions (location of schematic cross section, cf. Fig. 59).	117
Figure 55: Generalised conceptual model of salt water flow in the lower aquifer in the Gorleben channel	118
Figure 56: Conceptual model I to explain the presence of Holocene brines at the base of the Gorleben channel	122
Figure 57: Conceptual model II to explain the presence of Holocene brines at the base of the Gorleben channel	125
Figure 58: Hydrostratigraphic and hydrochemical vertical cross section through the Gorleben–Rambow salt structure around the Elbe-Löcknitz lowland (modified according to KLINGE et al. 2001)	127
Figure 59: Schematic diagram of salt water transport out of the Gorleben channel	130

List of appendices

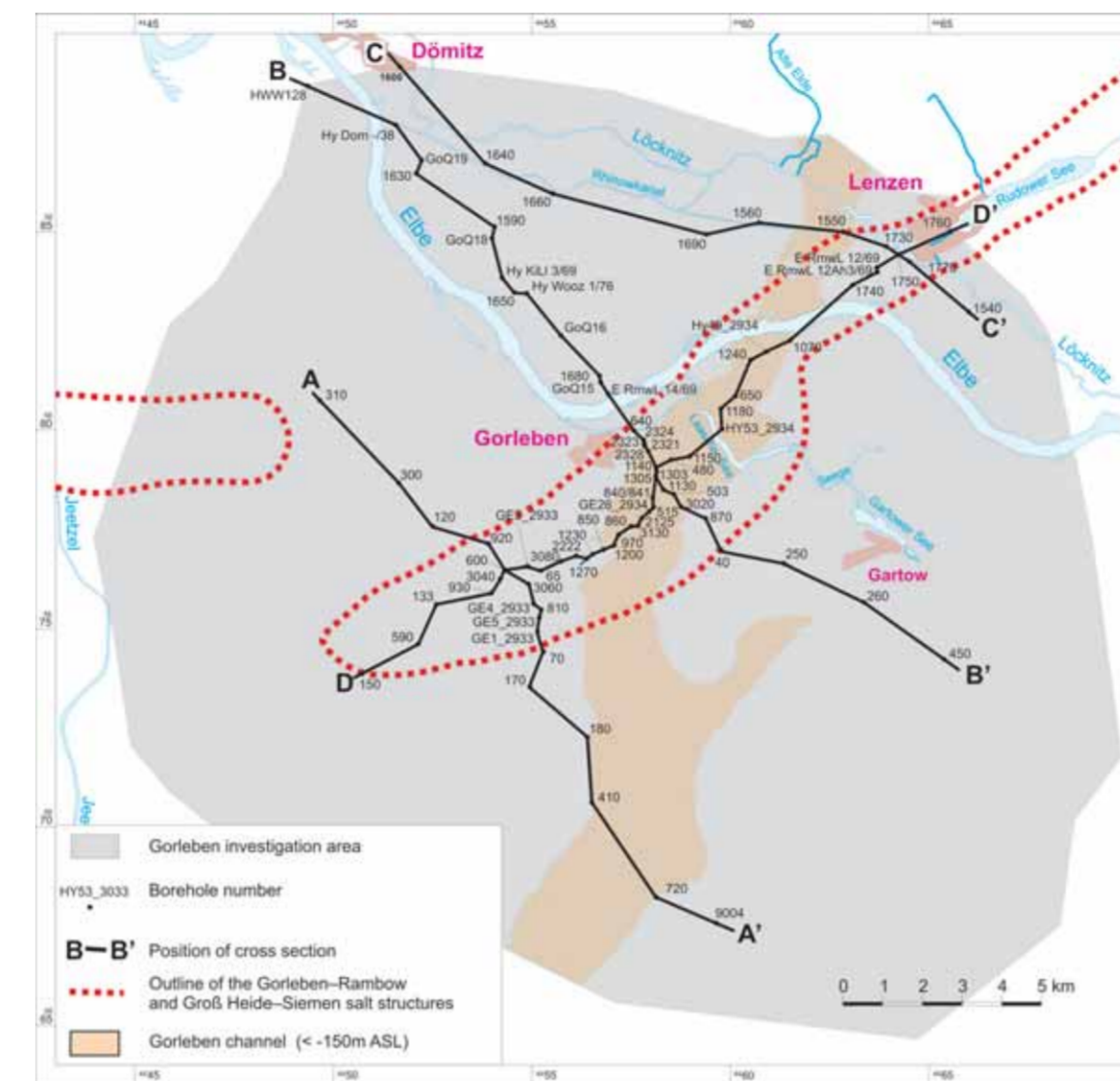
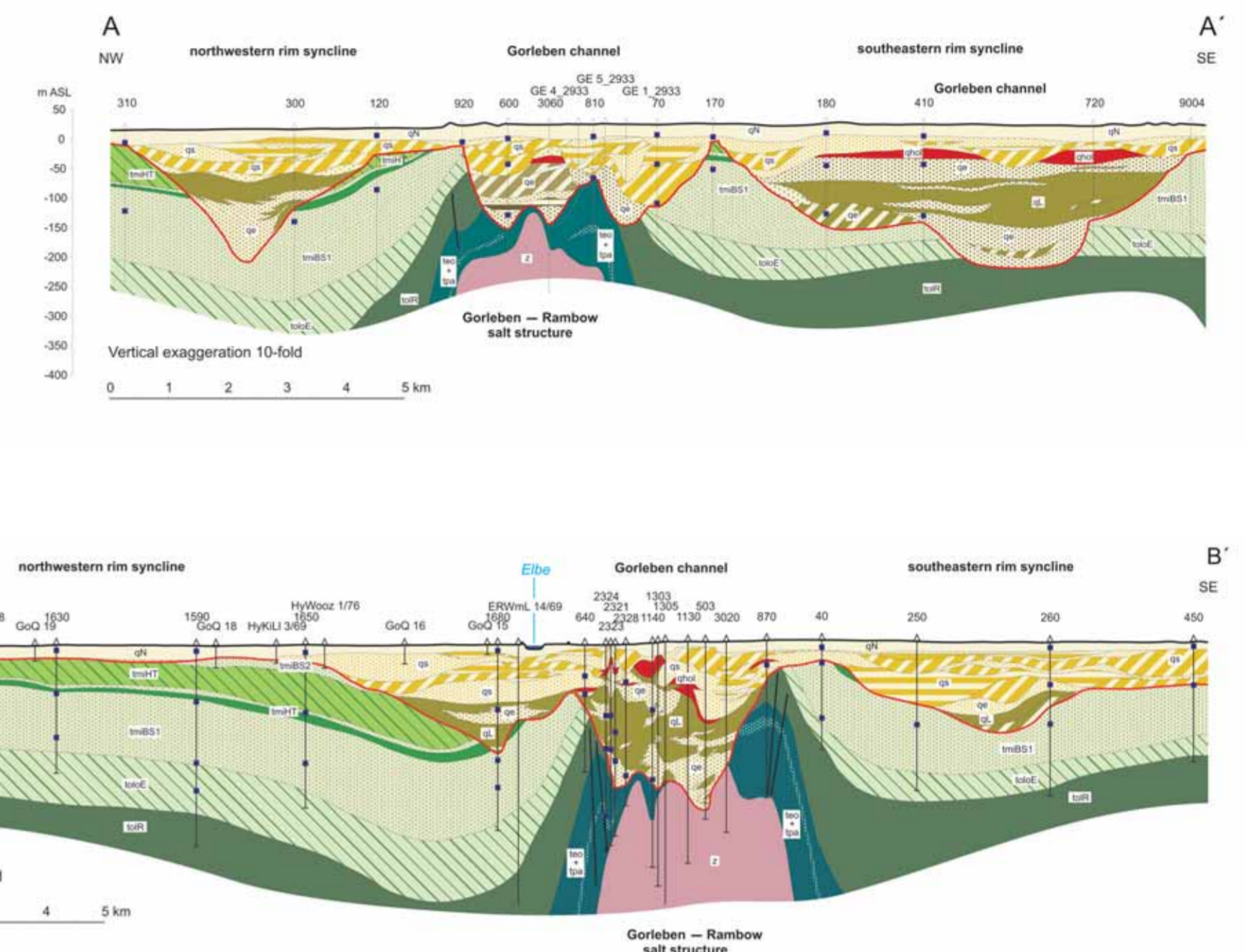
Appendix 1: Vertical cross sections through the study area Gorleben

Vertical cross sections through the study area Gorleben

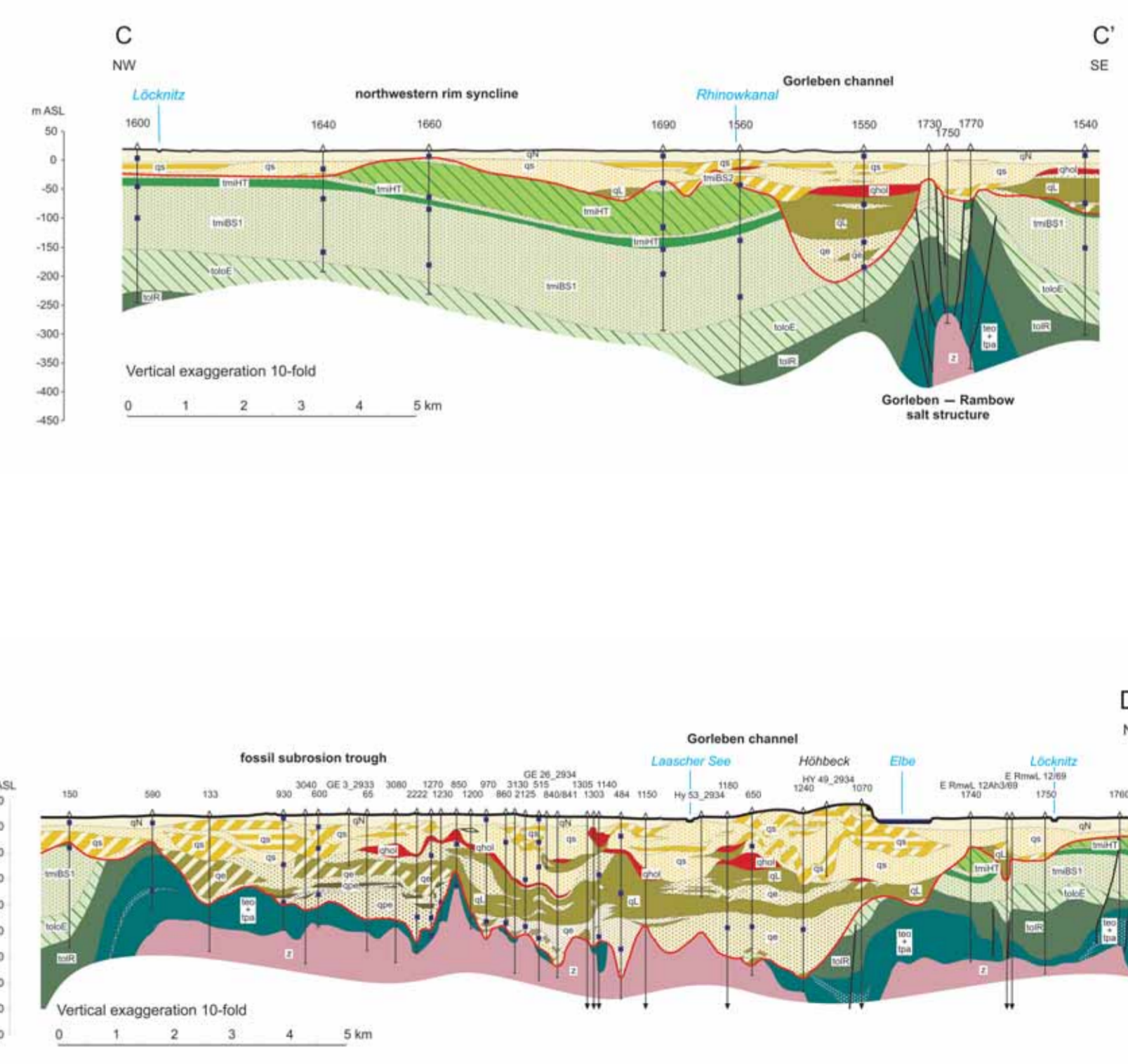
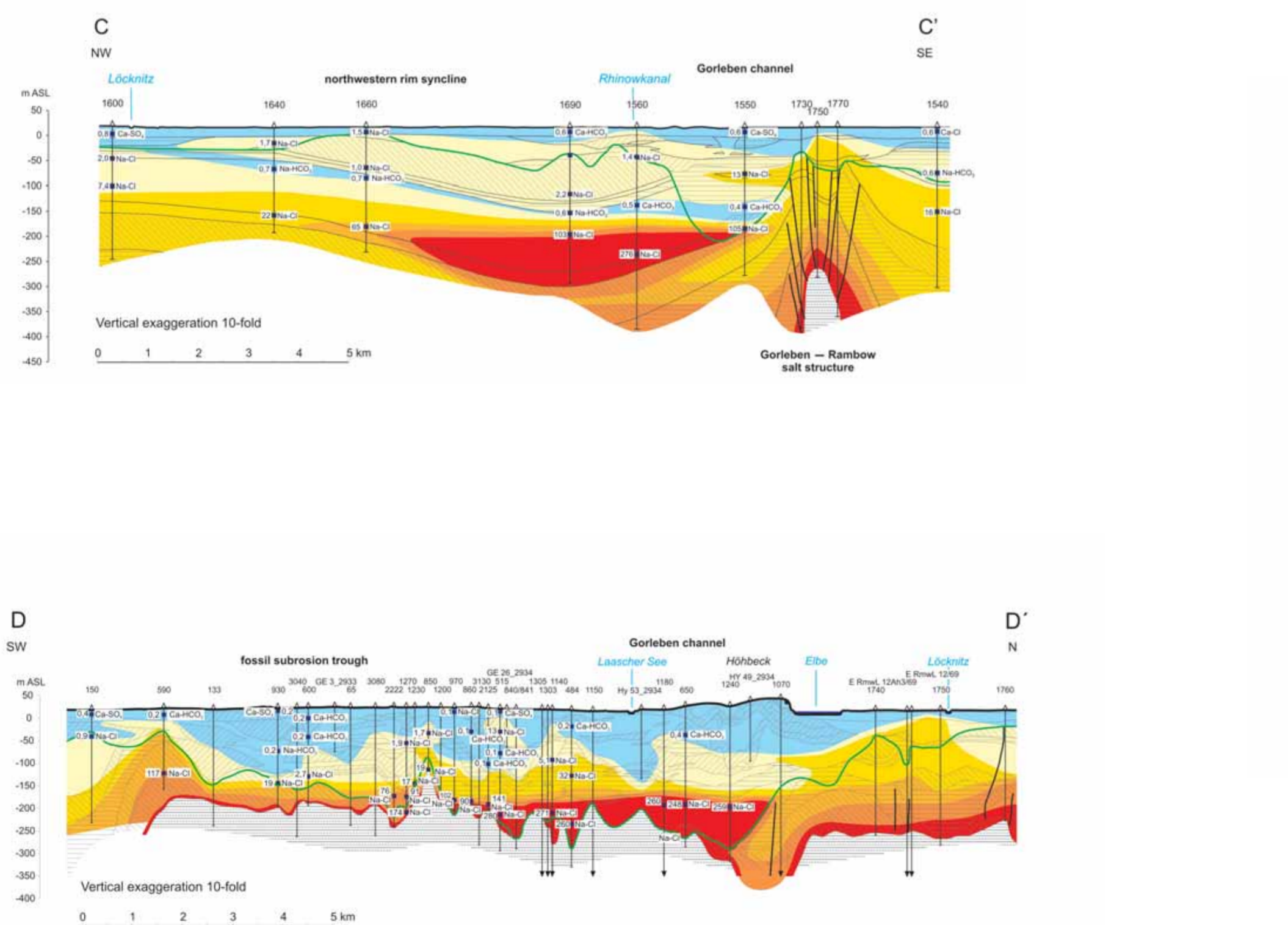
Hydrochemical vertical cross sections



Hydrostratigraphic vertical cross sections



Location and alignment of the vertical cross sections AA' to DD'



Legend (hydrostratigraphic cross sections)

- qN Sand: Weichselian lower terrace
- qs Sand: Saalian
- qs Bolder clay: Saalian
- qs Clay, silt: Saalian
- qhol Clay, silt partly sandy: Holsteinian
- ql Clay, silt: Elsterian (Lauenburger-Ton-Komplex)
- qe Sand: Elsterian
- qe Bolder clay: Elsterian
- ql Clay, silt: Elsterian
- qpe Silt, peat clay, fine sand: Bevel- and Cromer-Complex
- qpe Sand, with gravel: Menap glaciation
- tmBS2 Sand, silt: lower Miocene (obere Braunkohlsande)
- tmHT Silt, clay: lower Miocene (Hamburg-Ton)
- tmHT Sand, silt: lower Miocene (Hamburg-Ton)
- tmHT Clay, silt: lower Miocene (Hamburg-Ton)
- tmBS1 Sand, silt: lower Miocene (untere Braunkohlsande) incl. upper Oligocene (Neochattian)
- tmOE Clay, silt: upper Oligocene (Eochattian)
- tmOE Clay, silt: lower Oligocene (Rupelton)
- tm*pa Clay, silt: Eocene and Paleocene
- z Zechstein salts, incl. cap rock
- Base of Quaternary
- Fracture, locally simplified
- Borehole number
- Observation well

Legend (hydrochemical cross sections)

- Freshwater (TDS < 1 g/l)
- Saltwater (TDS 1 - 10 g/l)
- Saltwater (TDS 10 - 50 g/l)
- Saltwater (TDS 50 - 100 g/l)
- Saltwater (TDS 100 - 200 g/l)
- Saltwater (TDS > 200 g/l)
- Aquifer ($k_v > 10^{-6}$ m/s), Quaternary - Tertiary
- Aquifard ($k_v < 10^{-6}$ m/s), Quaternary - Tertiary
- Aquifard ($k_v = 10^{-4} - 10^{-5}$ m/s), Tertiary
- Zechstein evaporites, incl. caprock
- Base of Quaternary
- Fracture, locally simplified
- Observation well with TDS and chemical type of groundwater
- Borehole number

Bundesanstalt für Geowissenschaften und Rohstoffe (BGR)
Geozentrum Hannover
Stilleweg 2
30655 Hannover
Germany

www.bgr.bund.de

ISBN 978-3-9813373-4-1